國立臺灣大學工程學院機械工程學研究所

碩士論文

Department of Mechanical Engineering
College of Engineering
National Taiwan University

Master Thesis

運用數位微鏡裝置發展全域性掃描準單擊式共軛焦顯微形貌量測技術與系統

Development of quasi One-shot Full-field Confocal Microscopic Surface Profilometry and its Measuring Systems using Digital Micro-mirror Device

阮忠德
Nguyen Duc Trung

指導教授：陳亮嘉 博士
Advisor: Liang-Chia Chen, Ph.D.

中華民國 105 年 7 月
July 2016

doi: 10.6342/NTU201601083

Acknowledgements

I would like express special thanks to my advisor Prof. Liang-Chia Chen, lecturer in the Department of Mechanical Engineering- National Taiwan University for providing me with so many wonderful learning opportunities. It is an honor and a privilege to work with him and I am eternally grateful for his support, advice and mentorship.

Thanks to all my wonderful friends of AOI lab for being such supportive and inspiring.

Finally, I would like to thank my family and my girlfriend for their encouragement and inspiration throughout my life. To my mother Ho Thi Be who always cares about me with unconditional love. To my girlfriend Nguyen Thi Quynh who always believes in me.

I would like to dedicate this thesis to the memory of my father, Nguyen Van Thanh. He taught me to dream big and I know he would be immensely proud of my achievements.

doi: 10.6342/NTU201601083

摘要

本論文中，運用數位微鏡裝置(DMD)的準單擊式全域性掃描共軛焦顯微形貌量測術與量測系統獲得提出與執行。藉由精準的控制數位微鏡裝置上每一片微米鏡片來排列結構圖形，此微鏡裝置可視為針孔陣列，用以達到全域式共軛焦量測，不用任何橫向機械式掃描，同時能避免傳統共焦顯微術中遭遇到訊號橫向交談問題。研究中被發展出的兩個創新方法完全省略共軛焦垂直掃描。

第一個方法中，一個新方法被發展用來編碼並解碼表面形貌的深度資訊，藉由量測深度和相對應的共軛焦顯微鏡架構中表面繞射圖案之間的相關性。此發展系統可以將量測點與其周圍的光橫向交談最小化。因此，此系統在表面重建上可以有更高的強健性與效能和較少的橫向掃描可以說是準單擊式量測。

第二種方法利用彩色共焦顯微機構與寬頻光源，在深度-色散物鏡的量測範圍內，從偵測的光譜響應中編碼與解碼深度資訊。一個發展的訊號處理演算法可以建立一條光譜響應曲線，基於多光譜訊號擷取自擁有多頻光譜偵測功能的 IMEC 面形光譜相機。表面深度藉由偵測擁有最大光強的波長可以被精準的決定偵測光譜響應曲線中的峰值以取得最大光強值對應的波長。更重要的是，運用 DMD 排列設計的虛擬針孔陣列，將可使共軛焦橫向交談影響最小化。

根據使用二維正規化相關係數來建立正規化相關係數-深度響應曲線、在基於 DMD 的數位的繞射-共軛焦成像相關性原理、以及包含面型光譜相機的彩色共軛焦系統中運用一維正規化相關係數在光譜響應匹對程序，以上四項技術的發展，以克服光源能量波動或待測面反射率不同所造成的光強變化問題。

為檢驗被提出的方法之可行性與驗證系統的量測精度，用所發展的量測系統來測量校正過並擁有鏡面反射的階高塊。經由來自鏡射表面樣品的初步實驗結果，已證實基於 DMD 的數位的繞射-共軛焦成像相關性顯微鏡，在 400 μm 的量測範圍內高度量測的重複性在一個標準差是 0.03 μm，其量測的最大誤差為 0.1%在可量測深度範圍內。另一方面，包含面型光譜相機的彩色共軛焦系統中，用鏡面型樣品的隨機標準差低於 0.12 μm。將系統用在樣品表面粗糙度為 Ra=1.6 的案例中，高度量測的一個標準差可以保持於 0.67 μm 以內。

關鍵字：自動化光學檢測、彩色共軛焦顯微術、表面輪廓量測、正規化相關係數、全域量測、數位微鏡裝置(DMD)

doi: 10.6342/NTU201601083

Abstract

In the thesis, quasi one-shot full-field confocal microscopic surface profilometry and its measuring systems using digital micro-mirror device (DMD) is proposed and implemented. With precisely controlling each micro-mirror on DMD and modulated with structured patterns, a DMD can function as an array of pinholes to perform full-field confocal measurement without any lateral mechanical scanning and to avoid suffering lateral signal cross talk encountered in conventional confocal microscopy. Two novel approaches were developed in the study to omit confocal vertical scanning fully.

In the first approach, a new method was developed to encode and decode depth information of surface profile by the correlation between a measuring depth and its corresponding surface diffraction image pattern in confocal microscopic configuration. The developed system can minimize the light cross talk between each measuring point and its neighboring region. Thus, it can be more robust and efficient in surface reconstruction with less lateral scanning in a manner of quasi-one shot measurement.

The second approach uses a chromatic confocal microscope setup with broadband light, in which a depth-dispersion chromatic objective is used to encode and decode depth information from the detected spectrum response receiving at its measuring depth range. A developed signal processing algorithm can establish a spectrum response curve based on the multi-band spectral information captured by using an IMEC area spectral camera with multi-band spectrum detection capability. The surface depth can be accurately determined by detecting the wavelength with maximum intensity respected to its detected surface depth. More importantly, undesired confocal cross talk effect can be also minimized by applying a designed virtual pinhole array formed by DMD.

By applying 2-D normalized cross correlation to establish normalized cross correlation–depth response curve in the developed digital diffractive-confocal imaging correlation microscope, which is based on DMD and 1-D normalized cross correlation for spectrum response matching procedure in chromatic confocal system including spectral area camera, the developed confocal microscopes can be immune to light intensity variation being caused by light source's power fluctuating and reflectivity variation of sample's surface.

To test the feasibility of the proposed method and verify its measurement accuracy, a pre-calibrated step height with specular reflection was measured by the developed

doi: 10.6342/NTU201601083

measuring systems. From the preliminary experimental results with specular surface sample, it was verified that for digital diffractive-confocal imaging microscope based on DMD, the repeatability with one-standard deviation on height measurement is 0.03 μm in a measuring rage of 400 μm while the maximum measured error is 0.1 % of the measurable range. On the other hand, for chromatic confocal system including spectral area camera, one standard deviation is lower than 0.12 μm for mirror-like sample. Applying the system in the case of surface sample with roughness Ra = 1.6, one-standard deviation on height measurement still can be kept lower than 0.67 μm.

Keywords: Automated optical inspections (AOI), chromatic confocal microscopy, surface profilometry, normalized cross correlation (NCC), full-field measurement, digital micro-mirror device (DMD).

doi: 10.6342/NTU201601083

Table of Contents

1 Introduction 12

1.1 Background 12

1.2 Statement of the problem 15

1.3 Research objectives 16

1.4 Expected outcomes 17

2 Literature review 18

2.1 Traditional confocal microscope 19

2.2 Confocal microscope with Nipkow disks system 20

2.3 Noninterferometric differential confocal microscope 21

2.4 Polychromatic differential confocal microscope 23

2.5 Point-scan chromatic confocal microscope 24

2.6 Line-scan chromatic confocal microscope 26

2.7 3-D micro-inspection goes DMD 27

2.8 Time-resolved confocal microscopy using DMD 28

3 Research methodology 31

3.1 Confocal microscope 31

3.1.1 Basic structure and working principle of confocal microscope 31

3.1.2 Confocal microscope image formation 34

3.2 Digital micro-mirrors devices (DMD) 36

3.3 Digital diffractive-confocal imaging correlation microscope based on DMD………. 39

3.3.1 Pinhole's diffraction pattern 40

3.3.2 Confocal effect 43

3.3.3 Pinhole auto-locate algorithm 47

3.4 Digital diffractive-confocal imaging correlation microscope goes chromatic….. 48

doi: 10.6342/NTU201601083

3.5 Chromatic confocal system including spectral area camera 51
3.5.1 Chromatic confocal microscope 51
3.5.2 Spectral area camera 55
3.5.3 Chromatic confocal system included spectral area camera working principle…… 59
3.5.4 Alternative configurations 60
3.5.5 Efficient of the new DMD arrangement 62
3.5.6 Chromatic objective selection 64
3.5.7 Chromatic confocal depth response curve 65
4 Software development 67
5 Experiment setup and analyses 71
5.1 Digital diffractive-confocal imaging correlation microscope 71
5.1.1 General configuration 71
5.1.2 Alignment 72
5.1.3 Checking confocal configuration 75
5.1.4 Experiment results and analyses 77
5.2 Digital diffractive-confocal imaging correlation microscope goes chromatic….. 81
5.2.1 General configuration 81
5.2.2 Experiment result and analyses 82
5.3 Chromatic confocal system included spectral area camera 86
5.3.1 General configuration 86
5.3.2 IMEC camera calibration 87
5.3.3 Experiment results and analyses 90
6 Conclusions and future work 99
6.1 Conclusions 99
6.2 Future work 100

doi: 10.6342/NTU201601083

References 102

doi: 10.6342/NTU201601083

Table of figures

Figure 1 Surface measurement devices 13
Figure 2 Surface measurement devices measurement range 14
Figure 3 Commercial microscopes： (a) OLYMPUS Vertical scan laser confocal; (b) POLYTECH Vertical scan laser confocal; (c) KEYENCE Vertical scan white light interferometry; (d) SENSOFAR Virtual confocal; (e) STIL Chromatic confocal 15
Figure 4 Structure of traditional confocal microscope. 20
Figure 5 Nipkow disk structure 21
Figure 6 Noninterferometric differential confocal microscope's structure 21
Figure 7 Axial response curve of a confocal microscope 22
Figure 8 Differential response of our differential confocal microscope with various objective lenses: (a) 60X, NA = 0.85; depth resolution = 2 nm; dynamic range = 0.7 pm. (b) 40 X, NA = 0.65; depth resolution = 4 nm; dynamic range = 1.3 pm. (c) 20 X, NA = 0.40, depth resolution = 12 nm; dynamic range = 3.6 pm 22
Figure 9 Schematic diagram of DCMBPI (lasers 1, 22; focusing lens 2, 21; pinholes 3, 8, 10, 20, 25, 28; extender lens 4, 19; polarized beam splitters 5, 18; beam splitters 6, 23; λ / 4 wave plates 13, 17; depolarized beam splitter 14; collecting objectives 7, 9, 24, 27; center shaded filter 15; objective 16; detectors 11, 12, 26, 29; monochromatic filters 30, 31; focal planes O 1 , O 2) 23
Figure 10 Extended response range based on polychromatic illumination. (a) Response of the differential detector group. (b) Synthetic uniform response range of DCMBPI .. 24
Figure 11 Confocal intensity signal a) with mechanical depth scanning and b) with chromatic depth scanning 25
Figure 12 Structure of point-scan chromatic confocal microscope 25
Figure 13 Chromatic confocal line sensor 26
Figure 14 Confocal depth response 27
Figure 15 Image of a complete DMD 27
Figure 16 Schematic illustration of the DMD based optical surface profiler 28
Figure 17 Optical layout of a DMD-confocal microscopy system 29
Figure 18 Examples of employed DMD scan patterns: a) point scan, b) line scan, ... 29
Figure 19 Plot of the axial resolution of the DMD confocal scanning microscope........ 30
Figure 20 Point-scan confocal microscope (object at focal plane) 32
Figure 21 Point-scan confocal microscope (object out of focus) 33

doi: 10.6342/NTU201601083

Figure 22 Intensity respond curve 33
Figure 23 Point-scan confocal microscope modeling.. 34
Figure 24. Pixels in On and Off state.. 36
Figure 25 Pixel with Labeled Parts.. 37
Figure 26 DMD orthogonal and diamond arrangements 38
Figure 27 DMD incident light and reflected light configuration.................................... 38
Figure 28 Diagram of optical system setup for digital diffractive-confocal imaging correlation microscope... 40
Figure 29 Fraunhofer diffraction from a rectangular aperture.. 41
Figure 30 2-D and 3-D visualization for Fraunhofer pattern of a square aperture (computer generated)... 42
Figure 31 2-D and 3-D visualization of the same pattern but with increased exposure time to bring out some of the faint terms (computer generated).. 42
Figure 32 Pinhole's configuration 43
Figure 33 Auto-locate pinholes algorithm result 45
Figure 34 Diffraction pattern change by in- and out-focus effect of confocal configuration 45
Figure 35 Normalized cross correlation – depth response curve.................................... 47
Figure 36 Flow chart of auto-locate pinhole algorithms... 47
Figure 37 Digital diffractive-confocal imaging correlation chromatic microscope 49
Figure 38 Improve measurement range effect of chromatic objective 50
Figure 39. Bayer filter for color camera 50
Figure 40 Refraction occur between 2 isotropic media 51
Figure 41 Axial chromatic dispersion: each wavelength is focused at a different point along the optical axis 52
Figure 42 Basic configuration of point-scan chromatic confocal microscope 53
Figure 43 Intensity curve registered by the spectrometer... 54
Figure 44 Chromatic confocal calibration curve 55
Figure 45 Spectral Data Cube... 56
Figure 46 Typical spectral imaging approaches. (a) Whiskbroom. (b) Pushbroom. (c) Staring. (d) Snapshot... 56
Figure 47 Fabry Perot effect 57
Figure 48 Fabry Perot filters... 58

doi: 10.6342/NTU201601083

Figure 49. IMEC Mosaic spectral area camera.......... 58
Figure 50 Quasi one-shot full-field chromatic confocal microscope 60
Figure 51 Revised configuration for quasi one-shot full-field chromatic confocal microscope (illumination mode – configuration 1) 61
Figure 52 Revised configuration for quasi one-shot full-field chromatic confocal microscope (illumination mode – configuration 2) 61
Figure 53 Revised configuration for quasi one-shot full-field chromatic confocal microscope (illumination and detection mode) 62
Figure 54 Spectral response curve 63
Figure 55 Optical simulation of chromatic objective :(a) 20× chromatic.......... 64
Figure 56 Optical simulation of the dispersion range with respect to various light wavelengths for the design of the chromatic objective: (a) 20× chromatic objective, (b) 27× chromatic objective.......... 65
Figure 57 IMEC camera spectrum response corresponding to one pinhole at different depths 66
Figure 58 3 layers of control software 67
Figure 59 Software interface for digital diffractive-confocal imaging correlation microscopy.......... 68
Figure 60 Software interface for chromatic confocal microscopy using DMD and IMEC camera 69
Figure 61 Reducing database's size.......... 70
Figure 62 Timeline for parallel processing mode 70
Figure 63 Optical system setup on anti-vibration table 72
Figure 64 Alignment steps 73
Figure 65 Light collimating system 74
Figure 66 Placement of objective and tube lens 75
Figure 67 Flowchart for confocal effect checking.......... 76
Figure 68 Intensity–depth response curve for 2x objective 76
Figure 69 Intensity–depth response curve for 20x objective 77
Figure 70 Flowchart of digital diffractive-confocal imaging correlation microscope.. 78
Figure 71 3-D images of wafer surface at different position 79
Figure 72 2-D and 3-D views of step-height sample 80
Figure 73 Defected sample. 80

doi: 10.6342/NTU201601083

Figure 74 3-D view of defected sample 80
Figure 75 Optical system setup on anti-vibration table for digital diffractive-confocal imaging correlation microscope goes chromatic 82
Figure 76 Flowchart of digital diffractive-confocal imaging correlation microscope goes chromatic 83
Figure 77 Typical NCC-depth response curve for digital diffractive-confocal imaging correlation microscope goes chromatic at position 1 – blue range 84
Figure 78 Typical NCC-depth response curve for digital diffractive-confocal imaging correlation goes chromatic at position 2 – green range 84
Figure 79 Typical NCC-depth response curve for digital diffractive-confocal imaging correlation microscope goes chromatic at position 3 – red range 85
Figure 80 2-D and 3-D views of step-height sample 85
Figure 81 Optical system setup on anti-vibration table for chromatic confocal system using DMD and IMEC camera 87
Figure 82 IMEC 16 bands snapshot mosaic filter layout 88
Figure 83 Filter responses in the active range of a SSM 4x4 VIS hyper spectral sensor 89
Figure 84 Spectrum response after calibration 90
Figure 85 Typical response of IMEC camera (16 bands) 91
Figure 86 Typical response of IMEC camera (single bands) 91
Figure 87 Flowchart of chromatic confocal system using DMD and IMEC camera 92
Figure 88 Auto-locate pinholes algorithm output 93
Figure 89 Typical NCC response 93
Figure 90 Scatter plot for accuracy and precision test 94
Figure 91 Diffuse surface sample 95
Figure 92 Typical NCC response 96
Figure 93 NCC response with noise 96
Figure 94 Scatter plot for accuracy and precision test of diffuse surface sample 97

doi: 10.6342/NTU201601083

Nomenclature

DMD	Digital micro-mirror device
N.C.C	Normalized cross correlation
SPM	Scanning probe microscopy
SEM	Scanning electron microscopy
NA	Numerical aperture
PZT	Piezo electric transducer
FHWM	Full width half maximum
OPD	Optical path difference
DDCICM	Digital diffractive-confocal imaging correlation microscopy
$S(v,w)$	Light source distribution pattern function
$P(\xi,\eta)$	Pupil function
$D(v,w)$	Sensitivity function of detector
$I(u,v,w)$	Intensity function
$h(u,v,w)$	Fourier transform of the pupil distribution
$t(u,v,w)$	Projection pattern out-of-focus function
$J_0(x)$	First-order Bessel function
u,v,w	Normalized optical coordinates
$\Delta W(u,v,w)$	Wave front function including focusing and aberration terms
ξ and η	Normalized pupil coordinates
I_t	Total intensity in sub-image area
λ	Wavelength
n	Refractive index
σ	Standard deviation

doi: 10.6342/NTU201601083

1 Introduction

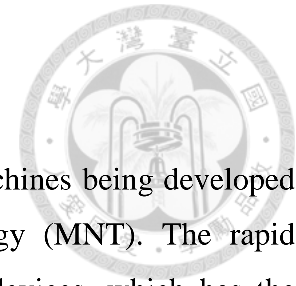

1.1 Background

For past few decades, there are many advantaged new machines being developed by the commercial exploitation of micro- and nanotechnology (MNT). The rapid development of micro-nano system technology requires new devices, which has the ability to control and measure the product features as we move into a miniaturized world.

Nowadays, inspection is extremely important in the manufacturing process. Inspection helps manufacturers control both catastrophic failure and defects, so they can increase the product's quality and reduce wasted product. In micro-nano scale product, the surface features play an important role for characteristics and quality of a part. Therefore, the key input information for micro-nano inspection processes usually is surface texture properties of micro-nano objects.

Surface profile measurement and areal surface texture measurement are both important input for micro-nano inspection processes. However, the measurement of areal surface texture has a number of benefits over profile measurement. There are currently many commercial instruments that can measure areal surface texture showed in Figure 1. We can classify these devices by judging their surface texture measuring performance (line profiling, areal topography, or area-integrating) or measuring procedure (non-contact or contact type) in Figure 2.

doi: 10.6342/NTU201601083

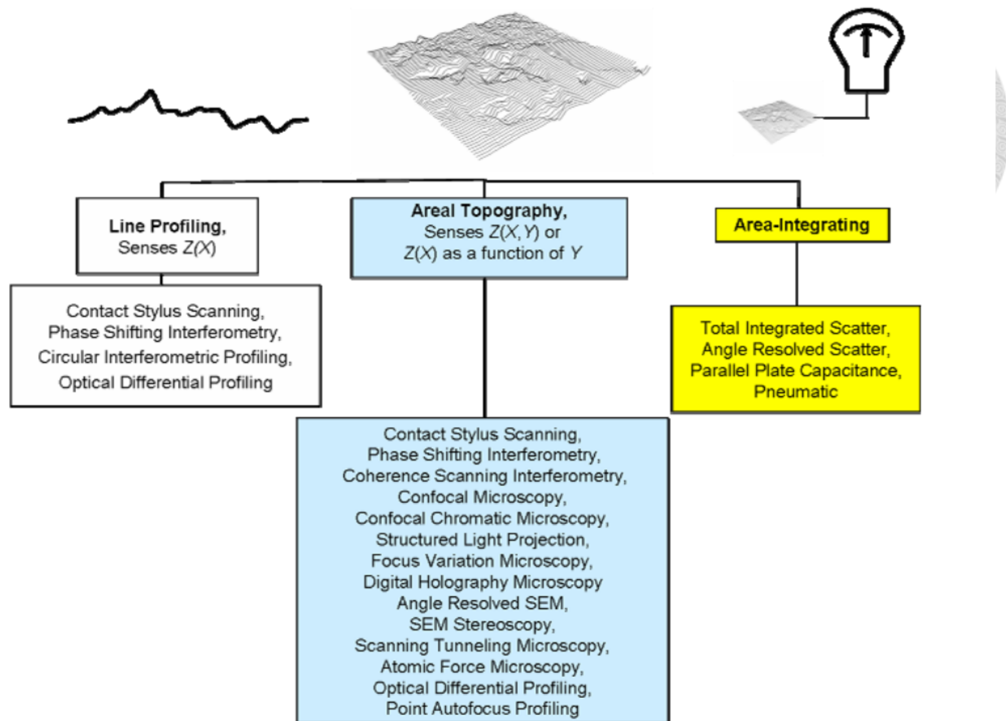

Figure 1 Surface measurement devices

Surface texture measurement can be divided into two categories: contact type (SPM, Stylus) and non-contact type (SEM, optical). For industrial sample measurement, the optical type is usually a better approach because it does not require contacting with the sample and is easy to integrate with available product lines. In the 21st century, there are a lot of different optical instrument developed for surface texture and form measurement. The interferometers with phase shifting technique could be accurately tracked for the peaks and valleys of the surface texture with nano-scale vertical resolution. The first of these was the phase shifting interferometry (PSI) microscope in the early 1980s, which was primarily useful for measurement of smooth optical surfaces. Flowing this invention, vertical scanning interferometer or scanning white light interferometer was developed in order to measure surfaces with higher roughness. Optical surface profilometry continues its success with confocal microscopes which were invented in the 1990s. Nowadays, these two types of instruments occupy big portion of the market for optical surface topography instruments.

doi: 10.6342/NTU201601083

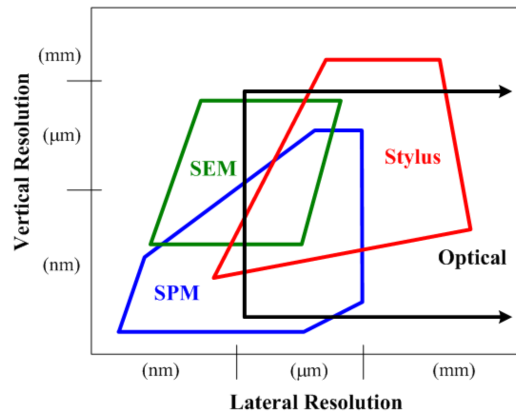

Figure 2 Surface measurement devices measurement range

Optical confocal microscope has become extremely important for surface topography because of its high longitudinal measurability range and excellent vertical resolution. This kind of microscope is widely used to measure volume structures or surface topographies. Before, confocal microscopes was used mainly in the field of biology and medicine to visualize the three-dimensional structure of cells. Now, those systems were widely used in semiconductor industries for inspection purposes. There are many inspection systems using optical confocal microscope principle, which are widely used in manufacturing processing. Figure 3 shows some product from OLYMPUS, POLYTECH, KEYENCE, SENSOFAR and STIL.

doi: 10.6342/NTU201601083

(a) (b) (c)

(d) (e)

Figure 3 Commercial microscopes： (a) OLYMPUS Vertical scan laser confocal; (b) POLYTECH Vertical scan laser confocal; (c) KEYENCE Vertical scan white light interferometry; (d) SENSOFAR Virtual confocal; (e) STIL Chromatic confocal

1.2 Statement of the problem

The goal of optical confocal surface profilometry is to measure volumetric structures or surface topographies with high accuracy and precision. This work is still a challenging task in this field because although traditional confocal microscope system help us to get higher accuracy and precision, it still requires scanning processes. Therefore, the time spent for measurement will be increased, and mechanical movement for scanning process can generate undesired errors in our measurement results.

Recent years, many different methods have been developed into confocal systems to improve the spatial resolution, the working distance, and scanning process. Most of the approaches try to maximize the simultaneous parallelization of confocal topography

doi: 10.6342/NTU201601083

measurements. Therefore, mechanical movement can be reduced or completely avoided, so the measuring times shortened. In general cases, to maintain the advantages of confocal microscope system, the approaches just can reduce the scanning process in 1 or 2 directions. However, almost the approaches still required complex setup, specific elements, troublesome calibration process and usually only applied for some specific samples. This makes these systems lack of flexibility.

Moreover, optical confocal surface profilometry is very time consuming in scanning process. To meet the requirements of industrial applications, the measuring time factor is the most important and, as such, it has the first priority to be improved.

Finally yet importantly, precedent confocal methods heavily relied on light intensity, the measured value can easily be effected by sample's surface reflectance or light source's power variation. Many confocal systems have been suffered from light intensity variation, so were hard to maintain with high precision and accuracy. Therefore, it is necessary to develop new methods, which can be immune to light intensity variation.

1.3 Research objectives

This research proposes an area-scan confocal surface profilometry system, which based on two new advanced devices: Digital Micro-mirror Devices (DMD) and IMEC spectral area-scan camera. In order to achieve maximum parallelization, we need to eliminate both lateral scanning and vertical scanning processes. By using DMD, lateral scanning will be reduced and mechanical movement in our system will be minimized, so measurement errors are also significantly reduced. Furthermore, with specific designed pinholes array arrangement being created by DMD, the cross-talk effect between adjacent measuring points can be significantly reduced, so lateral resolution could be also improved. In this study, the vertical scanning process will be eliminated by using two different approaches: innovative digital diffractive-confocal imaging correlation microscope and chromatic confocal system including spectral area camera.

In the first method, quasi one-shot full-field surface profilometry using digital diffractive-confocal imaging correlation microscope that is based on DMD is developed for quasi one-shot microscopic 3-D surface measurement. Optical configuration applied confocal microscope setup and was developed by using DMD to generate specific pinhole array arrangement for minimizing cross talk effect. The innovative method was developed to create normalized cross correlation – depth response curve from diffraction patterns of

doi: 10.6342/NTU201601083

pinhole. Using this approach, the sub-micrometer scale depth can be detected with high accuracy and precision.

In the second method, the spectral area camera will make are-scan chromatic confocal surface profilometry become robust and flexible. To apply these two devices to chromatic confocal system, we need to analyze the effect of virtual pinhole size, which is generated by the DMD light pattern, and the cross talk effect between adjacent virtual pinholes, then to develop an appropriate scanning strategy for the approach. On the other hand, spectral area camera have finite wavelength bands, so a new calibration process needs to be developed to increase the wavelength resolution. Moreover, a new method needs to be developed to establish the calibration curve based on the relationship between the scanning vertical distance and the spectral intensity.

1.4 Expected outcomes

In order to satisfy the high requirements in the modern industry about the speed, flexibility, precision, stability and reliability, this research will focus on developing area-scan confocal surface profilometry using DMD and spectral area camera, which satisfy the most important things as follows:

- Quasi one-shot full-field;
- Compact and lightweight;
- High accuracy and high precision with short measuring time;
- Robustness and efficiency.

doi: 10.6342/NTU201601083

2 Literature review

The confocal measurement principle makes use of a pinhole filter to filter the reflected stray light. When the sample is not in the focal position, the reflected light will not pass through the pinhole then to the light sensor; on the contrary, when the sample is on the focal position, reflected light will go through the pinhole to the light sensor, then gives a strong signal. This research focuses on maximizing parallelization of the developed confocal surface profilometry system, so literature review section will be divided into several subsections based on parallelization of each system. Literature review will come through from traditional confocal systems to chromatic confocal systems, from point scanning to area scanning confocal systems. All the systems in literature review section are grouped and listed in the table shown below:

Table 1 Classification of reviewed confocal system

direction scanning	direction scanning	direction scanning	Zero direction scanning
• Traditional confocal microscope • Confocal microscope using Nipkow disks • Noninterfero metric differential confocal microscope • 3-D inspection using DMD • Time-resolved confocal	• Polychromatic differential confocal microscope • Point-scan chromatic confocal microscope	• Line-scan chromatic confocal microscope	• Area-scan chromatic confocal microscope

doi: 10.6342/NTU201601083

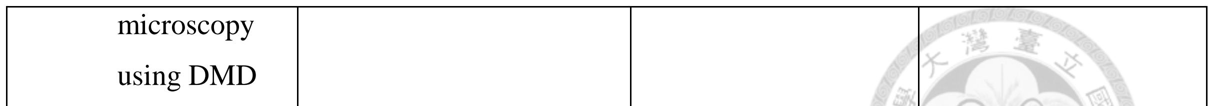

microscopy using DMD			

2.1 Traditional confocal microscope

Scanning confocal microscope is a well-established imaging tool, which has widely used for surface topography measurement because of its superior lateral and vertical resolution compared to conventional microscope [1]. It has played an important role in different fields, especially in *in-situ* automatic optical inspection (AOI) on microstructures [2]. Confocal microscopes are applied to surface profile detection for its high resolution, depth discrimination and unique sectioning capability; and, many efforts have been made to improve its property [3].

In a confocal microscope, a point light source illuminates the object through an objective, and the reflected light formed image on a point detector, which is employed to measure intensity of the reflected light. The point detector is achieved using a pinhole in front of the detector. A basic configuration of traditional confocal microscope is illustrated in Figure 4. Only the light that is reflected from the focal plane of the system, can pass through a pinhole, and then hit to the point detector. This create a strong optical sectioning property, which can be used to investigate the three-dimensional structure of thick objects. On the other hand, the pinhole also rejects light scattered from the optical system, so image clarity and measurement accuracy can be both improved [4].

Because the confocal microscopy only focuses on a single point in 3-D space, in order to build up a complete volumetric structure or surface topography of measuring sample, the system needs to perform both lateral scanning (X, Y direction) and vertical scanning (Z direction). Traditional confocal microscopes usually use a moving stage (servo motor stage or PZT) for scanning process. Based on the reflected light intensity signal, which will be maximum when the measuring sample is at the focal position, the volumetric structure of surface topography of measuring sample can be reconstructed.

doi: 10.6342/NTU201601083

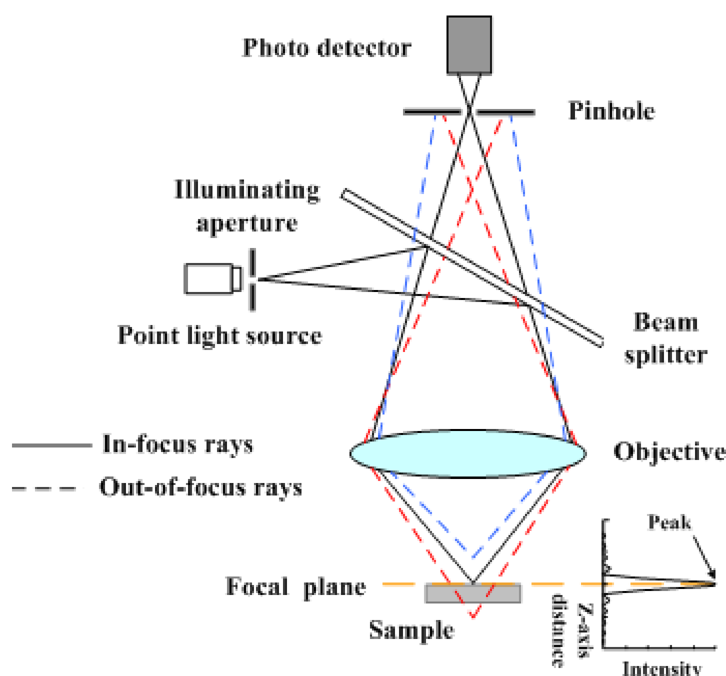

Figure 4 Structure of traditional confocal microscope.

2.2 Confocal microscope with Nipkow disks system

A compact high-resolution scanning confocal microscope, using a micro lens and Nipkow disks has been developed by Takeo Tanami and other researchers to improve the scanning speed of confocal microscope system [5]. Figure 5 illustrates the construction of the microscope, which consists of two disks. The upper disk consists of micro lenses and the lower disk consists of pinholes. The pinholes and micro lenses are placed on two disks with the same special pattern. The collimated light from a laser illuminates on the upper disk, and then the light is focused onto the lower disk by the micro lenses. After that, the objective lens focuses the light onto a spot on the specimen. Going through the same path reflected, a beam splitter would reflect light from the specimen, and then forms an image on the camera through a relay lens. The two disks are connected together, so when they finish one rotation, the confocal microscope will finish the whole area of measuring specimen. This mechanism can increase the lateral scanning speed and can also speed up to 1 frame/ms with the Nipkow disk consists of ~20000 pairs of pinholes and micro lenses. The system has a high lateral scanning speed but reduces image quality (depending on the number of micro lenses and pinholes pairs). Moreover, the rotating movement of Nipkow disk may induce undesired mechanical vibration, which affects measurement quality.

doi: 10.6342/NTU201601083

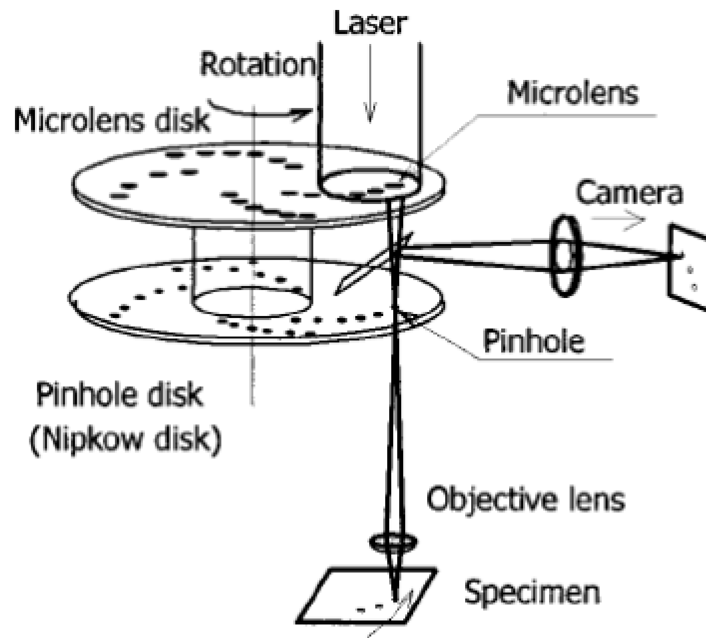

Figure 5 Nipkow disk structure [5]

2.3 Noninterferometric differential confocal microscope

The concept of differential confocal microscope was proposed to utilize a linear variance ratio of intensity at the slopes of the axial response curve to measure surface contours with high axial resolution [6].

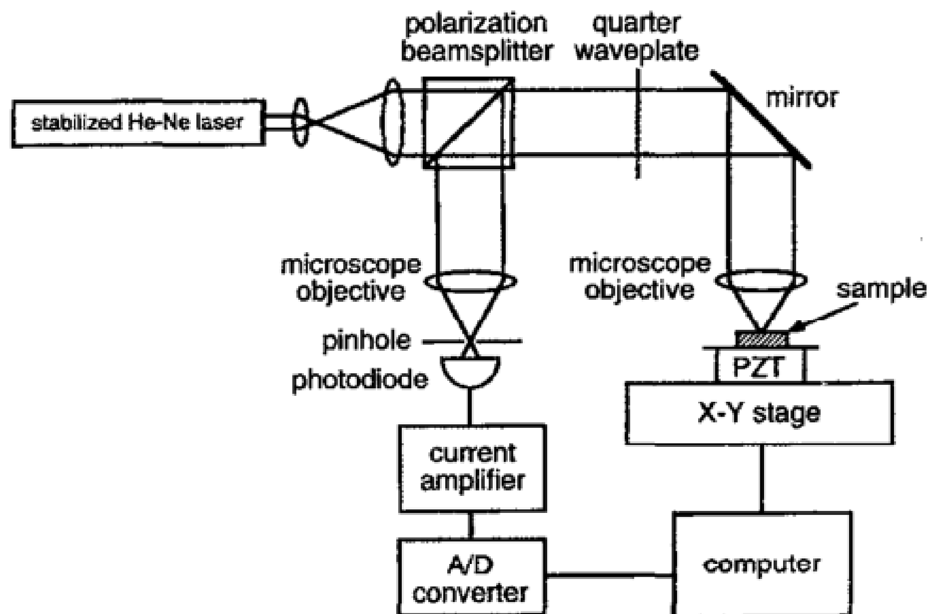

Figure 6 Noninterferometric differential confocal microscope's structure [6]

doi: 10.6342/NTU201601083

Although when the sample is at the focal point, the light intensity is maximum. The derivative of the response curve with respect to the sample position becomes zero as in Figure 7. In order to increase the sensitivity to sample height variation, the sample needs to be placed slightly away from the focal point. From this setup, we can create differential response curve as in Figure 8.

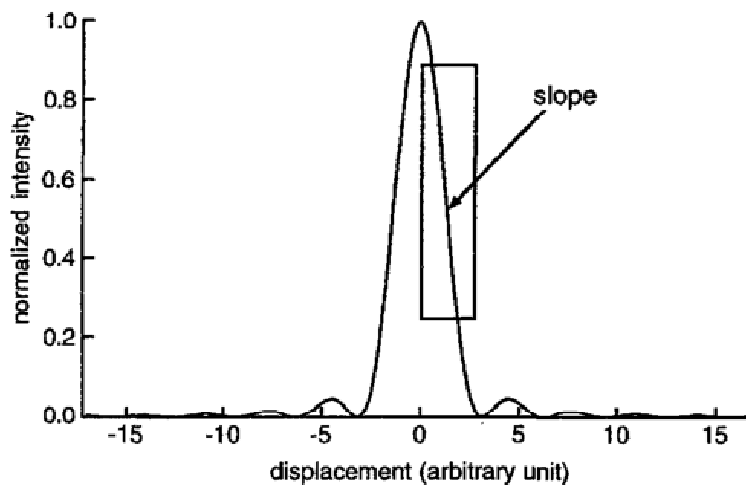

Figure 7 Axial response curve of a confocal microscope [6]

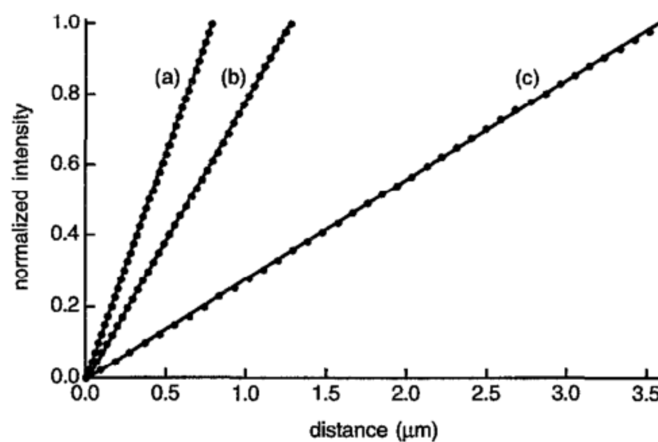

Figure 8 Differential response of our differential confocal microscope with various objective lenses: (a) 60X, NA = 0.85; depth resolution = 2 nm; dynamic range = 0.7 pm. (b) 40 X, NA = 0.65; depth resolution = 4 nm; dynamic range = 1.3 pm. (c) 20 X, NA = 0.40, depth resolution = 12 nm; dynamic range = 3.6 pm [6]

doi: 10.6342/NTU201601083

Even thought, the configuration made the system more insensitive to height variation, this system still needs to scan in X, Y and Z direction. There was no improvement in measurement parallelization.

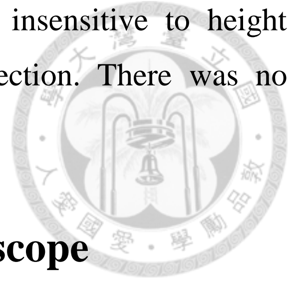

2.4 Polychromatic differential confocal microscope

A differential confocal microscope based on polychromatic illumination was developed in order to gain both a wide measurement range and a high lateral resolution [7].

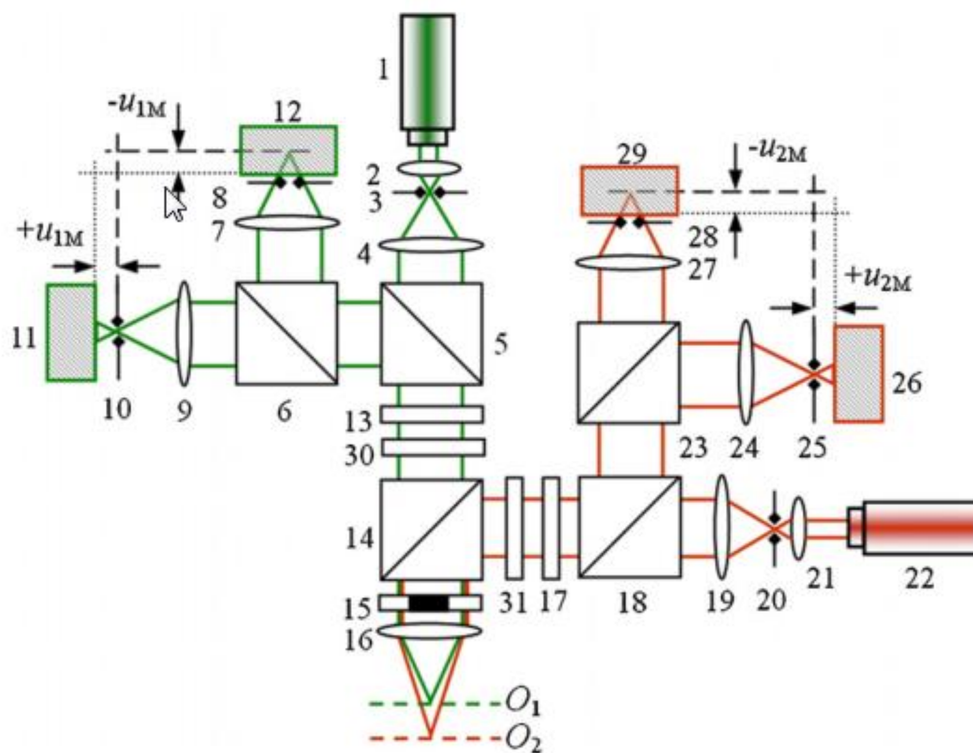

Figure 9 Schematic diagram of DCMBPI (lasers 1, 22; focusing lens 2, 21; pinholes 3, 8, 10, 20, 25, 28; extender lens 4, 19; polarized beam splitters 5, 18; beam splitters 6, 23; λ / 4 wave plates 13, 17; depolarized beam splitter 14; collecting objectives 7, 9, 24, 27; center shaded filter 15; objective 16; detectors 11, 12, 26, 29; monochromatic filters 30, 31; focal planes O 1 , O 2) [7]

The idea for this system based on the fact that axial response can be shifted with its curve when a detector is shifted from its imaging focal plane. That means that setting the detectors being defocused from their imaging focal planes will shift the axial response curves being shifted either forward or backward [8]. Figure 9 shows the configuration of

doi: 10.6342/NTU201601083

polychromatic differential confocal system. In this system these detector 11, 12 29 and 26 are shifted away from focal point, in order to generate differential signals. By using two light sources with different wavelength, this system can increase the measurement range. The differential signals are calculated by using the formula:

$$I(w,u)=\frac{I_1(w,u+u_m)-I_2(w,u-u_m)}{I_1(w,u+u_m)+I_2(w,u-u_m)}$$

With the differential signals detected, we can inverse one of those signal and combine it together to form a lager measurement range.

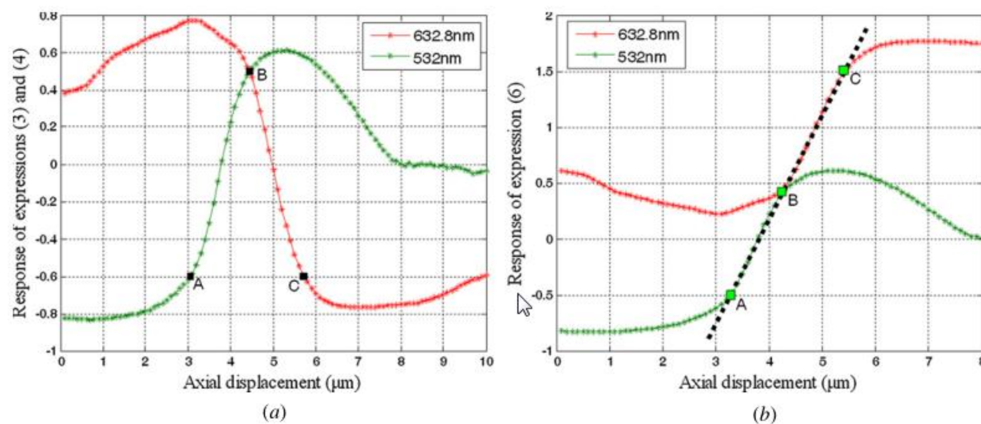

Figure 10 Extended response range based on polychromatic illumination. (a) Response of the differential detector group. (b) Synthetic uniform response range of DCMBPI [7]

By introducing polychromatic illumination, two independent ranges can be stitched together to form an extended measurement range. The system already eliminates vertical scanning but still requires lateral scanning. However, in this method, there still exist some drawbacks, which may affect the accuracy and its potential application. The system based on two light sources with four light detectors can make its structure more complex and hard to calibrate. Limited by the number of light sources, the measuring range cannot be extended further.

2.5 Point-scan chromatic confocal microscope

Chromatic confocal technique with an exemption for vertical scanning and can achieve real-time measurements [9, 10], and the advantage of long depth measurement

doi: 10.6342/NTU201601083

range [11]. The chromatic confocal point sensor achieves a complete parallelization of the depth scan.

Applying chromatic effects of the imaging lens is a possibility to eliminate the vertical scanning process. The intensity curve from traditional confocal microscope now transform to spectrum curve as described in Figure 11. After mapping the wavelength and the distance of focal plane for each wavelength, we can get the height of measuring sample from spectral intensity.

Figure 11 Confocal intensity signal a) with mechanical depth scanning and b) with chromatic depth scanning [9]

In a point scan, chromatic confocal setup can use a varying illumination wavelength or use a spectrally broad light source and a spectrometer as a detector. Figure 12 illustrates the second configuration.

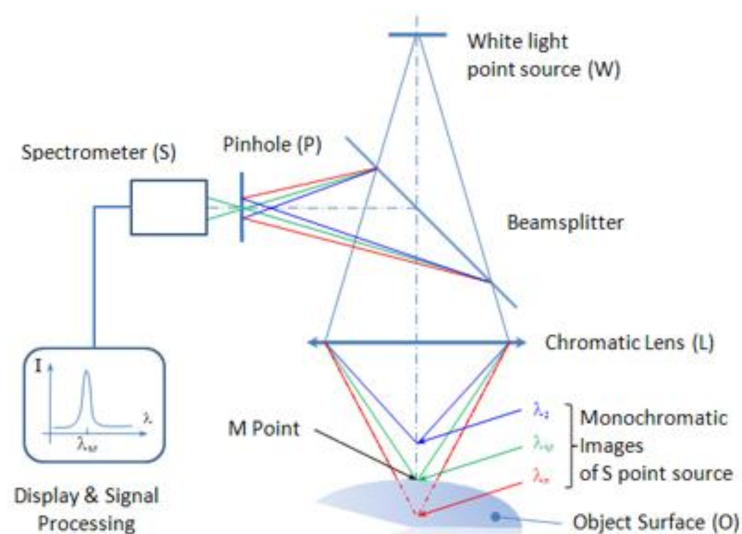

Figure 12 Structure of point-scan chromatic confocal microscope [9]

doi: 10.6342/NTU201601083

2.6 Line-scan chromatic confocal microscope

Chromatic confocal point sensors does not need vertical scanning but it is still necessary to perform spatial scanning to reconstruct a surface topography. A further parallelization can be achieved by using chromatic confocal line sensors.

By applying cylinder lens and using a slit aperture instead of a pinhole, this system can reduce lateral scanning in one direction. In this system, the line-spectrometer can be employed to maintain lateral resolution.

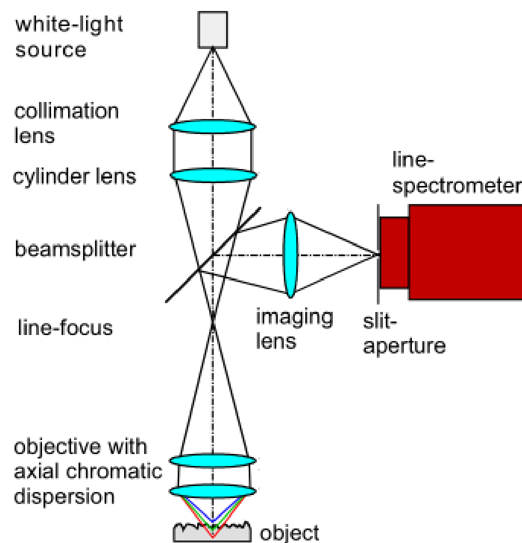

Figure 13 Chromatic confocal line sensor [9]

The line-scan chromatic confocal microscope can eliminate the depth scanning and reduce the lateral scanning in one direction. However, this system may suffer from cross-talk effect between adjacent points in scanning line.

In the developed system, the optical system was designed for a relatively high NA of 0.4 for a field diameter of 2.4 mm. The achieved chromatic depth measurement range was 0.7 mm. A slit aperture just can eliminate cross talk effect in one direction. Therefore, its depth discrimination property is poorer than that of a pinhole. The confocal depth is plotted in Figure 14 and it has a FWHM of 55 μm.

doi: 10.6342/NTU201601083

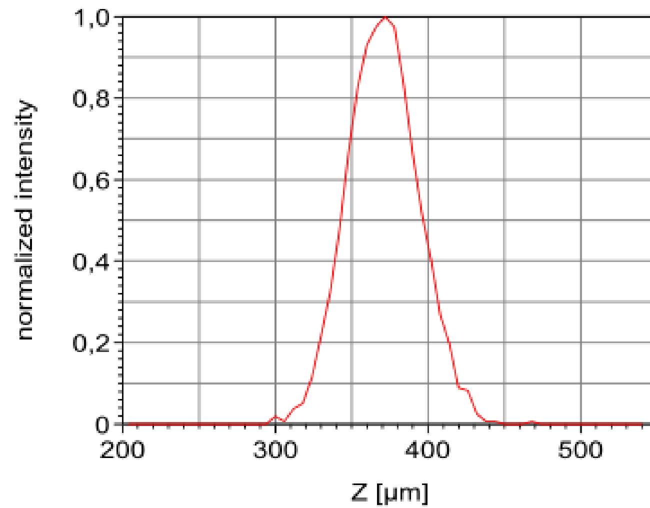

Figure 14 Confocal depth response [9]

2.7 3-D micro-inspection goes DMD

Digital Micro-mirror Devices (DMD) was employed for applications in the field of optical metrology are also possible. Modern DMDs consist of many micro-mirrors made of an aluminum alloy. The single micro-mirrors can be control to switch a tilting angle. Usually, a single micro mirror has 3 states: ON, OFF, and REST respectively to 3 different tilting angles.

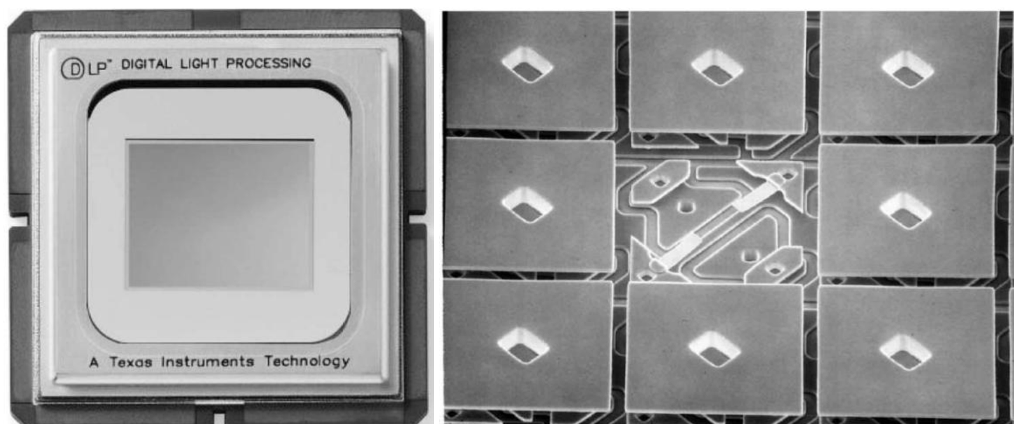

Figure 15 Image of a complete DMD [12]

F. Bitte and his partners already developed 3-D inspection system using the new devices [12] .In this configuration, the DMD is used to project an array of small spots resulting either from single mirror elements (pixels) or composed multiple mirror

doi: 10.6342/NTU201601083

elements (super pixels). These spots act as multiple point light source. The light from those spots are imaged onto the specimen surface by a microscope objective, then is reflected back and forms images onto the camera chip where their intensities are measured by specific camera pixels.

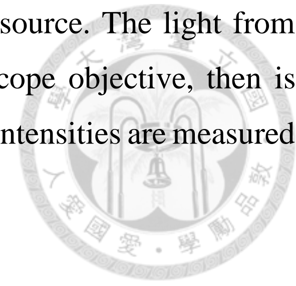

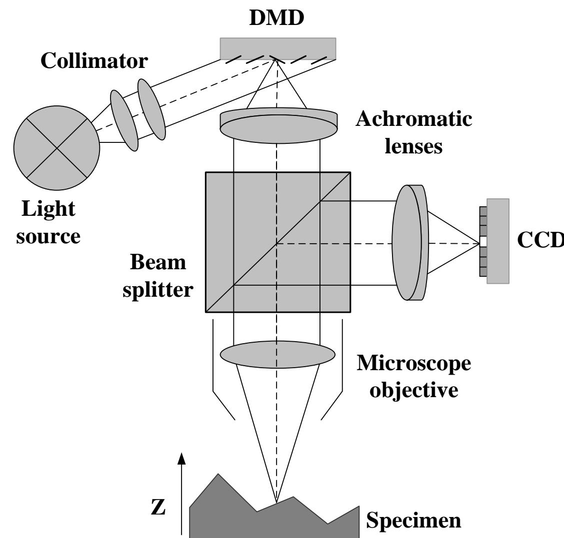

Figure 16 Schematic illustration of the DMD based optical surface profiler [13]

The pixel-intensities are maximum when the corresponding images, which created by DMD pixels are lying in the focal plane of the microscope objective. By doing vertical scanning, the intensity-depth response curves for every measurement point can be recorded. After detecting intensity peak in each intensity–depth response curves and link it to corresponding motor position, the 3-D profile of the specimen can be reconstructed.

In this system, by applying DMD for lateral scanning, the speed is significantly increased. However, this system still requires vertical scanning and lacking of pinhole. This may lead to reduce measurement accuracy and precision. Although special lateral scanning strategy was already developed, without using a real pinhole, the system may still suffer from the cross-talk effect between adjacent imaging points.

2.8 Time-resolved confocal microscopy using DMD

Time resolved 3-D-microscopy using DMD-arrays is a flexible confocal system. The system is optimized for optical imaging of reflective, transparent, and fluorescent objects [14. The configuration of this system is illustrated in Figure 17.

doi: 10.6342/NTU201601083

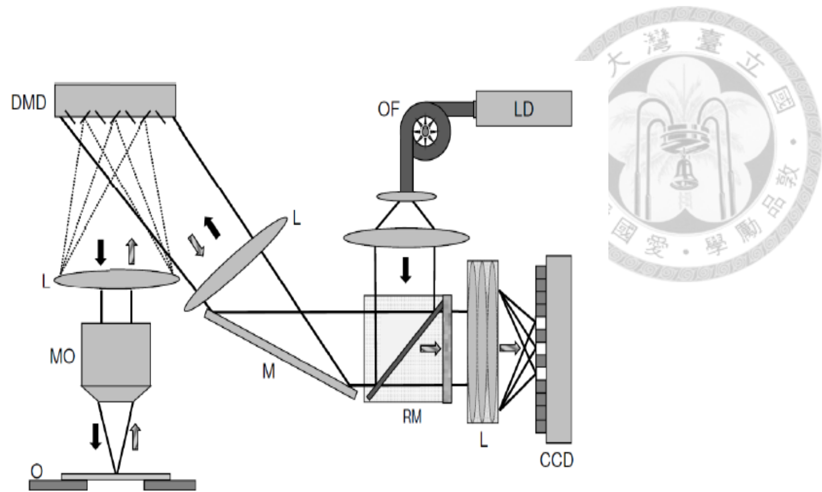

Figure 17 Optical layout of a DMD-confocal microscopy system [14]

The working principle of this system is almost the same with 3-D-inspection using DMD. However, in this application, DMD realizes both the illumination and the confocal sectioning through a DMD-array. Just by changing the order of beam splitter and DMD, the DMD now has a role acting like a virtual pinhole in front of the light source and in front of CCD. This configuration will improve the sectioning capability and reduce cross-talk effect between adjacent scanning points.

In this system, the DMD-array consists of a rectangular grid, in this case of 1024x768 square micro-mirrors. Each mirror measures 12.6 μm to a side, with a distance of 1 μm between mirrors, the overall dimensions of the array are approx. 14x10 mm. Each micro-mirror can be set into one of three states: on, off, and resting. The switch rate can be up to 8 kHz. Based on this device, the system can flexibly changes between different illumination modes such as point-scan, multiple point-scan, line-scan and multiple line-scan.

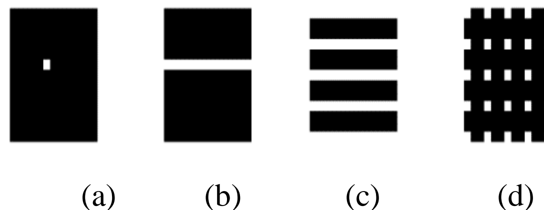

(a) (b) (c) (d)

Figure 18 Examples of employed DMD scan patterns: a) point scan, b) line scan, c) multi-line scan, d) multipoint scan [14]

Figure 18 shows the axial resolution of the DMD confocal scanning microscope for different scan pattern configurations (1x1, 2x2, and 4x4 mirrors).

doi: 10.6342/NTU201601083

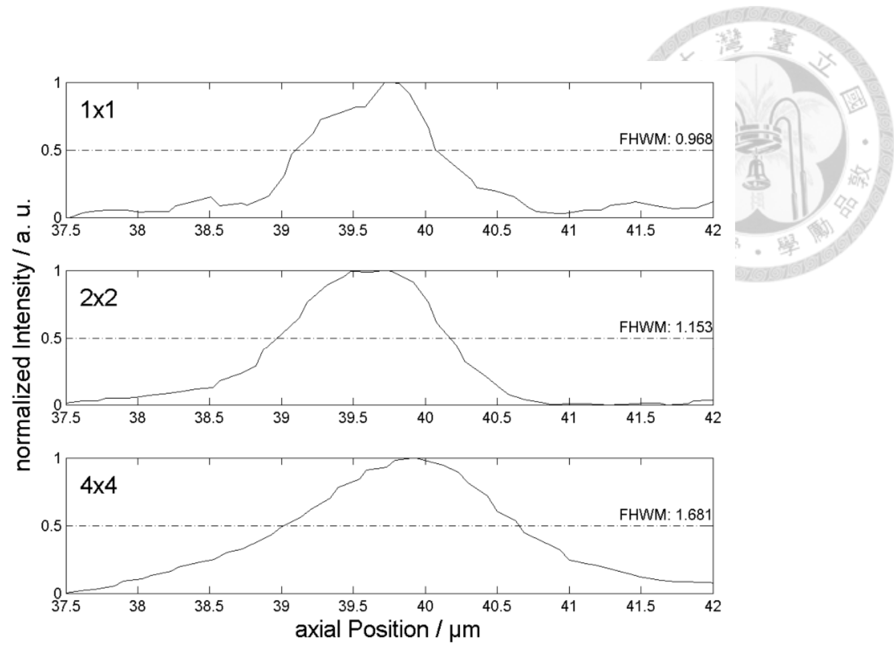

Figure 19 Plot of the axial resolution of the DMD confocal scanning microscope [14]

Like 3-D-inspection using DMD system, by applying DMD for lateral scanning, the scanning time of this system is reduced. On the other hand, because of no mechanical movement, the error due to mechanical vibration is eliminated. Furthermore, changing the order of DMD and beam splitter has solved the lacking-pinhole problem, leading to improvement of measuring result’s quality. However, this system still requires vertical scanning.

doi: 10.6342/NTU201601083

3 Research methodology

In order to archive quasi one-shot full-field confocal surface profilometry, in both developed methods (digital diffractive-confocal imaging correlation method and chromatic confocal system including spectral area camera), our systems relies on confocal microscope theory, specific designed pinholes array created by Digital Micro-mirrors Devices (DMD) and spectral area camera. Before illustrating how these two approaches can be suitable for quasi one-shot full-field confocal profilometry, background knowledge and working principle of confocal and chromatic confocal microscope system will be first introduced, and then followed by the overview of DMD.

3.1 Confocal microscope

A confocal microscope will take a series of images of object when doing vertical scanning through the depth of focus of the objective. By the way, it can detect the image with the highest intensity and calculate the height or depth of measuring object. Confocal microscopy has many advantages over other optical measuring techniques such as having a high numerical aperture that can bring in high measureable local slope with high light intensity efficiency or high lateral and vertical resolution. In the beginning, confocal microscopy was mainly used in biomedical field, however, the application field of the device quickly become very broad, ranging from biomedical to semiconductor, optics, and more.

3.1.1 Basic structure and working principle of confocal microscope

Basic configuration of confocal microscopy is described in Figure 20. In such a configuration, a pinhole is located right in front of laser point source (an illumination pinhole). The light goes through the illumination pinhole to a beam splitter and projects on the sample by an objective lens. The smallest illuminated spot is achieved on the focal plane of the objective and is typically a diffraction-limited spot. When the light hits the sample surface, it then reflects back and goes through the detection pinhole (confocal aperture) to the detector. The illumination pinhole and detection pinhole mutually have a conjugate optical relation.

doi: 10.6342/NTU201601083

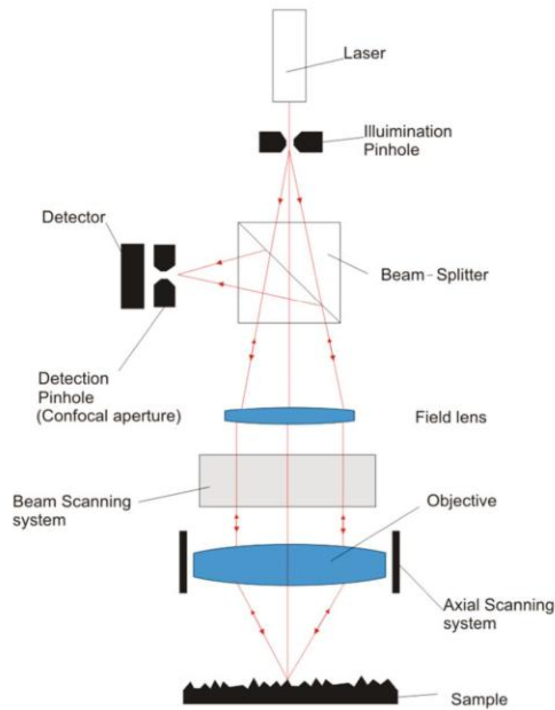

Figure 20 Point-scan confocal microscope (object at focal plane)

When the measured object's surface is placed exactly on the focal plane of the objective, the reflected light will have a maximum intensity. On the other hand, when the measured object's surface is not on focal plane, the reflected light defocuses away from detection pinhole (Figure 21). All the stray lights will be blocked by the detection pinhole, so the intensity of this measuring point on the detector will be significantly reduced.

doi: 10.6342/NTU201601083

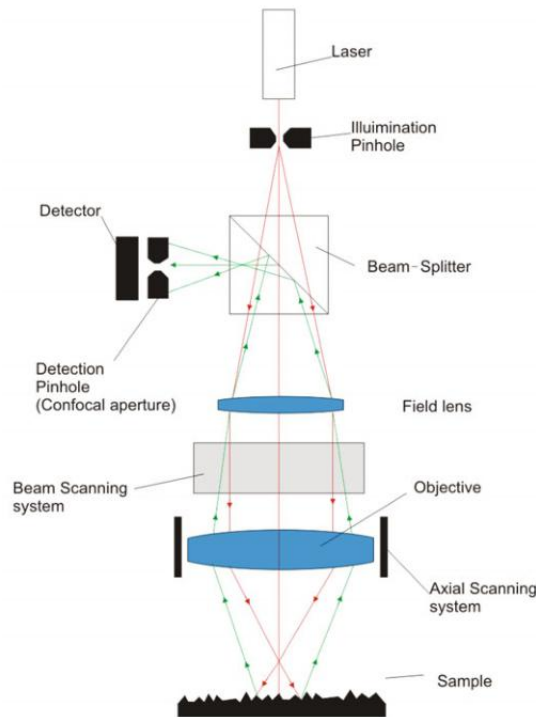

Figure 21 Point-scan confocal microscope (object out of focus)

Based on the characteristics of the confocal microscope, we can detect the height or the depth of measurement point on surface's sample. Vertical scanning procedure can be performed using a PZT or servo stage in order to generate intensity respond curves corresponding to individual points on the measured object's surface shown in Figure 22. Using peak detection algorithm and stage's depth location, we can calculate the height or depth of those points. To generate surface profile or surface 3-D topography, we can use mechanical (PZT or servo stages) or optical (Nipkow Disk or DMD) devices for lateral scanning to scan a line or an area on the object's surface.

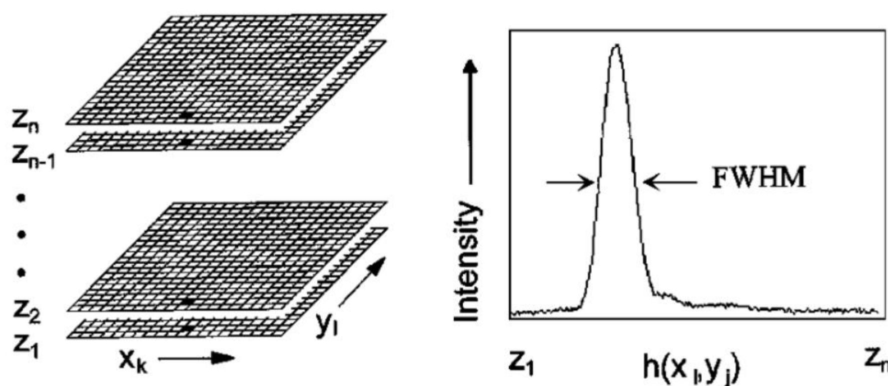

Figure 22 Intensity respond curve

doi: 10.6342/NTU201601083

3.1.2 Confocal microscope image formation

A schematic diagram of a typical scanning optical microscope is shown in Figure 23.

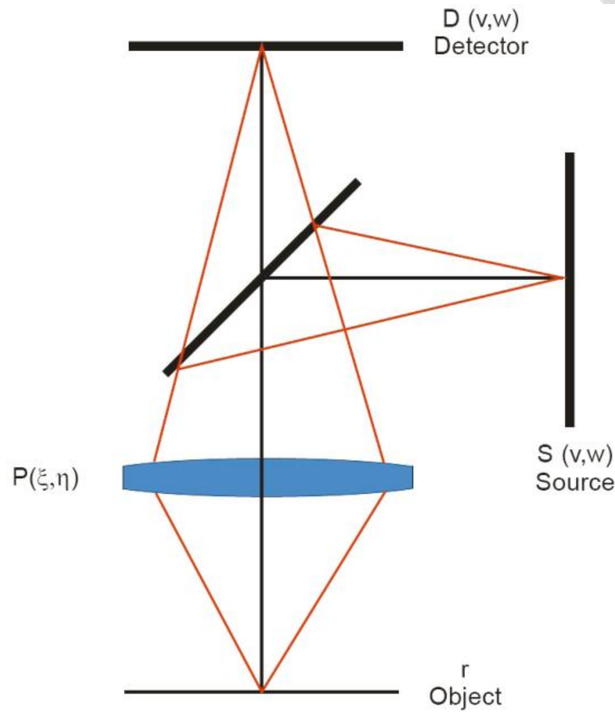

Figure 23 Point-scan confocal microscope modeling

A light source pattern of distribution $S(v,w)$ illuminates a microscope's objective with a pupil function $P(\xi,\eta)$. The light is focused onto the sample with reflectance distribution r and is reflected back to the objective with the same pupil function and then focused onto a detector with sensitivity $D(v,w)$. The intensity on a single point of the detector with incoherent propagation is given by

$$I(u,v,w)=\int_{-\infty}^{\infty}\int_{-\infty}^{\infty} D(v,w)t(u,v',w')\,\mathrm{h}(0,v-v',w-w')^2 dv'dw' \tag{1}$$

where $t(u,v',w')$ is the projection pattern out-of-focus by a quantity u, diffraction limited on the object plane, $u/2$ being the distance between the surface and the object plane, given by

$$t(u,v',\mathrm{w}')=\int_{-\infty}^{\infty}\int_{-\infty}^{\infty} S(v'',w'')h(u,v'-v'',w'-w'')^2 dv''dw''$$

doi: 10.6342/NTU201601083

(2)

where $h(u,v,w)$ is the Fourier transform of the pupil distribution

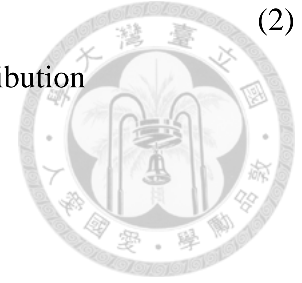

$$h(u,v,w)=\int_{-\infty}^{\infty}P(\xi,\eta)e^{i(\xi v+\mu w)}e^{i\Delta W(u,v,w)}d\xi d\eta$$

(3)

The terms v and w are the normalized optical coordinates

$$v=\frac{2\pi}{\lambda}x\sin\alpha$$
$$w=\frac{2\pi}{\lambda}\mathrm{y}\sin\alpha$$

(4)

And sinα is the numerical aperture of the objective, ξ and η are the pupil coordinates normalized to the aperture radius of the pupil, $\xi=\frac{x}{a},\eta=\frac{y}{a}$, and $\Delta W(u,v,w)$ is the wave front including focusing and aberration terms.

Equation (2) can be expressed as a convolution by

$$t(u,v,w)=S(v,w)\otimes|\mathrm{h}(u,v,w)|^2$$

(5)

Resulting in a simplified expression for equation (1) as

$$I(u,v,w)=(S(v,w)\otimes|\mathrm{h}(u,v,w)|^2)(D(v,w)\otimes|\mathrm{h}(0,v,w)|^2)$$

(6)

On a circular pupil, such as those present on a typical microscope objective

$$\xi=\eta=\rho\sin\theta$$

(7)

And Equation (3) is simplified to

$$h(u,v)=\int_0^1 P(\rho)J_0(v\rho)e^{i\Delta W(u,\rho)}\rho d\rho$$

(8)

doi: 10.6342/NTU201601083

where $J_0(x)$ is a first-order Bessel function of the first type. The defocus term for the wave front in the pupil region is expressed as

$$\Delta W(u,\rho) = -\frac{1}{2}u\rho^2 \tag{9}$$

where

$$u = \frac{8\pi}{\lambda} z \sin^2(\alpha/2) \tag{10}$$

Equation (8) is simplified to

$$h(u,v) = \int_0^1 P(\rho) J_0(v\rho) e^{-i\frac{1}{2}u\rho^2} \rho d\rho \tag{11}$$

3.2 Digital micro-mirrors devices (DMD)

Modern DMD consists of many micro-mirrors made of an aluminum alloy. The single micro-mirror is both an opto-mechanical element and an electro-mechanical element, which can be controlled to switch tilting angle.

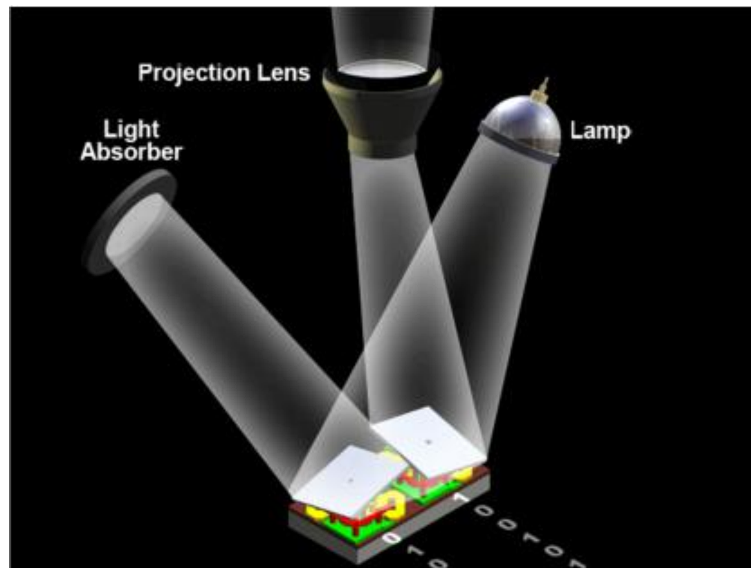

Figure 24. Pixels in On and Off state

doi: 10.6342/NTU201601083

The DMD pixel is an electro-mechanical element in that there are three stable micro-mirror states corresponding to different tilting angles. By programing the DMD controller, individual micro-mirror can be set into one of three working states (on, off and resting). In our systems, the DMD acts as a spatial light modulator as well as a pinhole array creator. By convention, the positive (+) state is tilted toward the illumination and is referred to as the "on" state. Similarly, the negative (–) state is tilted away from the illumination and is referred to as the "off" state.

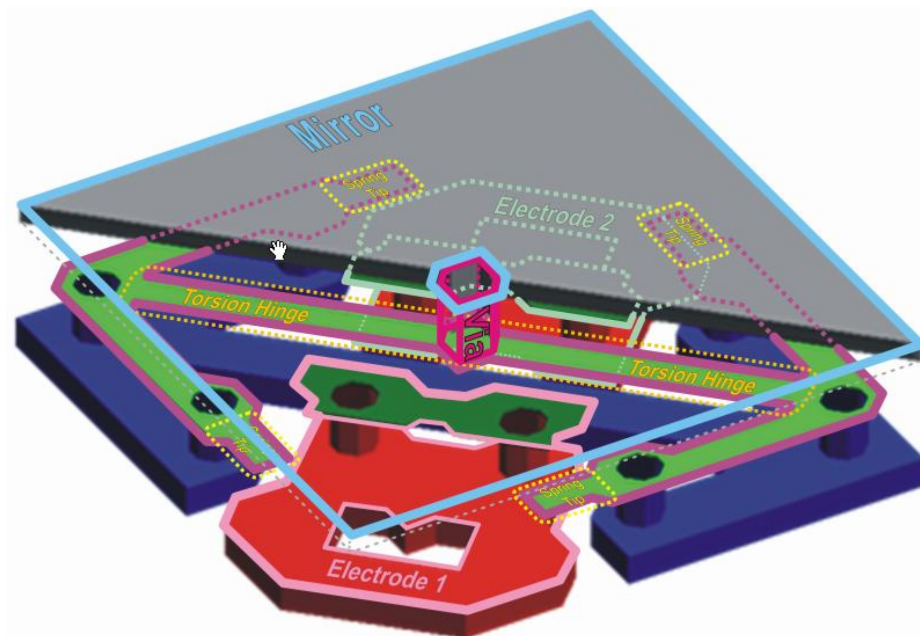

Figure 25 Pixel with Labeled Parts

Mechanical structure of a DMD pixel was illustrated in Figure 25. The diagram shows a micro-mirror in the unpowered state. The two electrodes shown are used in holding the micro-mirror in on or off positions (+12° and -12°).

Based on the characteristics of the device, it can be used to control illumination light and reflect light in confocal system. DMD not only reduces the measuring time and mechanical vibration error, but also makes the system more flexible because the system can switch among scanning mechanisms (point-scan, line-scan, area-scan) just by changing scanning pattern in software.

In our application, we use DMD from Texas Instrument. In order to get the highest on-off frequency, we use DMD with diamond arrangement micro-mirrors as described in Figure 26. Figure 27 shows the specific alignment to make incident light and reflected lights follow designed paths. Because of diamond arrangement, to setup our system on

doi: 10.6342/NTU201601083

anti-vibration table, which requires incident light and reflected lights to be co-planar, we need to rotate DMD 45 degree.

Chipset catalog - advanced light control

DMD Number	*Micromirror Array	Array Diagonal	Controller	Driver/PMIC	Max Pattern Rate	Optimized Wavelengths	Pixel Pitch	Pixel Orientation	EVM	DMD Package Dimensions (lxwxh)	DMD 100u Price ($ U.S.)	Controller 100u Price ($ U.S.)	Driver/PMIC 100u Price ($ U.S.)
DLP2010NIR	854 x 480	0.2"	DLPC150	DLPA2005	1,500 Hz (binary)	700 – 2500 nm	5.4 µm	Orthogonal	DLP NIRscan Nano	15.9 x 5.3 x 4 mm	125.28	26.17	6.33
DLP3000	608 x 684	0.30"	DLPC300	—	4,000 Hz (binary)	420-700 nm	7.6 µm	Diamond	LightCrafter	16.6 x 7 x 3.54 mm	95	16	—
DLP4500	912 x 1140	0.45"	DLPC350	—	4,225 Hz (binary)	420-700 nm	7.6 µm	Diamond	LightCrafter	20.7 x 9.1 x 3.33 mm	143	56	—
DLP4500NIR	912 x 1140	0.45"	DLPC350	—	4,225 Hz (binary)	700 - 2500 nm	7.6 µm	Diamond	NIRscan	20.7 x 9.1 x 3.33 mm	315	56	—
[illegible]	[illegible]	[illegible]	[illegible]	[illegible]	[illegible]	[illegible]	[illegible]	[illegible]	[illegible]	[illegible]	[illegible]	[illegible]	[illegible]
DLP6500FYE	1920 x 1080	0.65"	DLPC900	—	9,500 Hz (binary)	420 - 700 nm	7.6 µm	Orthogonal	DLP Light-Crafter 6500	32 x 32 mm	588	160	—
DLP6500FLQ	1920 x 1080	0.65"	DLPC900	—	9,500 Hz (binary)	400-700 nm	7.6 µm	Orthogonal	DLP Light-	32 x 41 mm	1,137	160	—
DLP7000	1024 x 768	0.7"	DLPC410	DLPA200	32,552 Hz (binary)	420-700 nm	13.6 µm	Orthogonal	Discovery™ 4100	40.64 x 31.75 x 6.01 mm	787	193	12.36
DLP9000	2560 x 1600	0.9"	DLPC900	—	9,500 Hz (binary)	400-700 nm	7.6 µm	Orthogonal	Crafter 9000	42.2 x 42.2 x 7 mm	2,783	160	—
DLP9500	1920 x 1080	0.95"	DLPC410	DLPA200	23,148 Hz (binary)	400-700 nm	10.8 µm	Orthogonal	Discovery 4100	42.16 x 42.16 x 7.03 mm	2,446	193	12.36

Figure 26 DMD orthogonal and diamond arrangements

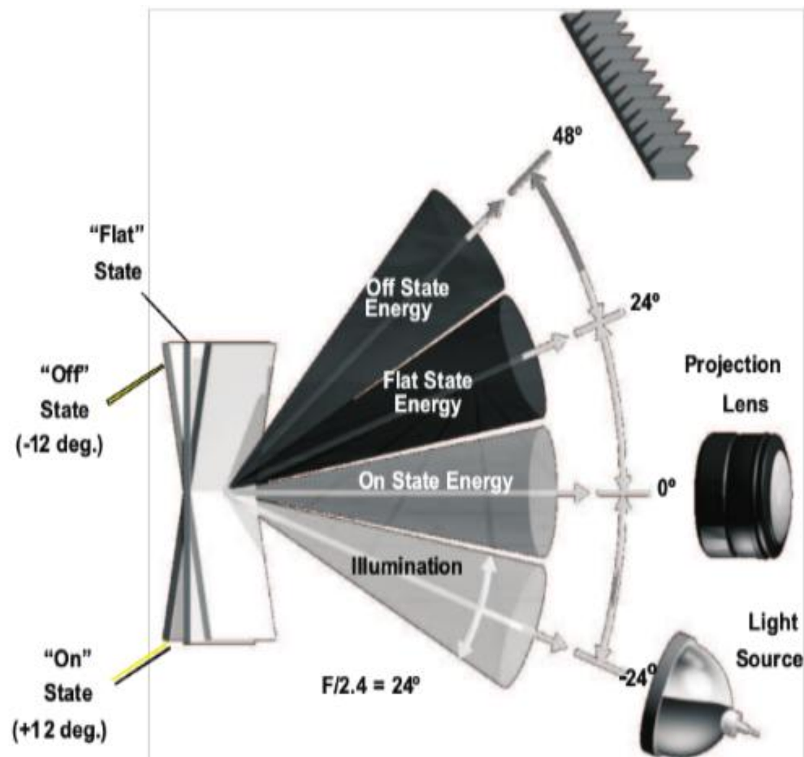

Figure 27 DMD incident light and reflected light configuration

doi: 10.6342/NTU201601083

3.3 Digital diffractive-confocal imaging correlation microscope based on DMD

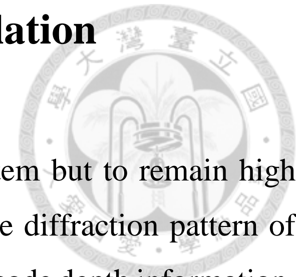

In order to speed up the measuring speed of confocal system but to remain high sectioning capability and spatial resolution, our idea is to use the diffraction pattern of virtual pinholes, which are created by micro-mirror on DMD to encode depth information. Then, using the reverse procedure to decode the depth information from pinhole's diffraction patterns to depth. Applying this principle will strengthen measurement efficiency by many factors. First, by building diffraction database and extract the depth information from this database, the vertical scanning process can be totally omitted. On the other hand, based on DMD, there are a large number of pinholes matrix can be created, so in *in-situ* application, spatial scanning processes can be skipped. For applications which require higher spatial resolution, spatial scanning processes can be performed using different specific pinhole matrix arrangement which created by DMD. In this method, there are no requirements for both axial and lateral scanning; therefore, the developed system can improve in both measurement speed and quality. Before, to omit one scanning direction in confocal microscope, we always need to stick with complex setup of differential confocal microscope or specific spectrometer in chromatic confocal microscope. In our method, we just based on simple optical configuration with a 12-bit mono CCD. With this approach, confocal microscope system can be optimistic for *in-situ* surface measurement because of quasi one-shot full-field capability.

To achieve the above-mentioned approach, this article proposes one novel optical configuration of confocal microscopy using DMD. The configuration uses digital micro-mirror device (DMD; Texas Instruments, Dallas, Tex.) as spatial light modulator in confocal microscope configuration with white-light light source. A white-light light source beam is collimated by lens L1 to illuminate the DMD. The reflected light from DMD is collimated again using tube lens L2 and imaged on the object plane of the objective. The mirror (or test sample) is placed perpendicular to optical axial of objective, so reflected light from the mirror go through objective again and is imaged on to high speed 12-bit CCD camera by tube lens L2 and beam splitter BS. In order to make optical configuration simple and flexible as much as possible, the configuration employed illumination only mode of Programmable Array Scanning Confocal Microscope configuration, where the pixels of DMD are used to restrict the light projected onto the surface while the optical sectioning is achieved by the use of the pixels of a CCD camera.

doi: 10.6342/NTU201601083

Each element of the micro-display corresponds to pixels on CCD camera. None the light from out-of-focus regions falls on neighboring pixels is taken into account. The system applies virtual pinhole configuration to remain high sectioning capability with a robust setup. To build database of diffraction patterns, the reference mirror is moved by piezoelectric stage. The diagram of optical system setup is described in Figure 28.

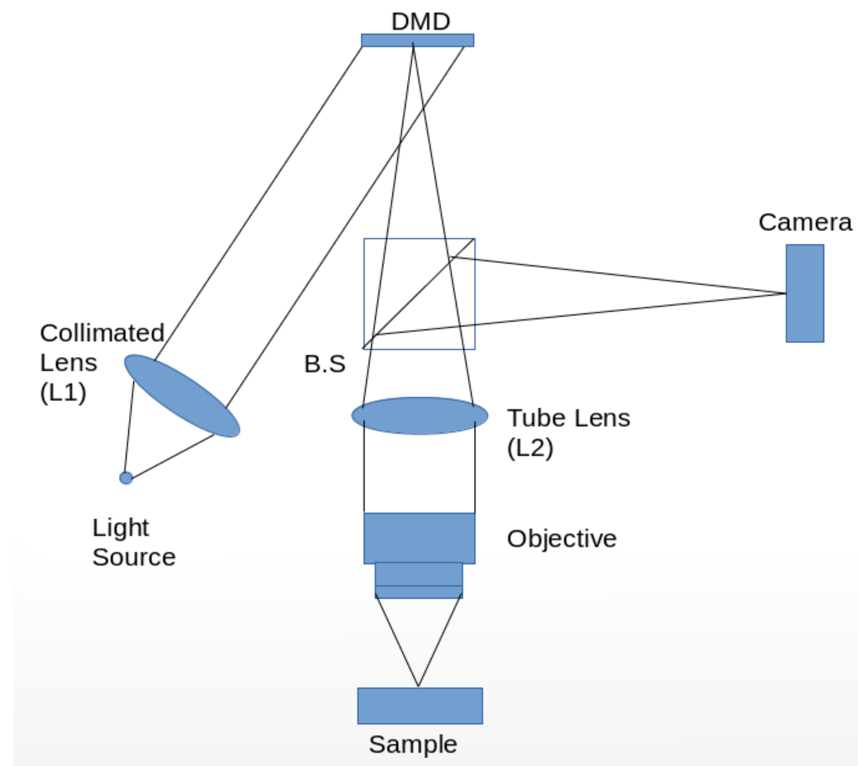

Figure 28 Diagram of optical system setup for digital diffractive-confocal imaging correlation microscope.

3.3.1 Pinhole's diffraction pattern

In digital diffractive-confocal imaging correlation microscope, those micro-mirrors of the DMD are used as square micro-pinholes and as square aperture, which can create diffraction patterns needed for encoding and decoding depth information. In this configuration, the light from point light source is collimated by lens L1, and then hit to DMD. Those micro-mirrors of the DMD act as square aperture, distance from DMD to sample are rather large compared to the size of square aperture, so the diffraction patterns created by DMD micro-mirrors need to follow Fraunhofer diffraction theory.

To understand the principle of calculation of the Fraunhofer diffraction from a simple rectangular aperture, let us consider Figure 29.

doi: 10.6342/NTU201601083

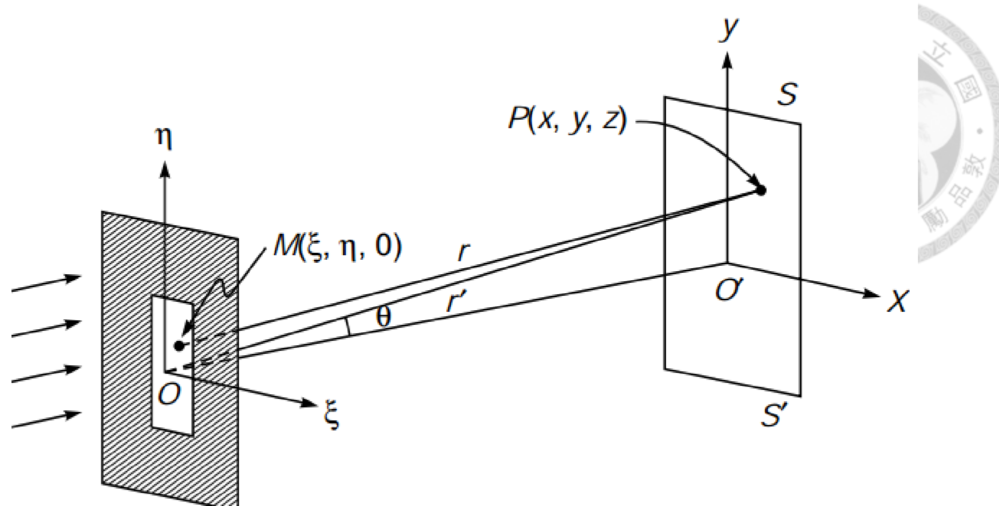

Figure 29 Fraunhofer diffraction from a rectangular aperture

The Fraunhofer diffraction of a plane wave incident normally on such a rectangular aperture will be given by

$$u(x,y,z)=\frac{A}{i\lambda z}e^{ikz}\exp\left[\frac{ik}{2z}(x^2+y^2)\right]\times\int_{-b/2}^{+b/2}e^{-iu\xi}d\xi\int_{-a/2}^{+a/2}e^{-iv\eta}d\eta \tag{12}$$

where we have chosen the origin to be at the center of the rectangular aperture (see Figure 29). Carrying out the integration, we obtain

$$u(x,y,z)=\frac{A}{i\lambda z}e^{ikz}\exp\left[\frac{ik}{2z}(x^2+y^2)\right]\left(\frac{\sin\beta}{\beta}\right)\left(\frac{\sin\gamma}{\gamma}\right) \tag{13}$$

where β is given by

$$\beta=\frac{ub}{2}=\frac{\pi bx}{\lambda z}\approx\frac{\pi b\sin\theta}{\lambda} \tag{14}$$

and γ is given by

$$\gamma=\frac{va}{2}=\frac{\pi ay}{\lambda z}\approx\frac{\pi a\sin\phi}{\lambda} \tag{15}$$

where ϕ represents the angle of diffraction along the y direction.

Thus, we may write for the intensity distribution

doi: 10.6342/NTU201601083

$$I(P) = I_0 \frac{\sin^2 \beta}{\beta} \frac{\sin^2 \gamma}{\gamma} \quad (16)$$

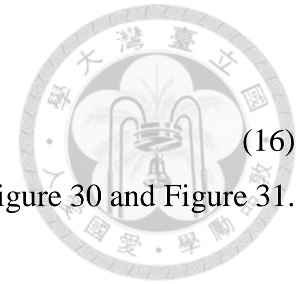

The diffraction pattern for square pinhole is illustrated by Figure 30 and Figure 31.

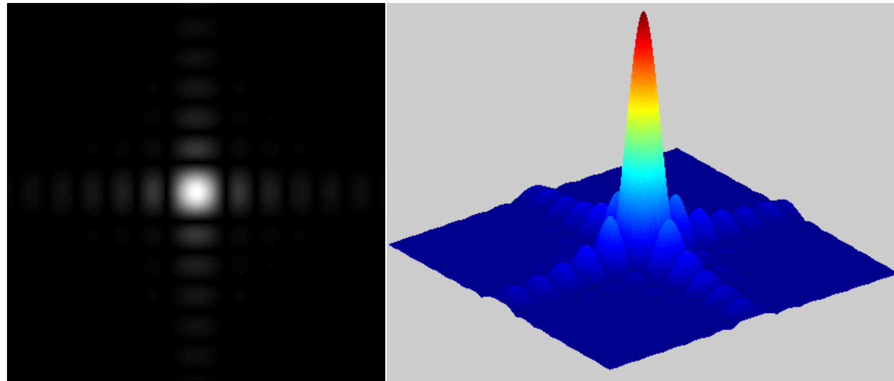

Figure 30 2-D and 3-D visualization for Fraunhofer pattern of a square aperture (computer generated)

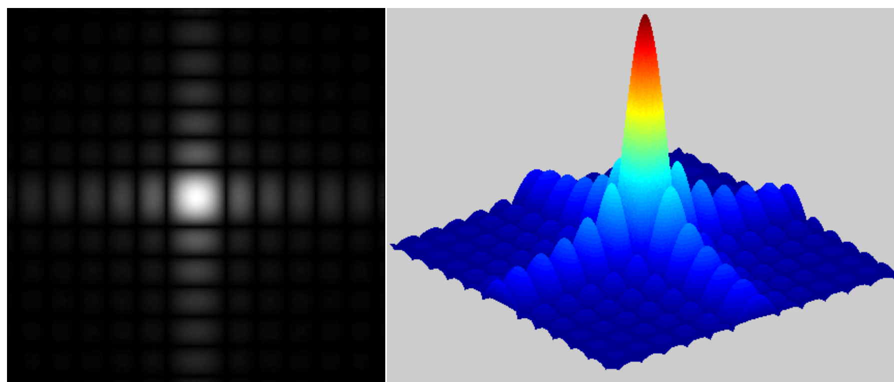

Figure 31 2-D and 3-D visualization of the same pattern but with increased exposure time to bring out some of the faint terms (computer generated)

For far field diffraction, when the distance between aperture and screen is increased, the diffraction pattern will become larger and less contrasted but it tends to keep the same pattern. However, by applying confocal microscope setup, with in- and out-focus effect the diffraction pattern we see on camera will change when the distance between sample and objective is increased or decreased. Therefore, with each depth position, we will have the corresponding imaged diffraction pattern. This will be signature pattern for this depth and can be used for depth encoding and decoding process.

In our application, because of light intensity, these pinholes created from DMD micro-mirrors consist of four micro-mirrors arranged in symmetric configuration as

doi: 10.6342/NTU201601083

showed in Figure 32. The diffraction pattern generated by this configuration is different from a simple single rectangular aperture. The diffraction pattern will be superposition of four Fraunhofer diffraction patterns from four square micro-mirrors.

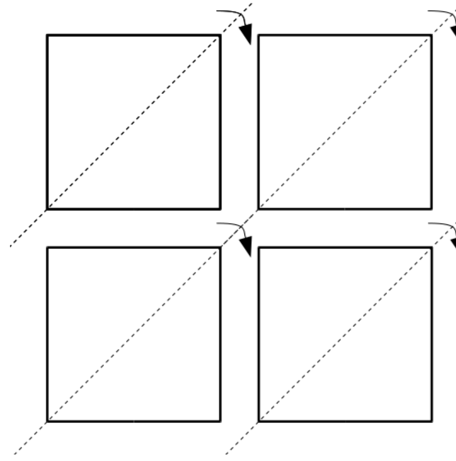

Figure 32 Pinhole's configuration

3.3.2 Confocal effect

In the traditional confocal principle, pinholes are used to eliminate stray light get into optical system, also to prevent cross-talk effect between adjacent measuring points and between adjacent detecting sensors. When the object locates on the focal plane of a confocal layout, the reflected light from the object's surface can pass through a pinhole and reach to the detector with a maximum light intensity. For the traditional confocal microscope, a vertical scanning process is required to generate a depth response curve of the light intensity. The light intensity being detected in the above conjugative optical configuration can be represented by Eq. (17).

$$I(u) = \left[\frac{\sin(u/2)}{(u/2)} \right]^2 \tag{17}$$

where

$$u \approx \frac{8\pi}{\lambda} z \sin^2(\frac{\alpha_0}{2})$$

where λ is the wave - length of the light source; z is the vertical distance; and $\sin\alpha_0$ is the numerical aperture.

doi: 10.6342/NTU201601083

In the developed system, these pinholes created by controlling micro-mirrors on DMD are used to form one-to-one conjugate relation between each incident light and its corresponding detecting pixels. The conjugate relation will help to avoid the cross-talk problem in the full-field measurement. The DMD will be loaded with a specific pinhole array pattern, which is designed to spatially filter unfocused light and other possible stray lights away from the corresponding detecting sensor, thereby minimizing the lateral cross-talk between the detected image sensors.

When one lens is used for both objective and imaging lens, the light intensity function of acquired signals can be described as follows.

$$I(u,v) = \left| 2\int_0^1 P(\rho) e^{(ju\rho^2/2)} J_0(\rho v)\rho d\rho \right|^4 \tag{18}$$

where $P(\rho)$ denotes the pupil function of objective; J_0 is the zero-order Bessel function, u and v are the normalized optical radii.

$$v \approx \frac{2\pi}{\lambda} r \sin\alpha_0 \qquad u \approx \frac{8\pi}{\lambda} z \sin^2(\frac{\alpha_0}{2}) \tag{19}$$

Furthermore, this configuration will cause the change of diffraction pattern when the incident light goes through the objective, hits with measuring sample's surface or reference mirror's surface, then reflects back and finally is imaged on the camera's sensor. Based on this principle, we can replace the intensity-depth response curve by using normalized cross correlation-depth response curve and achieve a quasi one-shot full-field confocal microscope system. First, the specific pinhole array will be loaded into DMD, and then a reference mirror used to build a reference database. Vertical scanning calibration procedure was performed by using PZT. At each step – each vertical position, the 12-bit mono camera will take one corresponding picture. When measuring a sample, we just need to take one picture, and with the help of multiple pinholes array configuration generated by controlling DMD, we can achieve full-field measurement with one picture imaging. With the reference database being established, we can do special searching algorithm to find the best focus imaged position, size and location of each pinhole on the database images. The sample result of this step is showed in Figure 33. Because of in- and out-focus effect of the confocal configuration, each diffraction pattern of each pinhole is unique for each step height and can be used as a signature identifier for this

doi: 10.6342/NTU201601083

corresponding step. The change of diffraction pattern by in- and out-focus of confocal microscope setup is showed in Figure 34.

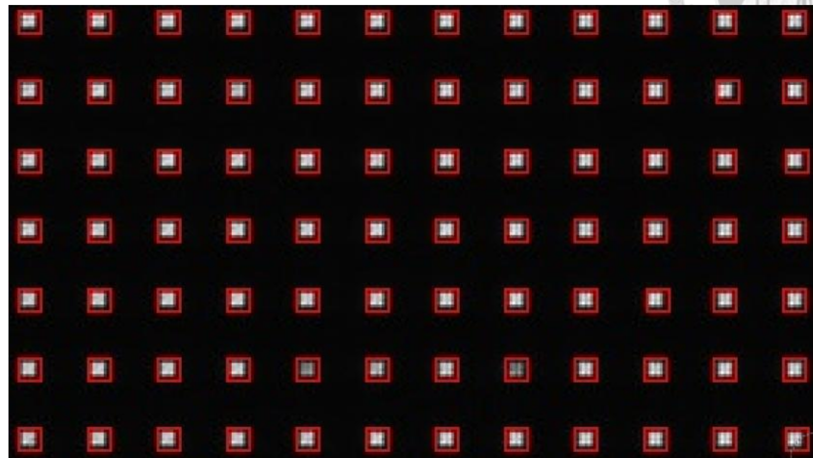

Figure 33 Result generated by using auto-locating pinholes algorithm.

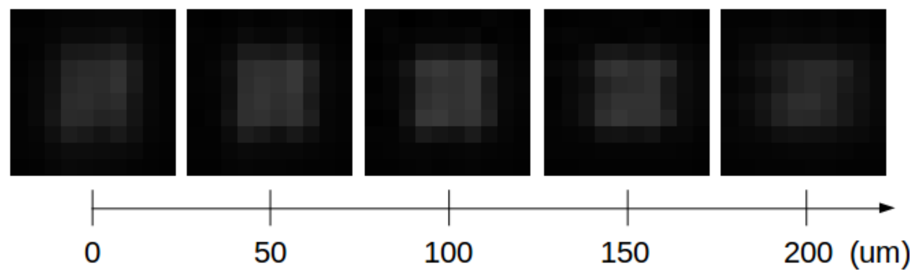

Figure 34 Diffraction pattern change by in- and out-focus effect of confocal configuration.

With this process, each pinhole will have an array of sub-image being contained with diffraction patterns corresponding with step heights.

When measuring a sample, the camera just needs to take only one shot and based on pinhole's locations which can get from the last step, the sub-image contain diffraction patterns of those pinholes can be extracted. The extracted sub-images can be used to calculate the normalized cross correlation value based on the reference sub-images array of each pinhole by the Eq. (20).

$$N.C.C = \frac{\sum_{x,y}(I(x,y)\cdot R(x,y))}{\sqrt{\sum_{x,y} I(x,y)^2 \cdot \sum_{x,y} R(x,y)^2}}$$

doi: 10.6342/NTU201601083

(20)

Therefore, each pinhole as well as each measurement point will have its own normalized cross correlation–depth response curve, illustrated in Figure 35. When the normalized cross correlation factor reaches to peak, this means the diffraction pattern of measuring point is identical with the diffraction pattern of reference point at this specific step. From that, we can convert the normalized cross correlation factor to depth information.

For the previous confocal microscope, an important factor affecting mesurement results is light intensity variation caused by undesired light source's power fluctuating and reflectivity variation of sample's surface. In our system, those disturbances can occur in both reference database image and measured image. In here, we assume that our light spot is small enough, so in this area, the sample's surface has uniform reflectivity. Therefore, those two disturbances can be modelled as one multiplicative mode disturbance n in Eq. (21); n_I is disturbance in measured image and n_R is disturbance in references database image. Eq. (21) will make our system immune to light intensity and surface reflectivity variations. This method can be practical to the object surface having a different absorb rate of optics from point to point.

$$N.C.C = \frac{\sum_{x,y}(n_I \cdot I(x,y) \cdot n_R \cdot R(x,y))}{\sqrt{\sum_{x,y}\left[n_I \cdot I(x,y)\right]^2 \cdot \sum_{x,y}\left[n_R \cdot R(x,y)\right]^2}}$$
$$= \frac{n_I \cdot n_R \cdot \sum_{x,y}(I(x,y) \cdot R(x,y))}{n_I \cdot n_R \cdot \sqrt{\sum_{x,y} I(x,y)^2 \cdot \sum_{x,y} R(x,y)^2}}$$
$$= \frac{\sum_{x,y}(I(x,y) \cdot R(x,y))}{\sqrt{\sum_{x,y} I(x,y)^2 \cdot \sum_{x,y} R(x,y)^2}}$$

(21)

where x, y are coordinate of pixels, I is intensity one measured image and R is the intensity in diffraction pattern database images.

doi: 10.6342/NTU201601083

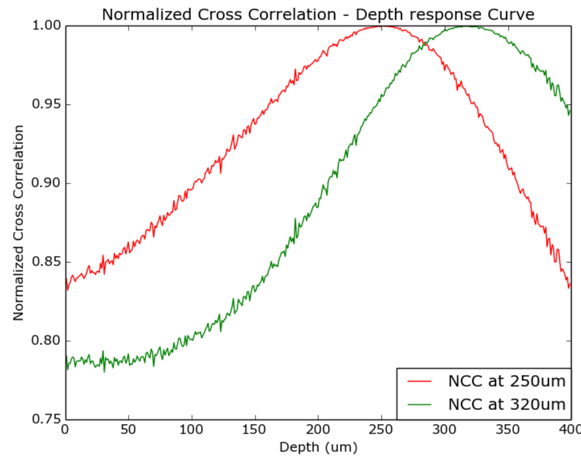

Figure 35 Normalized cross correlation – depth response curve

3.3.3 Pinhole auto-locate algorithm

In our system with the purpose to increase measurement flexibility of the system, we need to create an adaptive algorithm to find pinhole locations whenever we change virtual pinhole arrangement on DMD for different measuring samples. As described above, after archiving the reference database, we can do special searching algorithm to find best focus imaged position, size and location of each pinhole on the database images. The follow chart of this algorithm is illustrated in Figure 36.

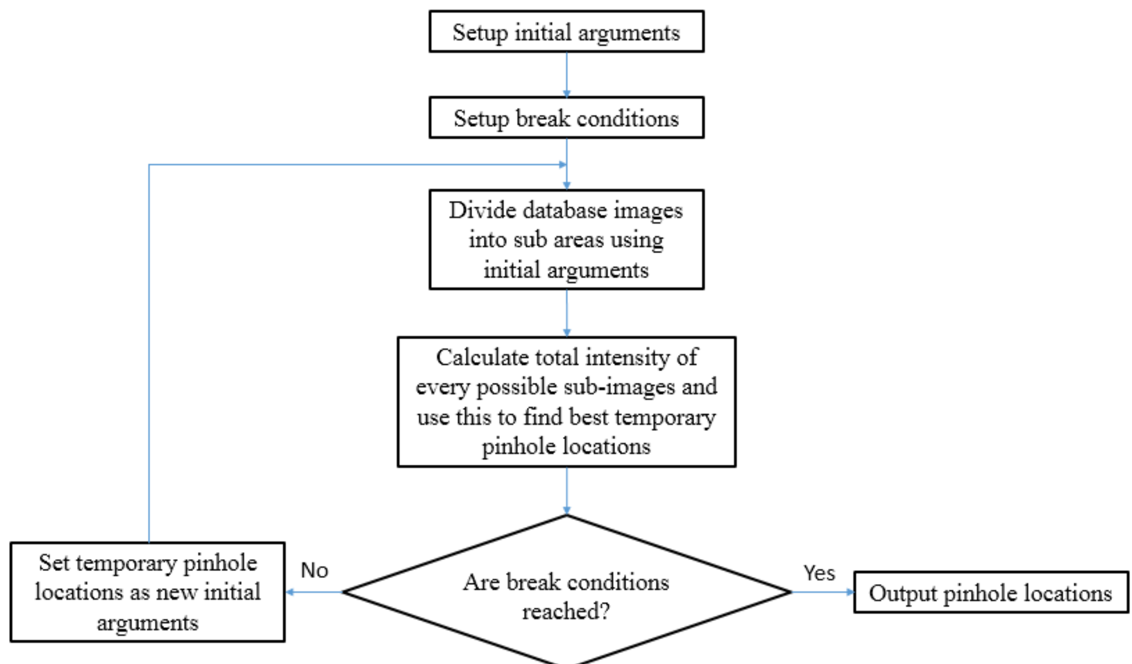

Figure 36 Flow chart of auto-locate pinhole algorithms

doi: 10.6342/NTU201601083

First, we need to setup initial arguments, which are temporary location of the first pinhole, the temporary distance between two neighboring pinholes, the size of pinhole and the size of database images. After that, we need to input the stop (break) conditions for our algorithms. In this algorithm, we can have two break conditions, where the first one is the loop time and the second one is the distance between the temporary location and the new found location. Following all initial setups, the database images will be divided into sub-areas; in each sub-area, we perform a specific function to calculate the total intensity of every possible sub-image in this sub-area by Eq. (22).

$$I_t = \sum_{x,y} I(x, y) \tag{22}$$

After that, the location of sub-image with maximum total intensity in each sub-area will be selected as the new temporary pinhole location and be used as new arguments for the next loop. When loop break condition or distance break condition is reached, the algorithm will output all pinhole's location as a list.

3.4 Digital diffractive-confocal imaging correlation microscope goes chromatic

Measurement range of digital diffractive-confocal imaging correlation microscope heavily depends on the depth of focus of objective. If we use the objective with high NA (this means a better signal and measuring slope), the depth of focus will be reduced, so the measurement range will be reduced. In order to improve the measurement range for high NA with a high magnification objective, we need to modify our system into a normalized cross correlation chromatic confocal microscope. In this system, we just replace conventional objective by chromatic objective and replace the mono camera by a color camera. The basic setup of the new system is illustrated in Figure 37.

doi: 10.6342/NTU201601083

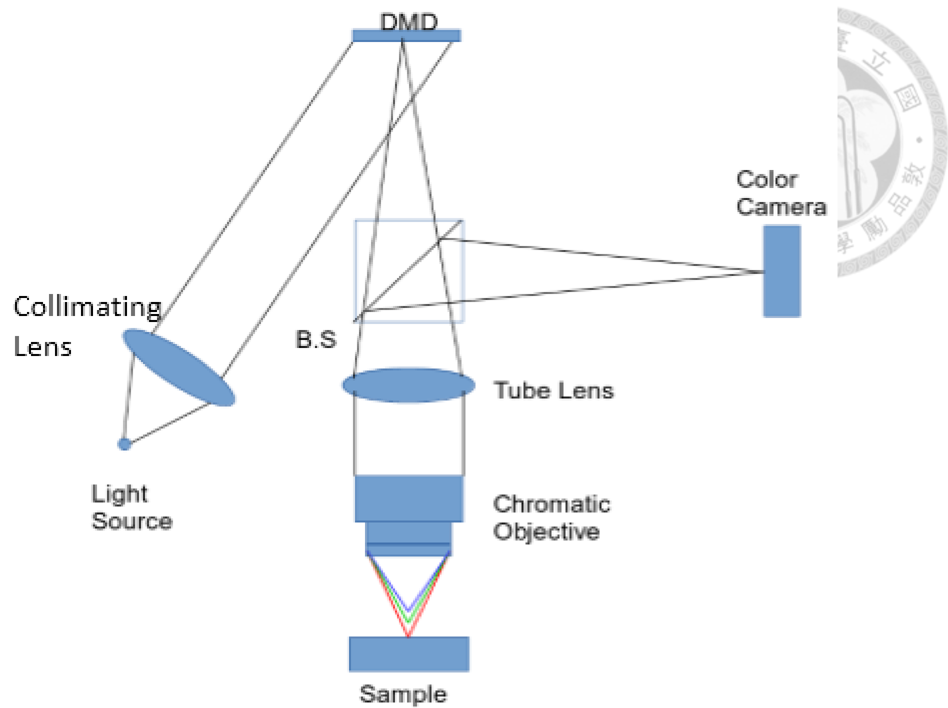

Figure 37 Digital diffractive-confocal imaging correlation chromatic microscope

In order to maintain quasi one-shot full-field capability of our system, we decide to use color camera instead of any specific spectrometer. On the other hand, when we use a chromatic objective, each wavelength has a different focus position as well as a different depth of focus. Therefore, if we use a sensing device with much larger spectrum, the diffraction pattern can be the same for different wavelengths at some positions. In this case, we cannot detect the right peak, neither achieve the right depth (or height information) of the measured surface.

Therefore, in our modified system, we use a color camera, which means we just focus on three different bands: red, green and blue. To get the best from this configuration, we need to choose a suitable chromatic objective with a suitable dispersion range as shown in Figure 38.

doi: 10.6342/NTU201601083

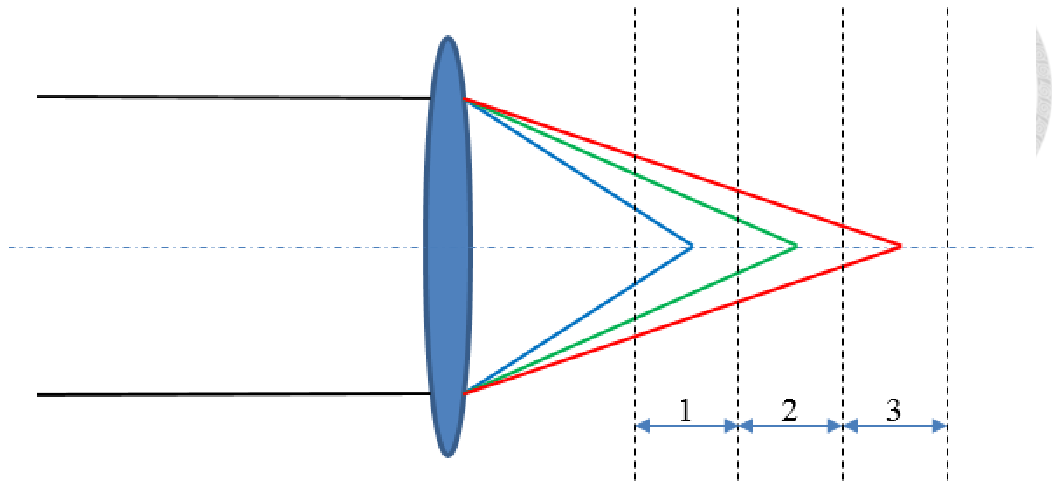

Figure 38 Improve measurement range effect of chromatic objective

We can see that the focus positions for those three wavelengths are separated, so the focus ranges will not overlap. By this way, we can find an appropriate position to stitch the RGB different measurement ranges.

For a color camera, every pixel is covered by Bayer filter in specific arrangement as described in Figure 39. Using color cameras, we will have four different diffraction patterns for depth mapping corresponding to three wavelengths. In different measurement range, we will find the most suitable one from the RGB color-band spectrum sensor and can rely mainly on this to calculate the measured depth from the reference diffraction pattern database.

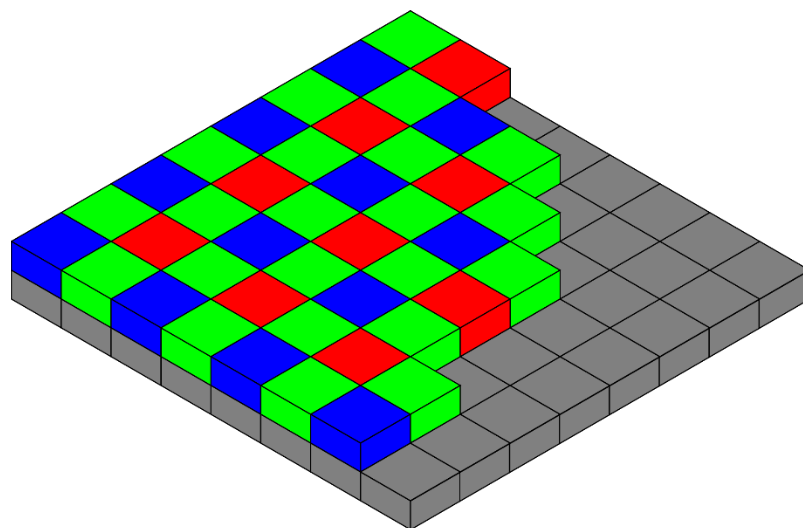

Figure 39. Bayer filter for color camera

doi: 10.6342/NTU201601083

3.5 Chromatic confocal system including spectral area camera

3.5.1 Chromatic confocal microscope

3.5.1.1 Chromatic dispersion

Chromatism is a physical property, which indicates refractive index of isotropic media, such as water, glass, or air depends on wavelength of the incident light. Based on Snell's law:

$$\frac{\sin\theta_1}{\sin\theta_2} = \frac{\lambda_1}{\lambda_2} = \frac{n_2}{n_1}$$

(23)

Based on this equation, when a broadband light source coming in to a lens or a system of lens (optical objective) the lights with different wavelength will be bent with different angles.

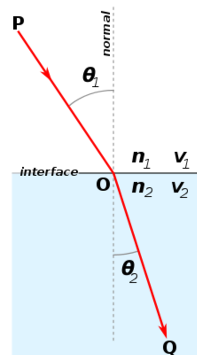

Figure 40 Refraction occur between 2 isotropic media

In a chromatic confocal microscope, we can employ the chromatism physical property of chromatic objective or different chromatic elements as a space-coding method. Employing axial chromatic dispersion, each wavelength in broadband light will be focused in different position on optical axis. The relationship between wavelength and focus position on optical axis could be used to find the sample surface's height when it is in the focus range.

doi: 10.6342/NTU201601083

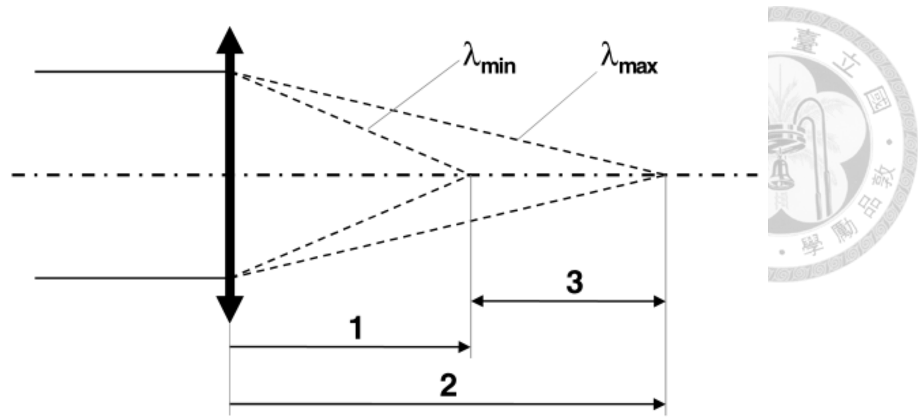

Figure 41 Axial chromatic dispersion: each wavelength is focused at a different point along the optical axis

As described in Figure 41, short wavelengths will focus closer to the objective than long wavelengths. The measurement range of chromatic confocal system is equal to the dispersion range, which is defined by the distance between the focal points of shortest wavelength and the longest wavelength,

$$\text{dispersion range} = \text{focal distance}(\lambda max) - \text{focal distance}(\lambda min) \tag{24}$$

In chromatic confocal system, vertical scanning just needs to be performed one time to build the calibration curve, which shows the relation between wavelengths and focus position on the scanning optical axis.

3.5.1.2 Basic setup

Basic configuration for point-scan chromatic confocal microscope is shown as Figure 42.

doi: 10.6342/NTU201601083

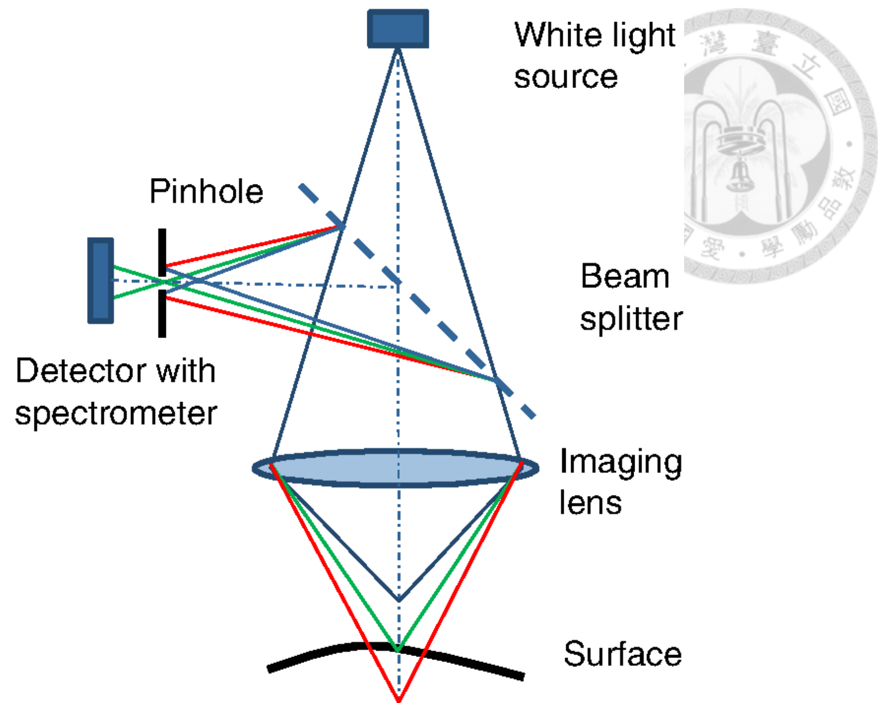

Figure 42 Basic configuration of point-scan chromatic confocal microscope

The configuration is almost identical with point-scan confocal microscope, except we change from the CCD to a spectrometer and the microscopic objective is replaced by a chromatic objective.

3.5.1.3 Spectral encoding and decoding

As shown in Figure 42, the light source is a point light source. The light source is focused onto the sample surface by an imaging lens. The reflected light then goes back through the same imaging lens, then passes through pinhole and forms an image on the detector of spectrometer. With chromatic dispersion, different wavelengths in the white light can be focused at different positions along the optical axis; therefore, a single wavelength is in focus on the surface with a specific depth. By this way, there are only one wavelength to be peaked in spectrum response curve. By detecting this specific wavelength and using a calibration curve to calculate the corresponding focus position, the height of the measured surface can be detected.

The detector pinhole will ideally block all out of focus wavelengths, so those wavelengths will not generate any intensity on the detector. Only the focused wavelength, which can pass through the detector pinhole, can generate an intensity peak. The spectrum response curve has the shape like shown in Figure 43.

doi: 10.6342/NTU201601083

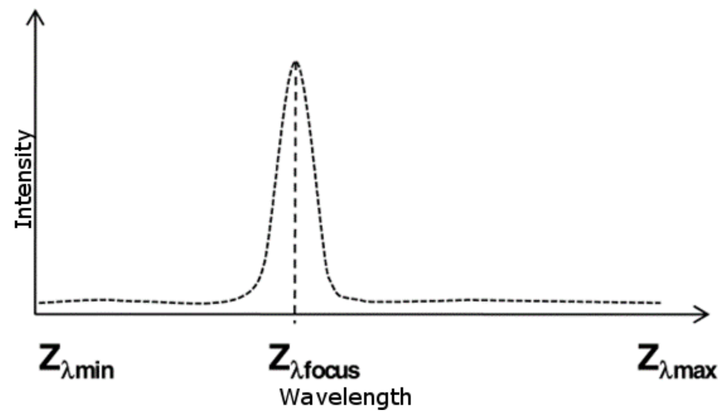

Figure 43 Intensity curve registered by the spectrometer

Working principle of chromatic confocal are based on the following two main processes: spectral encoding and spectral decoding. First, for the spectral encoding process, we need to build a calibration curve by using a vertical scanning mechanism by moving a referent plane (mirror) through the measurement range of the employing chromatic objective. For each step, we will get a spectrum response curse as described in Figure 43. By detecting the maximum intensity, the focused wavelength can be located. Based on the calibration curve being achieved by performing vertical scanning in calibration step, the surface height can be calculated. There are many different methods capable of finding the intensity peak such as interpolation, center of mass or curve fitting. Those methods can provide high accuracy and sub-pixel detection but requires higher computational resources. After performing spectral encoding process, we can build a calibration curve as shown in Figure 44. From a raw data curve, we can calculate the fitting curve for conventional computation. However, the look-up-table method is more adequate to the developed method since the calibration curve is not quite linear.

doi: 10.6342/NTU201601083

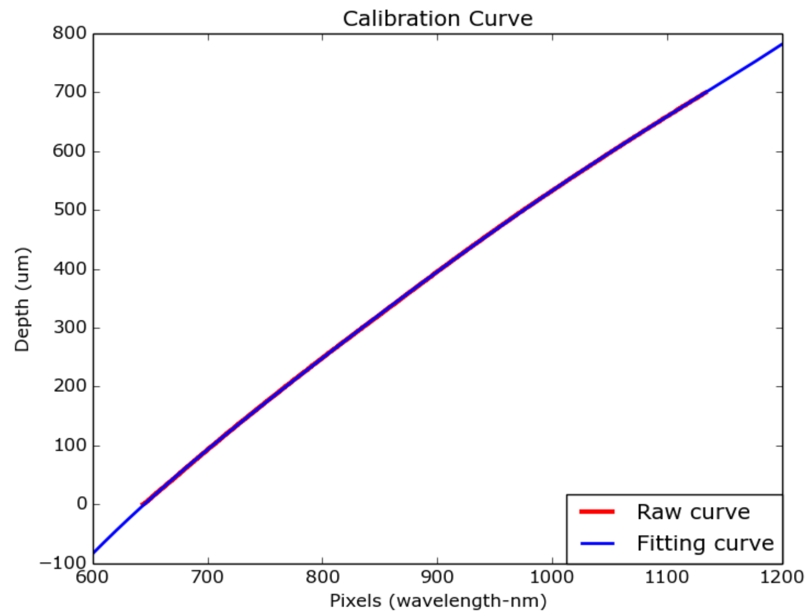

Figure 44 Chromatic confocal calibration curve

For height detection, we propose a reverse process, in which the spectral decoding is performed. To generate surface profile or surface 3-D topography, we can use mechanical (PZT or servo stages) or optical (Nipkow Disk or DMD) devices for lateral scanning to scan a line or an area on object's surface. For each measuring point on object's surface, we can obtain the corresponding spectrum response curve. Applying the same peak detection algorithm, we use on spectrum encoding process, so the wavelength with maximum intensity respected to the point cab be detected. Using calibration curve and the look up table method as well as the curve fitting, we can convert wavelength information into the height of object's measured surface point.

3.5.2 Spectral area camera

Spectral imaging technology can provide both spatial and spectral information from an object. It is widely used in the biomedical engineering field as a powerful analytical tool for biological and biomedical research. For further development spectral imaging is used in optical inspection system, in order to get more meaningful data from measuring sample. In literature review section, spectral imaging is used in chromatic confocal microscope system.

Spectral data cube is the concept helping to understand how spectral data can be represented with the corresponding spatial data. The data cube contains two spatial

doi: 10.6342/NTU201601083

dimensions (x and y) and one spectral dimension, in which the cube face is a function of the spatial coordinates and the depth, is a function of wavelength (Figure 45).

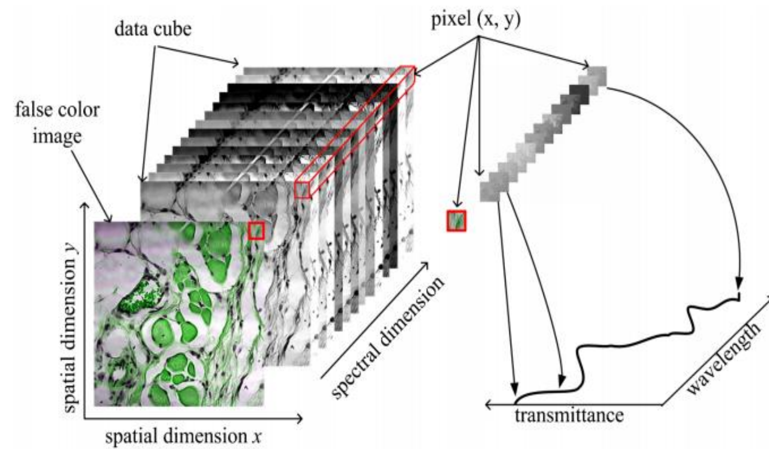

Figure 45 Spectral Data Cube [15]

Based on spectral information gathering mechanism, imaging methods can be divided in point-scan (Whiskbroom), line-scan (Pushbroom), and area-scan. Area-scan methods consist of staring and snapshot. All of the methods are illustrated in Figure 46.

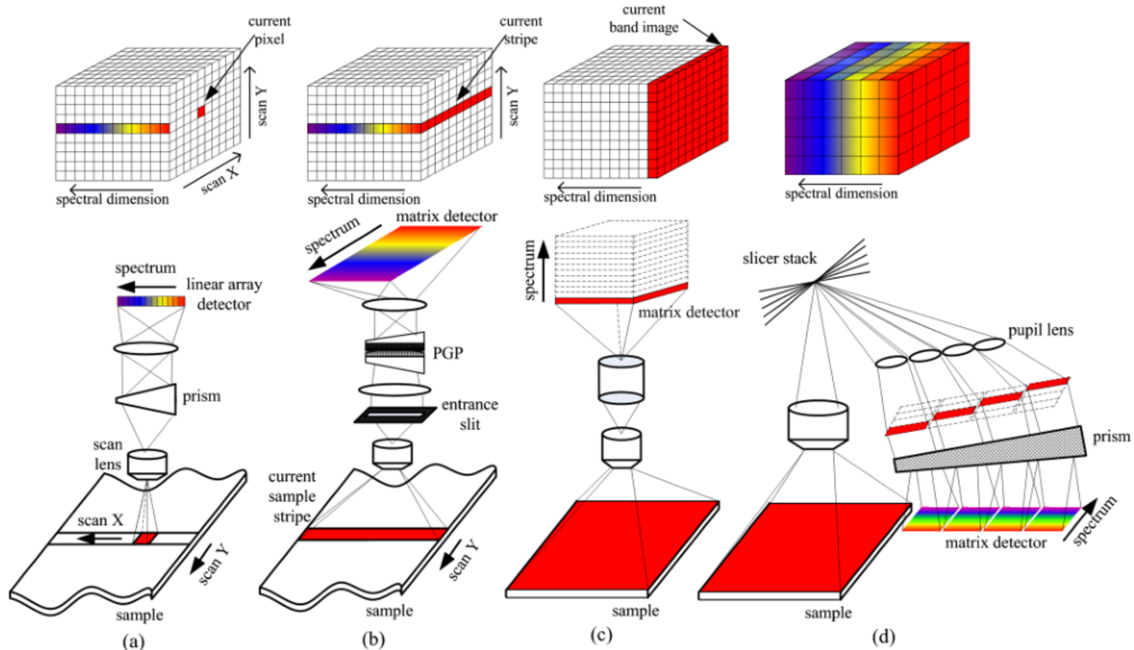

Figure 46 Typical spectral imaging approaches. (a) Whiskbroom. (b) Pushbroom. (c) Staring. (d) Snapshot [15]

doi: 10.6342/NTU201601083

Because our research objective is to develop an area-scan chromatic confocal microscopy, so staring and snapshot are more adequate for our development. Staring method uses a spectral filter to take 2-D image in one wavelength at a given time while the image cube is filled by tuning the output wavelength of the filter as a function of time. On the other hand, the snapshot method can be considered as a single-shot method, which relies on an array of pupil lenses acting as optical duplicators and prisms, in which a complete spectral data cube can be acquired in a single integration by directly imaging the remapped and dispersed image zones onto a CCD detector simultaneously.

However, the staring method has limited spectral bands (3 to 10) and the snapshot method is complex with a system of optical duplicator. These two methods are not appropriate for our system. Our developed system is designed to be compact and flexible. If this is chieved, the developed prototype can be easily integrated into available product line.

Fortunately, one of the possible solutions comes from the IMEC new spectral area camera. Appling Fabry Perot effect to select specific wavelength by varying cavity length, IMEC created a new spectral area camera with the integrated Fabry Perot Filters stick right at standard image sensor's surface, shown in Figure 48.

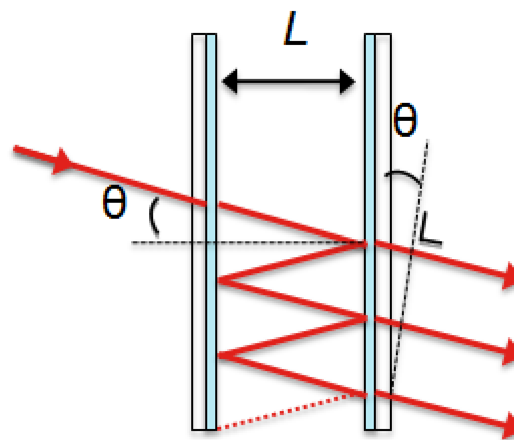

Figure 47 Fabry Perot effect

doi: 10.6342/NTU201601083

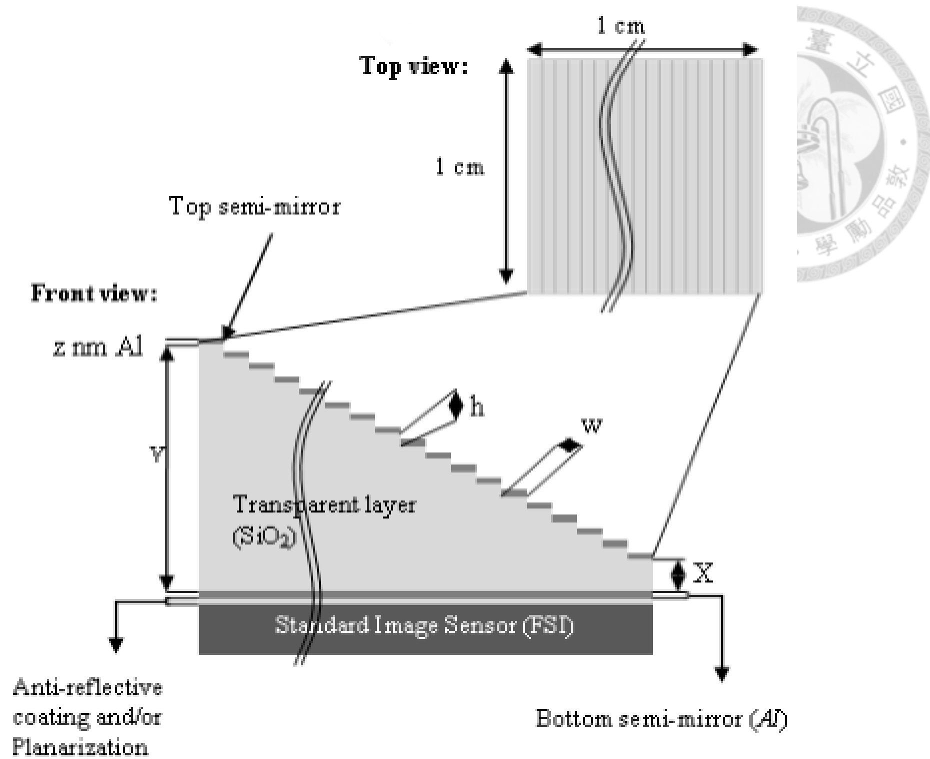

Figure 48 Fabry Perot filters

For area-scanning, IMEC has one special module: IMEC Mosaic spectral area camera, in which its structure is illustrated in Figure 49.

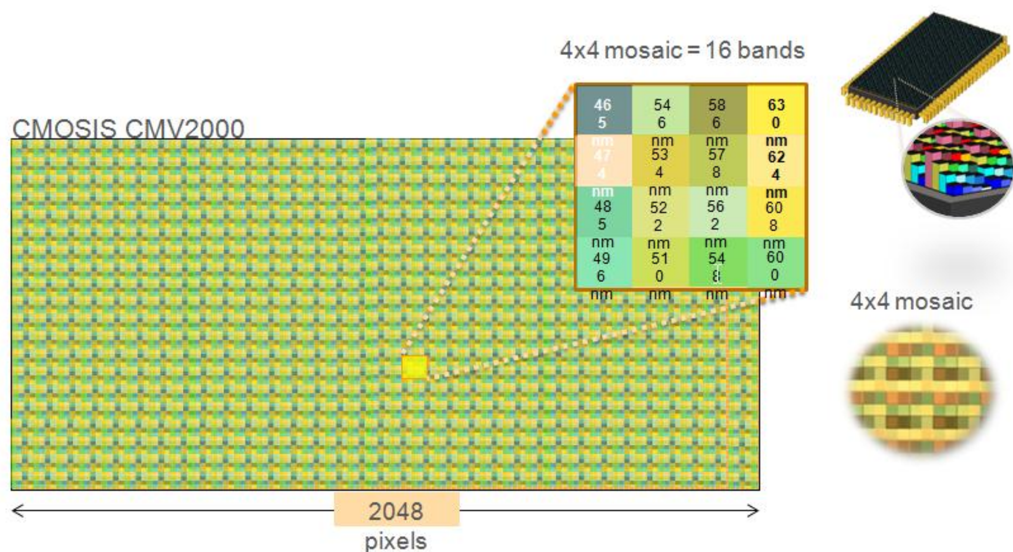

Figure 49. IMEC Mosaic spectral area camera

Mosaic spectral area camera's key specifications:

doi: 10.6342/NTU201601083

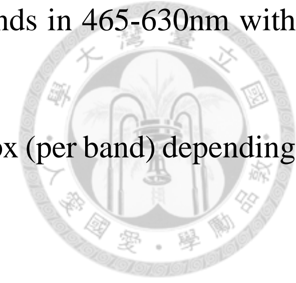

1. **Spectral resolution**: 4x4 mosaic (1filter / pixel) = 16 bands in 465-630nm with ~11nm incremental steps
2. **FWHM**: ~15nm
3. **Spatial resolution**: from 512x272 (per band) → up to 2Mpx (per band) depending on de-mosaicing algorithm
4. **Speed**: up to 340 data-cubes / s (max sensor limit)

Although the spatial resolution is reduced because each Mosaic pixel needs 16 sub-pixels for 16 spectral bands and the number of spectral bands is limited. However, we can still increase the depth discrimination by using an interpolation algorithm.

3.5.3 Chromatic confocal system included spectral area camera working principle

In order to achieve quasi one-shot full-field chromatic confocal profilometry, a DMD-based chromatic confocal method needs to be developed. By using DMD and chromatic confocal principle, we can enhance the measurement efficiency by completely removing the need in lateral and vertical scanning. The potential cross-talk problem, which usually appeared in line-scan or area-scan microscopy, will be solved by specially designed DMD scanning process. A digital micro-mirror device (DMD) can be deployed as an array of pinholes for confocal lateral scanning.

In this research, DMD can be deployed as an array of pinholes for confocal lateral scanning. These pinholes both control the point-spot illumination light and reflected light. The FWHM of the depth response curve will be significantly sharpened, thus improving the vertical measurement resolution and repeatability of the depth detection. Using the IMEC Mosaic spectral area camera can make our developed system to be more compact and flexible. However, limited number of spectral bands (16 bands) and sensor pixel may reduce spatial resolution and optical sectioning capacity of the system. To overcome this, spectrum response curve of measuring point and spectrum response curves in reference database are matched by NCC principle. By this way, the measurement range and depth resolution can be increased. Basic structure of the developed system is illustrated in Figure 50.

doi: 10.6342/NTU201601083

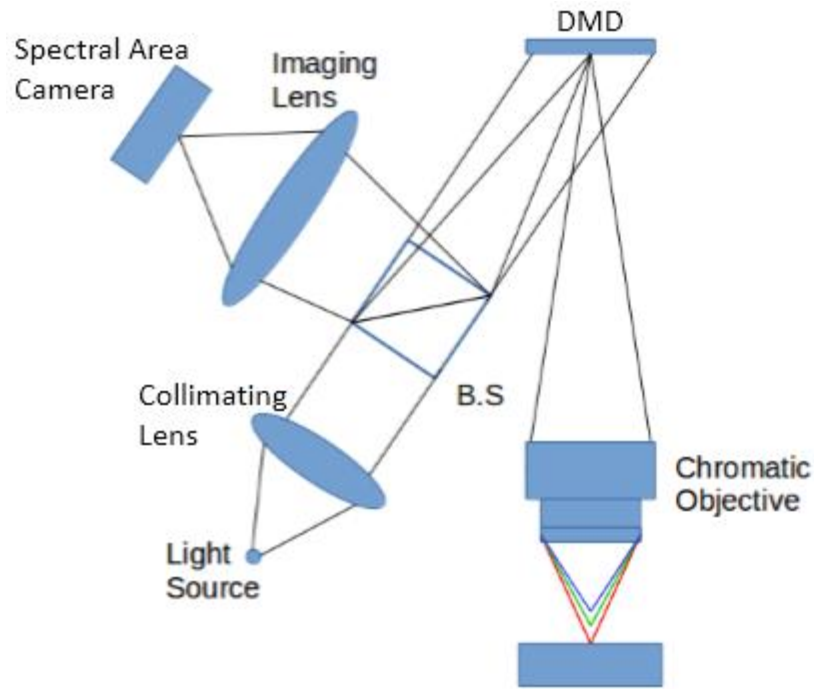

Figure 50 Quasi one-shot full-field chromatic confocal microscope

3.5.4 Alternative configurations

In first setup, just only one tube lens is used for both collimating light and forming image on camera's sensor Figure 51. This is the simplest setup, which requires matching DMD size and camera sensor size. On the other hand, in Figure 52 collimated lens is used for collimating light and tube lens is used for forming image on camera sensor. In this manner, we can easily change the image size to fit with the camera sensor size.

doi: 10.6342/NTU201601083

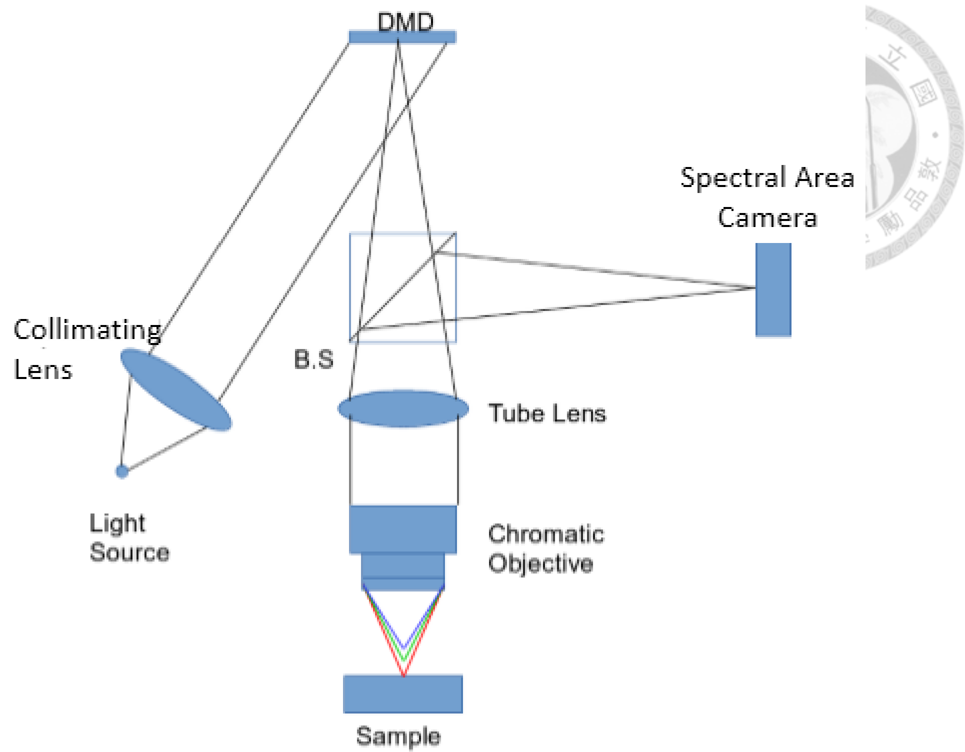

Figure 51 Revised configuration for quasi one-shot full-field chromatic confocal microscope (illumination mode – configuration 1: O-I confocal structure)

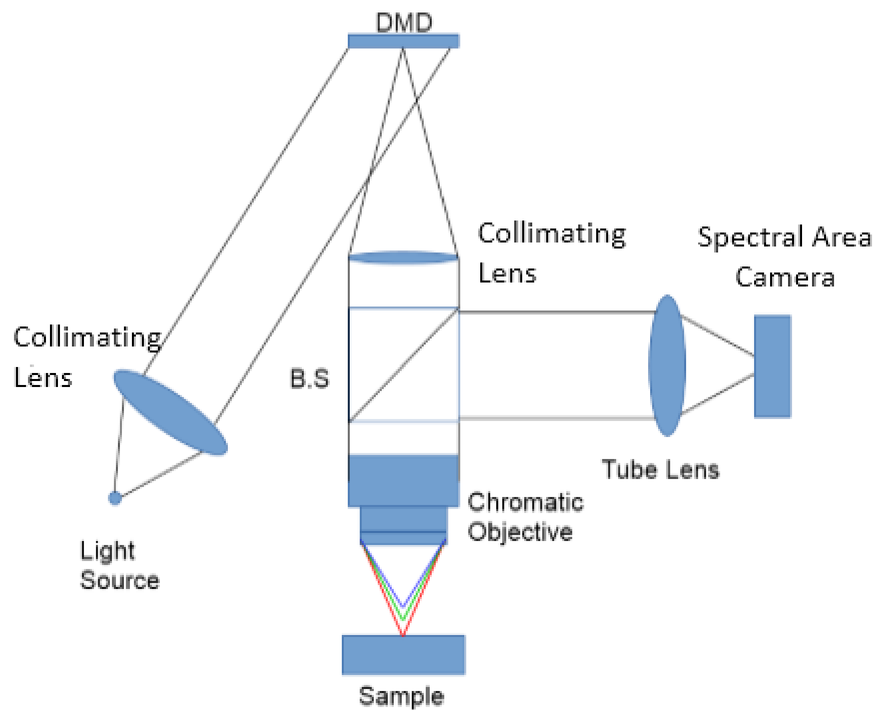

Figure 52 Revised configuration for quasi one-shot full-field chromatic confocal microscope (illumination mode – configuration 2: Infinitive confocal structure)

doi: 10.6342/NTU201601083

In both configurations for Figure 51 and Figure 52, the lights just go through DMD one time, so those pinholes created by DMD just have effect on illumination side. In contrast, in Figure 53, the light go through DMD twice, so the pinholes created by DMD have double light narrowing effect on both detection and illumination sides. The configuration can effectively increase confocal effect for increasing sectioning capability (axial resolution) of the measuring system. However, the setup in Figure 53 is much more complicated and need many efforts for optical alignment.

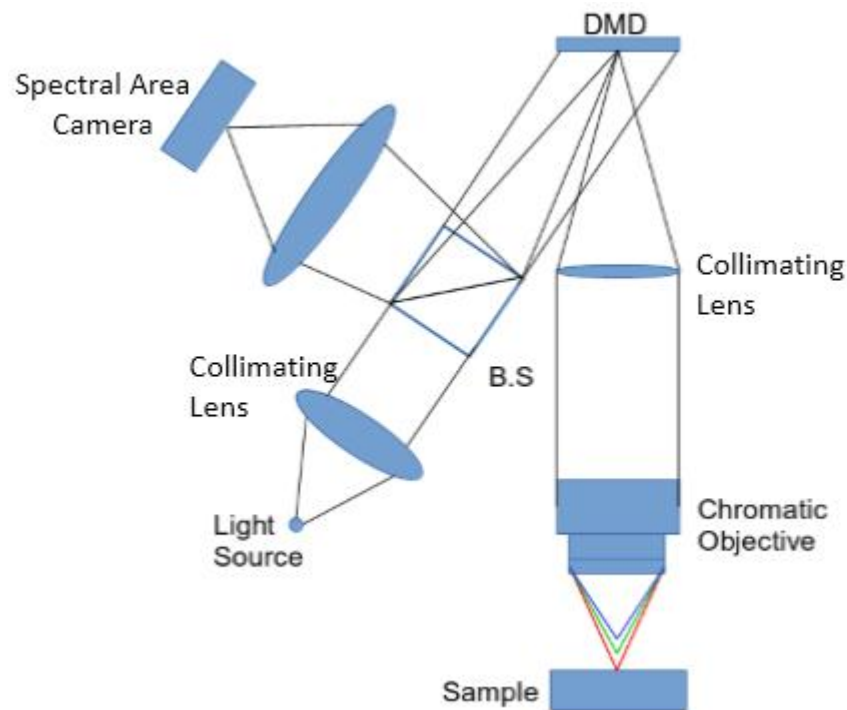

Figure 53 Revised configuration for quasi one-shot full-field chromatic confocal microscope (illumination and detection mode) with double light narrowing effect.

3.5.5 Efficient of the new DMD arrangement

In the traditional confocal microscope, a depth response curve of the light intensity, which primarily depends on the light wavelength and the numerical (NA) of the objective can be generated by using vertical scanning process. The intensity light intensity at the light sensor can be calculated by Equation (25):

$$I(u) = \left[\frac{\sin(u/2)}{(u/2)} \right]^2 \tag{25}$$

doi: 10.6342/NTU201601083

where

$$u \approx \frac{8\pi}{\lambda} z \sin^2(\frac{\alpha_0}{2})$$

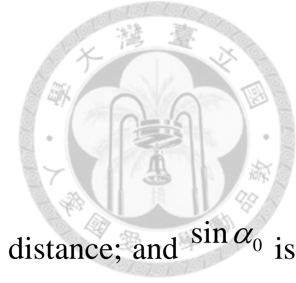

λ is the wave - length of the light source; z is the vertical distance; and $\sin\alpha_0$ is the numerical aperture.

For the chromatic confocal microscope system, optical sectioning capacity can be evaluated by the FWHM of spectral response curve as described in Figure 54.

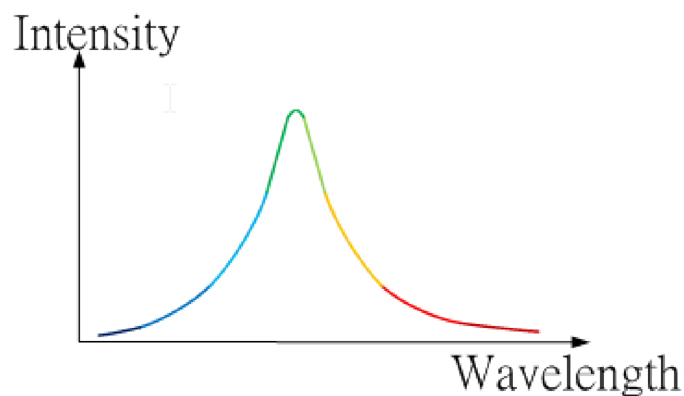

Figure 54 Spectral response curve

In section 2.7, the 3-D inspection using DMD system just uses DMD to manipulate illumination light. It projects many small light spot on the sample and using specific pattern for lateral scanning. On the other hand, our system uses DMD for both controlling the incident light and receiving reflected light. Our DMD's micro-mirrors can act as pinholes to create multipoint light source and eliminate stray light reflected back from those point, which are not in focal position. There is the predictable result that our system can have better optical sectioning capacity. In order to confirm the result, we should setup 4 systems as in Figure 50, Figure 51, Figure 52, and Figure 53 above and measure the FWHM of spectral response curve. We can see how much depth discrimination ability has been improved. The second configuration can become point-scan chromatic confocal microscope using DMD. We can use the system to test the effect of rectangular virtual pinhole's size.

doi: 10.6342/NTU201601083

3.5.6 Chromatic objective selection

Spectral resolution of IMEC Mosaic camera: 4x4 mosaic (1filter / pixel) = 16 bands in 465-630 nm with ~11nm incremental steps

Our research objective is to use the wavelength range 400~700nm for maximizing the IMEC Mosaic performance. Our laboratory already manufactured two chromatic objectives, which have a working wavelength ranging from 400 to 700 nm.

Table 1 Chromatic objective specification.

	20× Chromatic objective	27× Chromatic objective
Wavelength range (nm)	400 ~ 700	400 ~ 700
Dispersion range (μm)	350	600

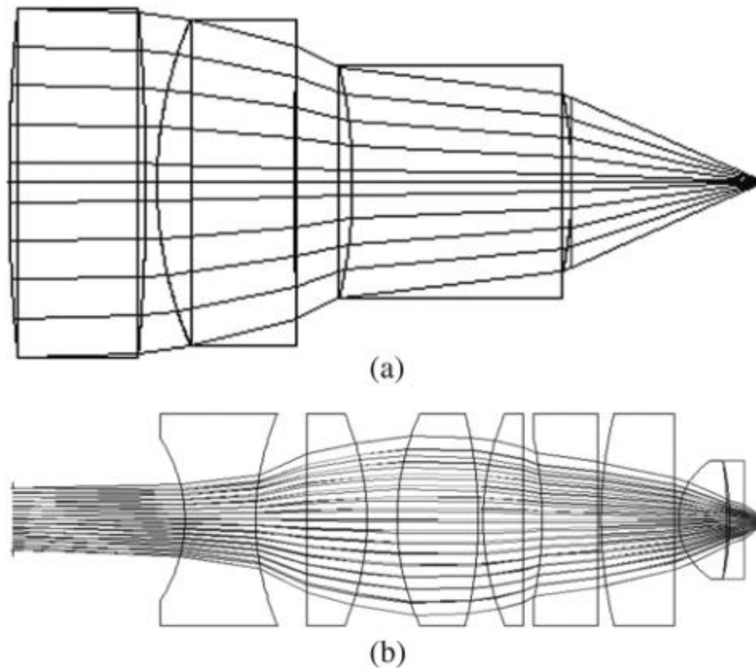

Figure 55 Optical simulation of chromatic objective :(a) 20× chromatic Objective and (b) 27× chromatic objective [16]

doi: 10.6342/NTU201601083

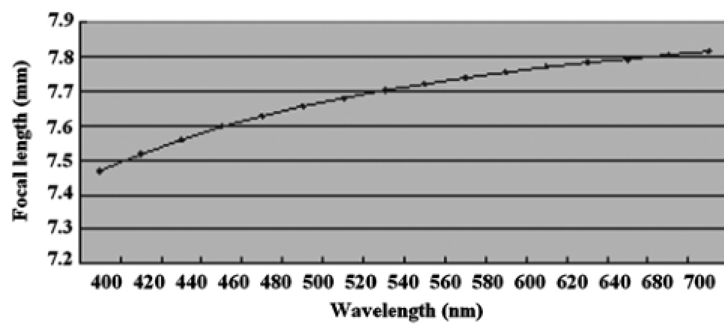

(a)

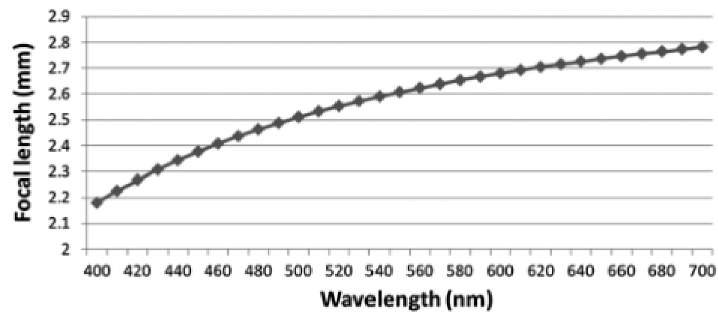

(b)

Figure 56 Optical simulation of the dispersion range with respect to various light wavelengths for the design of the chromatic objective: (a) 20× chromatic objective, (b) 27× chromatic objective [16]

3.5.7 Chromatic confocal depth response curve

As described above, IMEC Mosaic spectral area camera just can provide 16 spectral bands in spectrum from 470 to 620nm. In chromatic confocal microscopy using DMD system, reconstruction of the full spectrum response from IMEC spectral area camera data is required. That means we need to build a database of spectrum response for each calibrated depth through vertical scanning process and matching measured spectrum to one of spectrum in database and assign it back to the depth. Typical spectrum response of IMEC camera for chromatic confocal setup is shown in Figure 57, in which this typical response normally corresponds to only one pinhole.

doi: 10.6342/NTU201601083

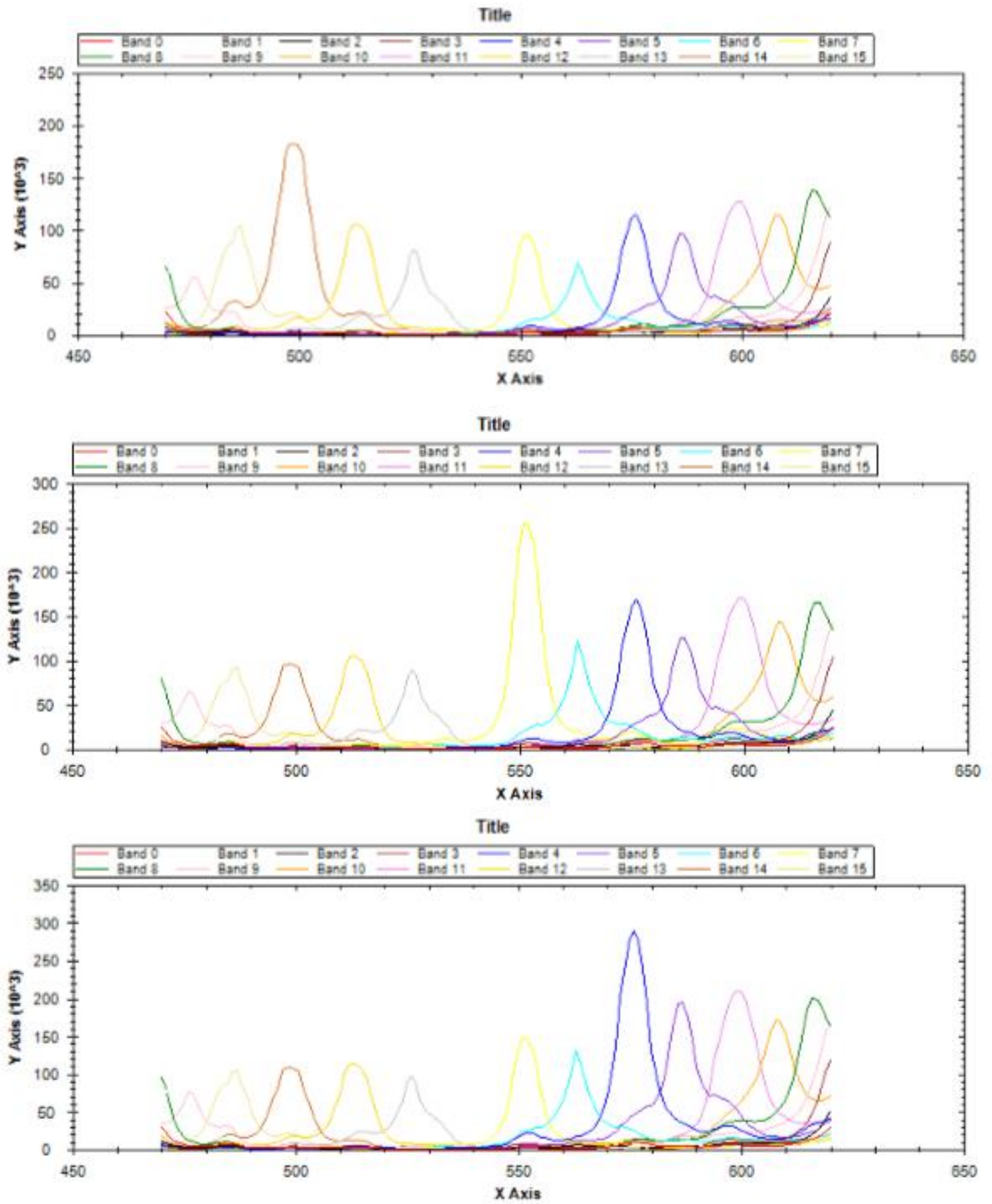

Figure 57 IMEC camera spectrum response corresponding to one pinhole at different depths

doi: 10.6342/NTU201601083

4 Software development

Software is developed in order to control all systems proposed in this thesis. The main software was built on OOP (object-oriented programming) and 3-layer structure as in Figure 58. With the focus on easy control, update and maintenance, all functions are divided into classes and written as independent modules. The top layer is the user interface being programmed in MFC dialog based application. It provides a compact and easy interface for users. The second layer is data flow layer, all function for scanning, and measuring procedure included in this layer. In order to prevent any misuse from users, top layer can communicate with second layer but cannot connect directly with hardware control layer (third layer).

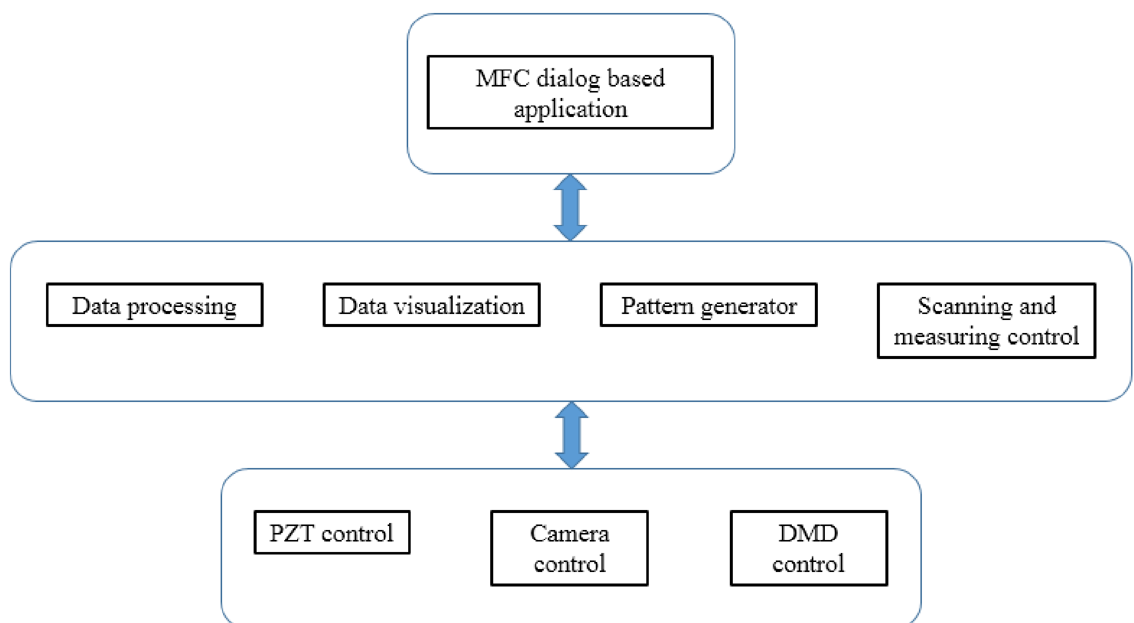

Figure 58 3 layers of control software

In data flow layer, data processing module was built on OpenCV library and focused on functions as auto-locate pinhole, NCC-depth response curve generation, peak detection, or depth encode and decode. Data visualization module acts as 2-D and 3-D generator from measured data, it also include function to extract profile and areal information. This module employed VTK open source library. Pattern generator module mainly communicates with DMD control module in hardware layer to generate specific designed pinhole pattern on DMD. On the other hand scanning and measuring control

doi: 10.6342/NTU201601083

module takes charge of experiment flow as describe in Figure 67, Figure 70 and Figure 76.

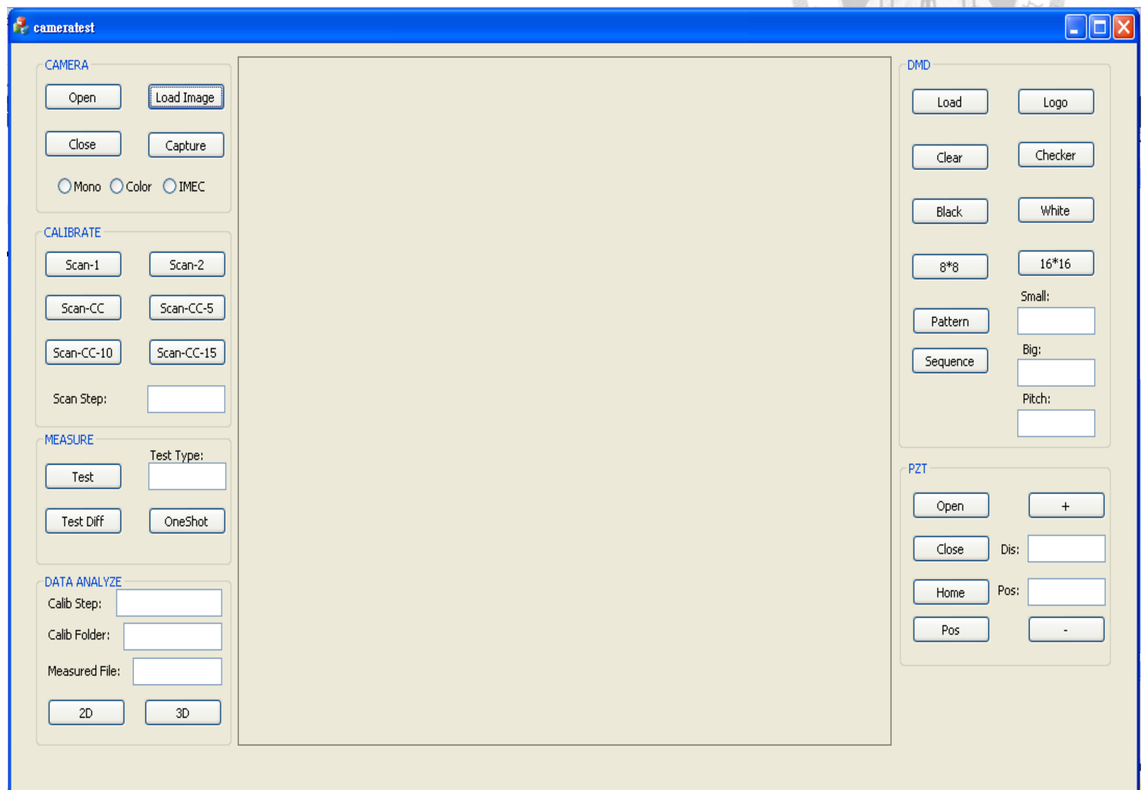

Figure 59 Software interface for digital diffractive-confocal imaging correlation microscopy

doi: 10.6342/NTU201601083

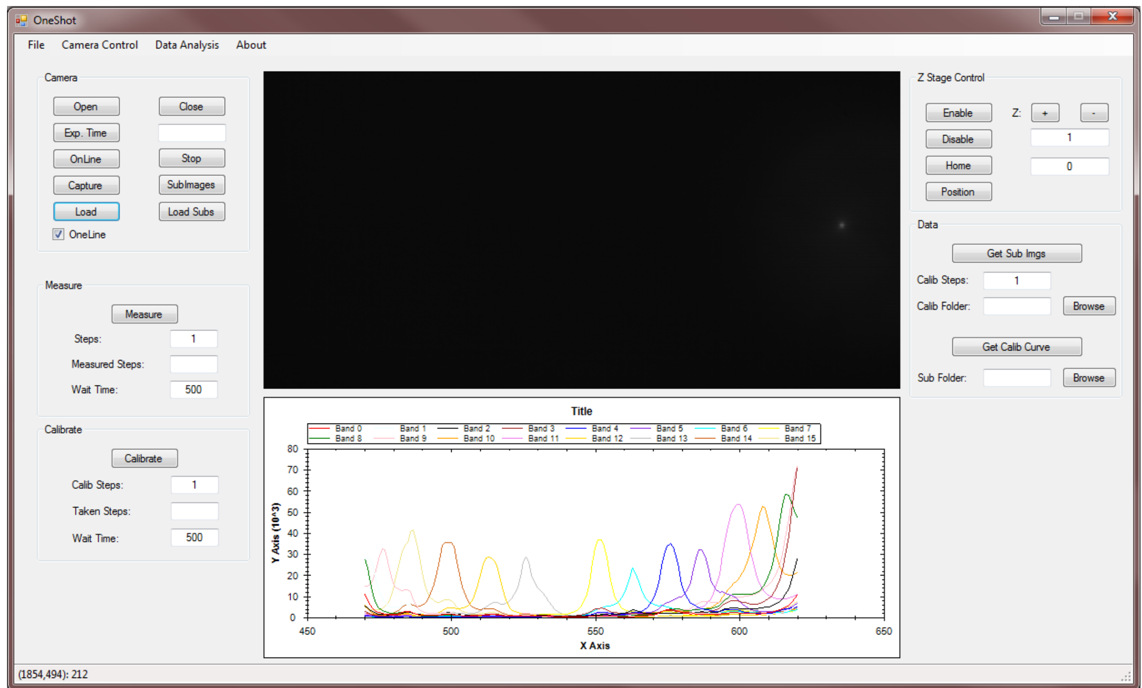

Figure 60 Software interface for chromatic confocal microscopy using DMD and IMEC camera

In order to put the system in in-line product chain, high speed is required. The speed of the system can exponentially be increased by reducing database size and forcing every procedure to work on a parallel mode instead of a serial mode. For all quasi one-shot full-field methods proposed in this thesis, we just care about the area equal to pinhole's image size and can neglect the gap area between any two adjacent pinholes. Therefore, after building database in traditional way and located pinholes' locations, database's size can be reduced by eliminating the gap area between two adjacent pinholes. For example, as described, in our system in which we used a specific designed pinhole pattern with a pinhole size of 2*2 pixels with the peak between 2 adjacent pinholes of 8 pixels. This means that the size of database can reduce 25 times as in Figure 61 when removing all gap areas. To get more measurement point, those systems can work in multiple-scanning mode. In multiple-scanning mode, database's size is relatively large, gap-removing process will make loading database into computer's RAM possible.

doi: 10.6342/NTU201601083

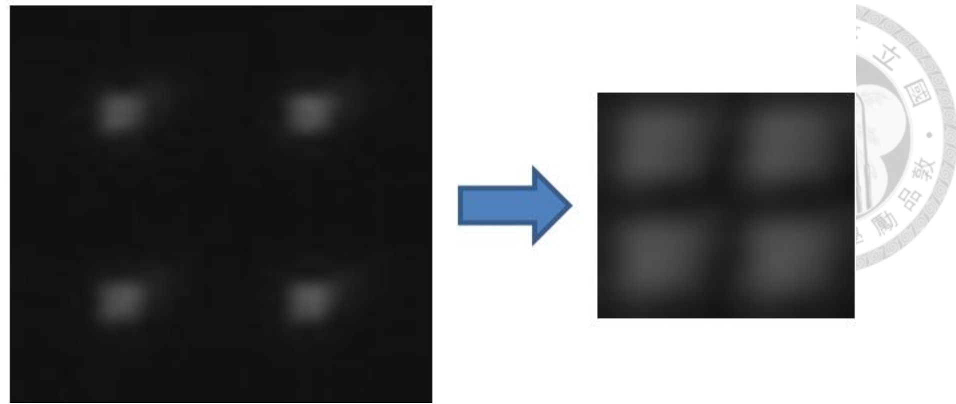

Figure 61 Reducing database's size

Computing speed will be significantly improved when all the data are stored in RAM. In that setup, the measuring speed can be maintained high enough for operating parallel processing mode. Parallel processing mode's diagram is depicted in Figure 62. This technique has the most benefit when using in multiple-scanning mode, it will make the proposed system to be compatible for *in-situ* applications.

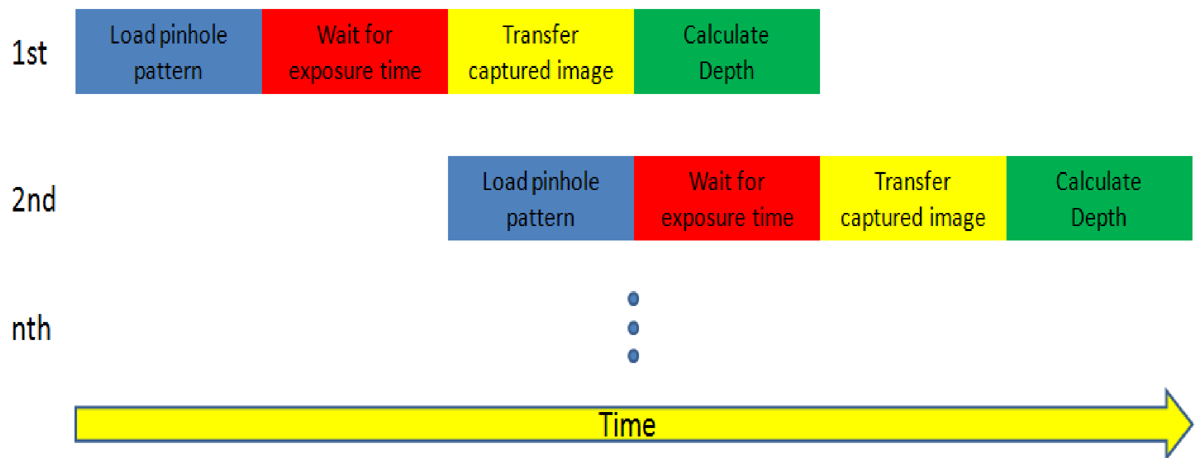

Figure 62 Timeline for parallel processing mode

doi: 10.6342/NTU201601083

5 Experiment setup and analyses

5.1 Digital diffractive-confocal imaging correlation microscope

5.1.1 General configuration

To implement the above-mentioned approach, this study proposes one novel optical configuration of confocal microscopy using DMD. The configuration uses digital micro-mirror device (DMD; Texas Instruments, Dallas, Tex.) as a spatial light modulator in confocal microscope configuration with white-light light source. A white-light source beam is collimated by a lens L1 to illuminate the DMD. The reflected light from DMD is collimated again using a tube lens L2 and imaged on the object plane of the objective. The mirror (or test sample) is placed perpendicular to the optical axial of the objective, so the reflected light from the mirror goes through the objective again and is imaged on to a high speed 12-bit CCD camera by using a tube lens L2 and a beam splitter. In order to make optical configuration simple and flexible as much as possible, the configuration employs illumination only mode of Programmable Array Scanning Confocal Microscope configuration, where the pixels of DMD are used to restrict the light impinging onto the surface while the optical sectioning is achieved by the use of the pixels of a CCD camera. Each element of the micro-display corresponds to pixels on CCD camera. None of the light from out-of-focus regions falls on neighboring pixels is taken into account. The system applied the virtual pinhole configuration to remain high sectioning capability with a robust setup. To build database of diffraction patterns, the reference mirror is moved by a piezoelectric stage. The diagram of the developed optical system setup is described in Figure 63.

doi: 10.6342/NTU201601083

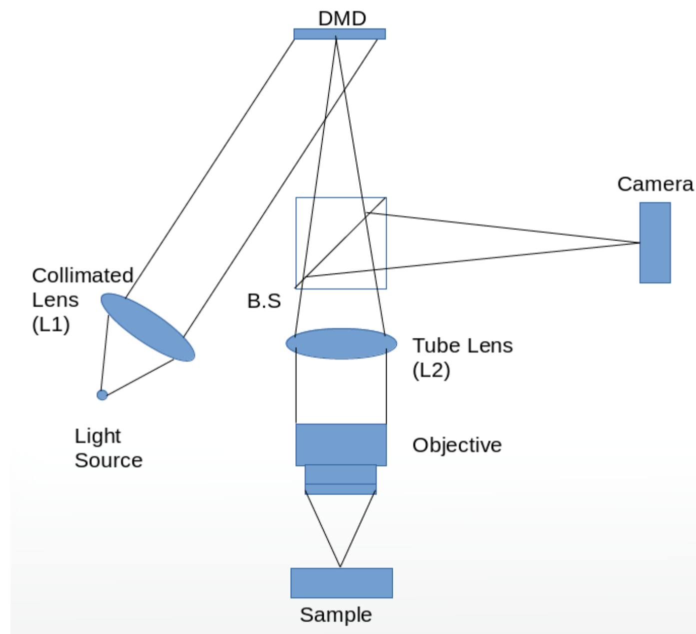

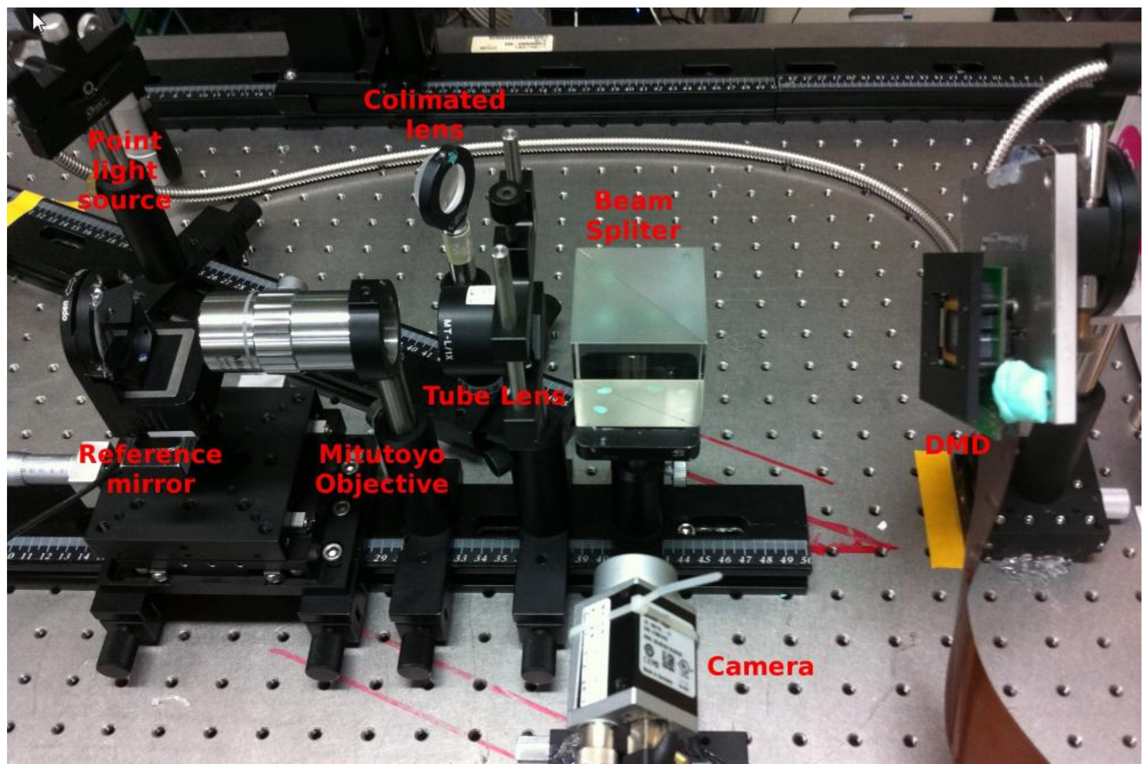

Figure 63 Optical system setup on anti-vibration table

5.1.2 Alignment

In digital diffractive-confocal imaging correlation microscope system, the most important point in configuration is alignment. There are three main steps to align the system, which were illustrated in Figure 64 .

doi: 10.6342/NTU201601083

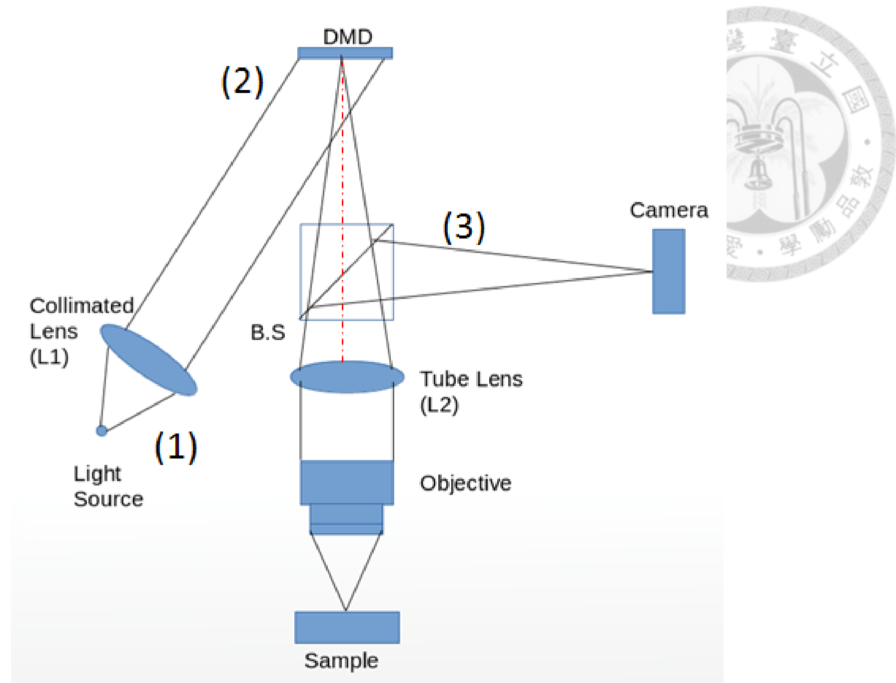

Figure 64 Alignment steps

First, incident lights that go to DMD need to be collimated and as uniform as possible. In order to have incident lights to be collimated, we just can use a single simple collimated lens. However, to achieve the uniformity we need to consider using more complex lens system as described in Figure 65. The reason for requiring uniform light is that when all incident lights are uniformed, we can use whole dynamic range of 12-bit mono camera when building database, which will increase accuracy and precision of the measuring system.

doi: 10.6342/NTU201601083

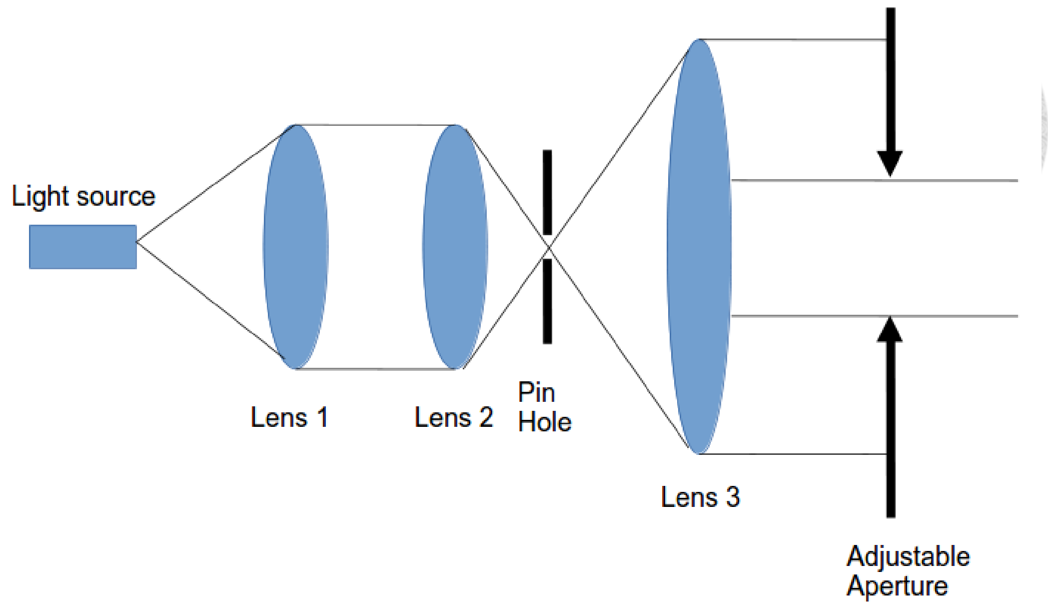

Figure 65 Light collimating system

Secondly, the light source and light collimating system need to be arranged in order to make incident lights form an angle of 24 degree with DMD surface's normal vector as shown in Figure 27. With this configuration, when micro-mirrors are in ON state, reflected lights will flow the direction of DMD surface's normal vector.

Finally, the distance between DMD and the tube lens (L2) needs to be equal to the back focal length of this tube lens. Furthermore, the distance between DMD and surface of beam splitter needs to be equal to the distance between the surface of beam splitter and the camera's sensor.

In addition, we also need to care about the distance between objective and tube lens to maintain light efficiency in our system as shown in Figure 66.

doi: 10.6342/NTU201601083

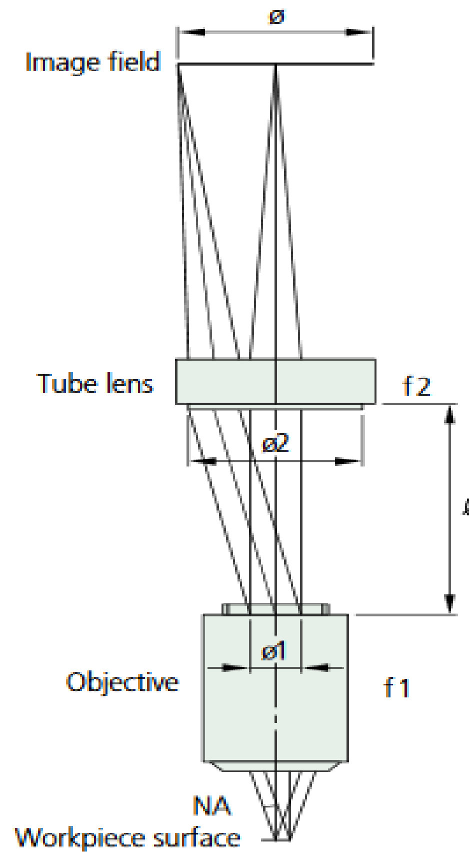

Figure 66 Placement of objective and tube lens

The distance can be calculated based on Equations (26) and (27) shown below:

$$\phi_1 = 2.f.NA \tag{26}$$

$$l = (\phi_2 - \phi_1).f_2 / \phi \tag{27}$$

where:

ϕ_1 : Objective exit pupil diameter (mm);

ϕ_2 : Effective diameter of tube lens (mm);

f_2 : Focal length of tube lens (mm);

ϕ : Image field diameter (mm).

5.1.3 Checking confocal configuration

Digital diffractive-confocal imaging correlation microscope system heavily depends on its confocal design configuration, so it is critical to check the confocal setup

doi: 10.6342/NTU201601083

after alignment procedure. The flowchart for checking confocal configuration is illustrated in Figure 67.

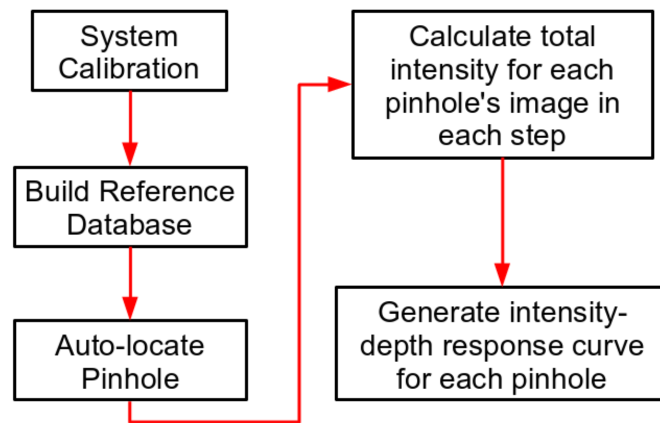

Figure 67 Flowchart for confocal effect checking

We performed the confocal configuration checking on two different objectives (20x and 2x Mitutoyo objective), with the same virtual pinhole size.

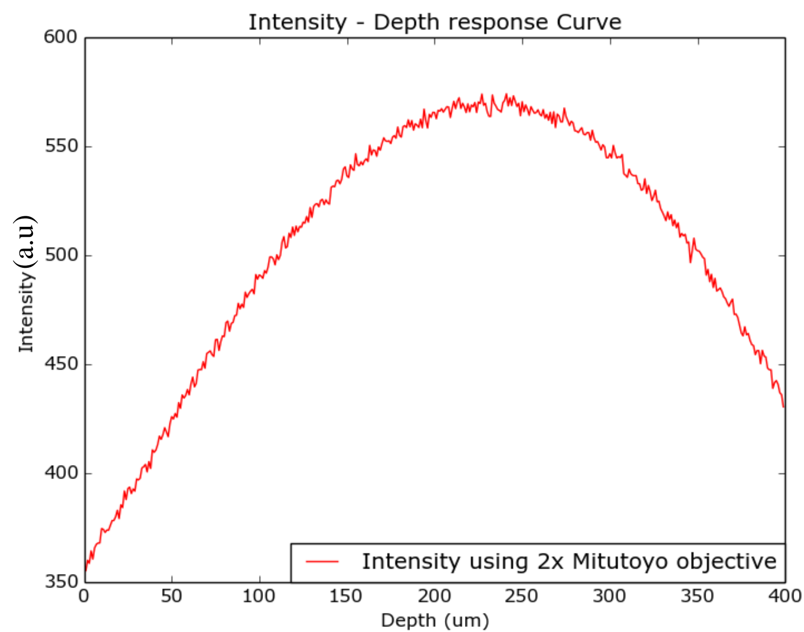

Figure 68 Intensity – depth response curve for 2x objective

doi: 10.6342/NTU201601083

國立臺灣大學 愛・學・勵・敬

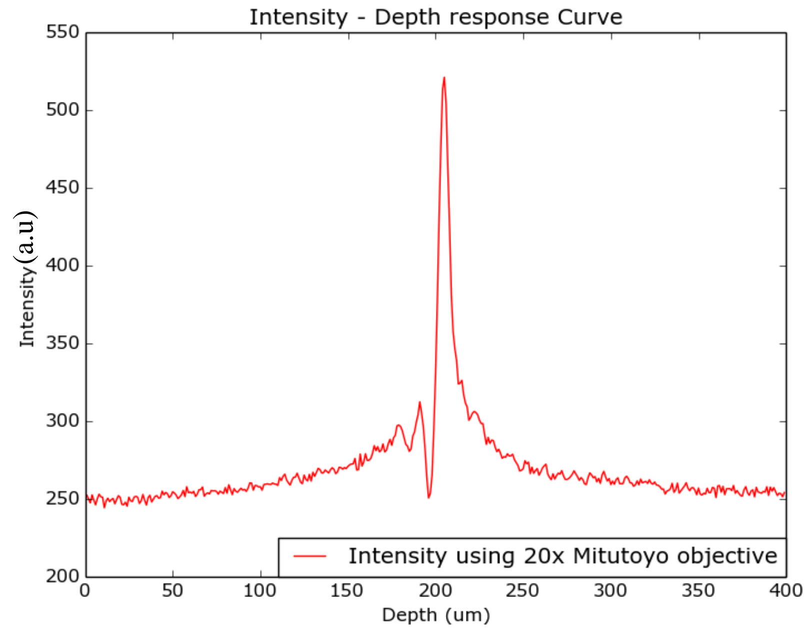

Figure 69 Intensity – depth response curve for 20x objective

5.1.4 Experiment results and analyses

We already developed the complete system being consisting of both software and hardware parts for quasi one-shot full-field surface profilometry using digital diffractive-confocal imaging correlation microscope with digital micro-mirror device. The flow chart of the developed system is shown in Figure 70. First, a system calibration procedure needs to be performed in order to optimize light intensity. A specific DMD pinhole pattern was designed and the best light exposure time is chose for achieving best image contrast. After this, a reference database is built by using reference mirror and PZT device as revealed in confocal effect section. The software will take care of pinholes auto located from achieved database. When measuring the sample, the position of object, light source intensity and camera exposure time also need to be calibrated to achieve the best image contrast and put the sample in the measurement range. The normalized cross correlation–depth response curve can be determined with respected to the surface property. The developed system can work in quasi one-shot or multiple shot for measuring more points by considering the requirement of applications. From measured picture, 2-D and 3-D view of sample can be generated and provide the reconstructed line profile or areal surface information.

doi: 10.6342/NTU201601083

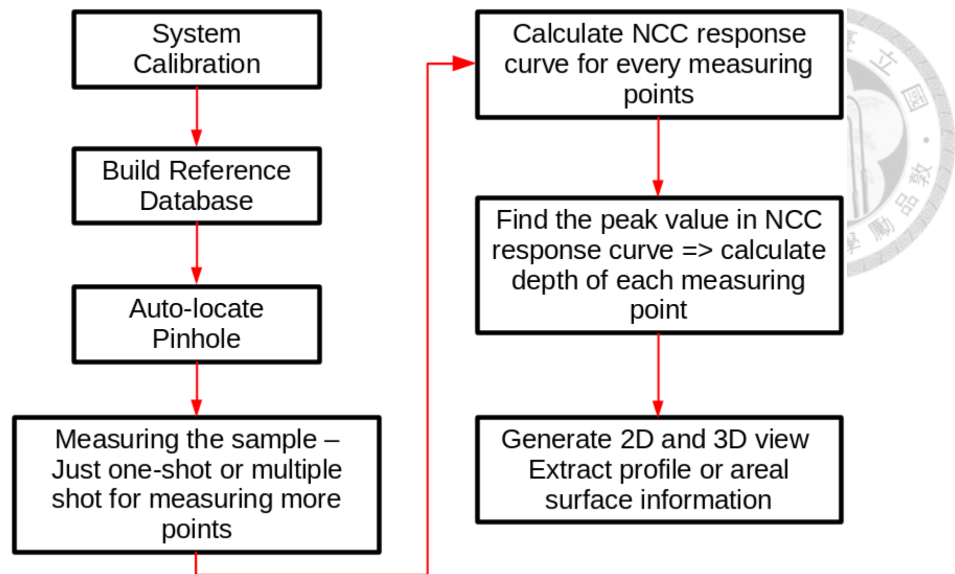

Figure 70 Flowchart of digital diffractive-confocal imaging correlation microscope

To check accuracy and precision of developed system, we designed a DMD pinhole pattern with a pinhole size of 2x2 pixels and the pitch between two pinholes as eight pixels. The smaller the pitch is the better lateral resolution to be achieved. However, the pitch also needs to be chosen, so a cross talk should be minimized to ensure a satisfactory vertical resolution in profile measurement. With the configuration we can measure almost 10000 points with quasi one-shot in FOV. Using this pinhole pattern and a standard flat mirror, we build a reference database consisting of 400 images for 400 steps, in which the distance between each step is one μm. After this, we change the mirror to an empty wafer and use an accurate linear PZT to move the wafer into measurement range. First, we take one image shot and move the wafer to a new location of 50 μm apart from the previous location, and take the other shot. From two consecutive measured images, we can calculate the position of every measuring point and the distance of this measuring point between two measurement times. We repeat this testing procedure for 30 times and then perform statistical analysis to determine the sample mean value and random standard deviation.

For different measure times, sample mean values were in a range from 49.6 to 50.1 μm and random standard deviations were in a range from 0.02 to 0.03 μm calculated on a group of 9852 measured points. Because our developed method is immune to not only light intensity but also sample surface reflectivity, so the precision of this method is extremely good. Moreover, the measurement accuracy still can be further enhanced by

doi: 10.6342/NTU201601083

adapting an imaging device with cooling temperature control and high dynamic range for maximizing signal to noise ratio of images. 3-D images of wafer surface at different positions was showed in Figure 71.

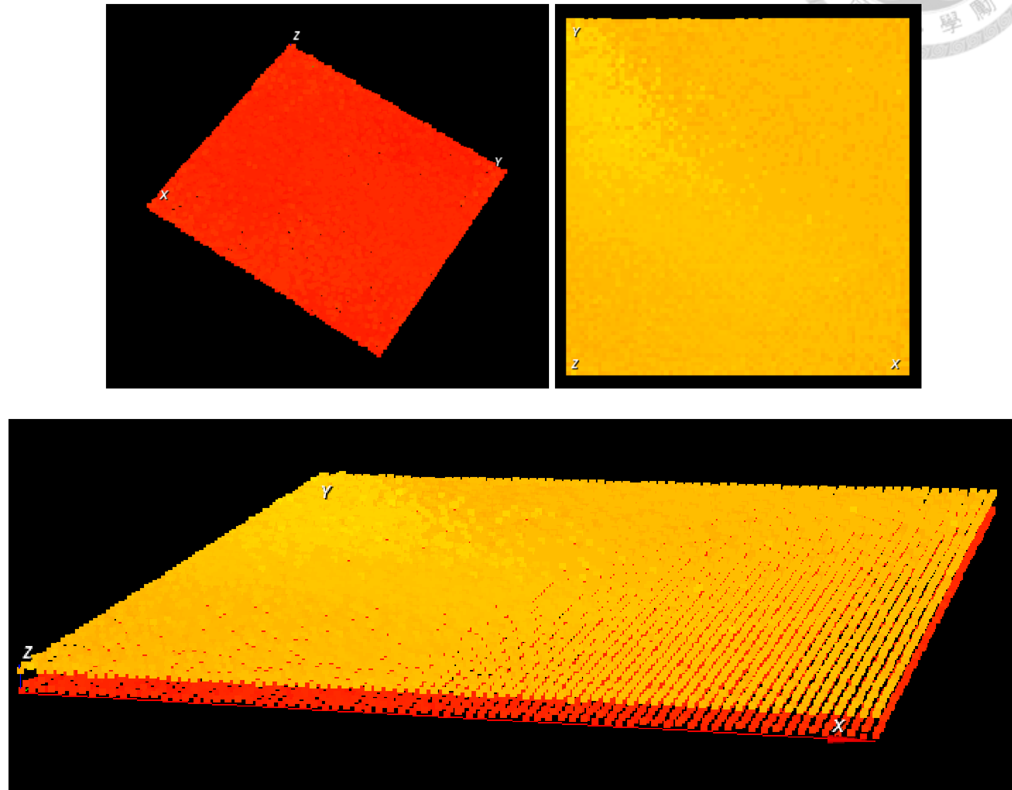

Figure 71 3-D images of wafer surface at different position

To attest the measurement accuracy of the developed measurement approach, we conducted an experimental measurement on a calibrated step-height surface target with a step height of 70 μm. With the same setup with above experiment, the average height of target was 70.16 μm. 2-D and 3-D views of this measured step height was showed in Figure 72.

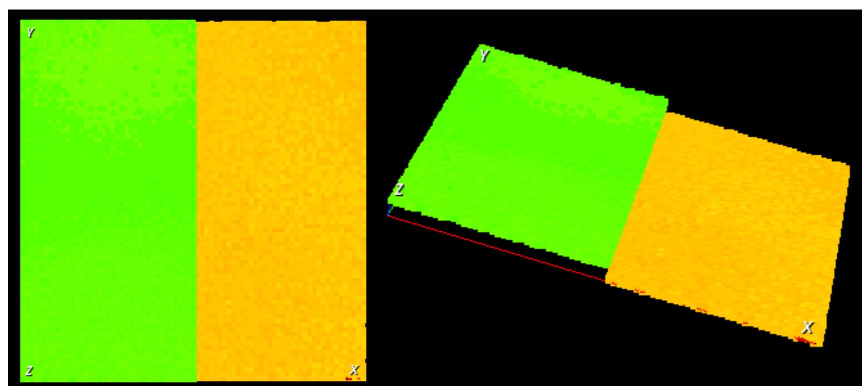

doi: 10.6342/NTU201601083

Figure 72 2-D and 3-D views of step-height sample

Moreover, to evaluate the efficiency of our system with surface reflectivity and NA of objective, we also measured one defected sample, which has some defected coating area without reflection, shown in Figure 73. Figure 74 shows the measuring results, in which at some part of the sample we cannot get reflected signals due to low surface reflectance, so the height information is lost.

Figure 73 Defected sample.

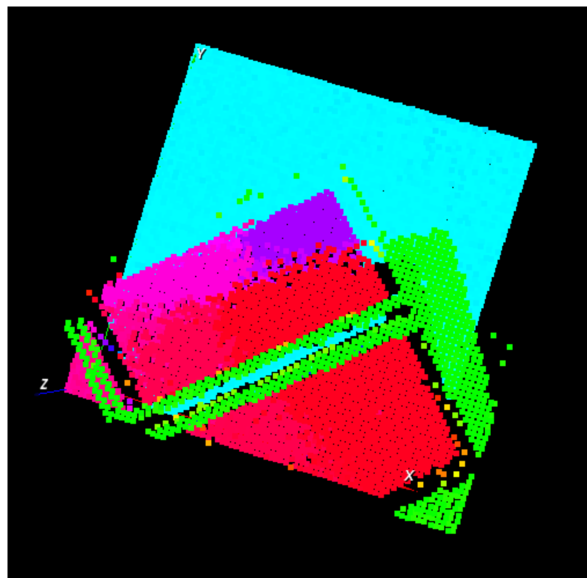

Figure 74 3-D view of defected sample

doi: 10.6342/NTU201601083

5.2 Digital diffractive-confocal imaging correlation microscope

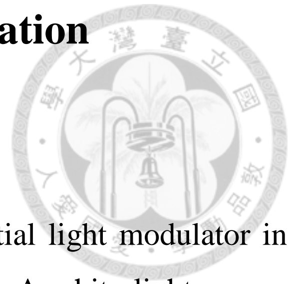

5.2.1 General configuration

The configuration uses digital micro mirror device as spatial light modulator in confocal microscope configuration with white-light light source. A white-light source beam is collimated by collimated lens to illuminate the DMD. Because of DMD characteristic, the reflected light from DMD will be dispersed, and then collimated again by a tube lens. After going through a beam splitter, reflected light goes directly to an infinite chromatic objective and re-focuses on the mirror (or test sample) surface which is placed perpendicular to the optical axial of the objective. The light is reflects again and forms an image on 12-bit color CCD camera by tube lens. In order to make optical configuration simple and flexible as much as possible, the configuration employed illumination only mode of Programmable Array Scanning Confocal Microscope configuration, where the pixels of DMD are used to restrict the light impinging onto the surface while the optical sectioning is achieved by the use of the pixels of a CCD camera. To build the database of diffraction patterns, the reference mirror is moving by an accurate linear piezoelectric stage. Diagram of optical system setup is described below and the real setup on optical table is shown in Figure 75.

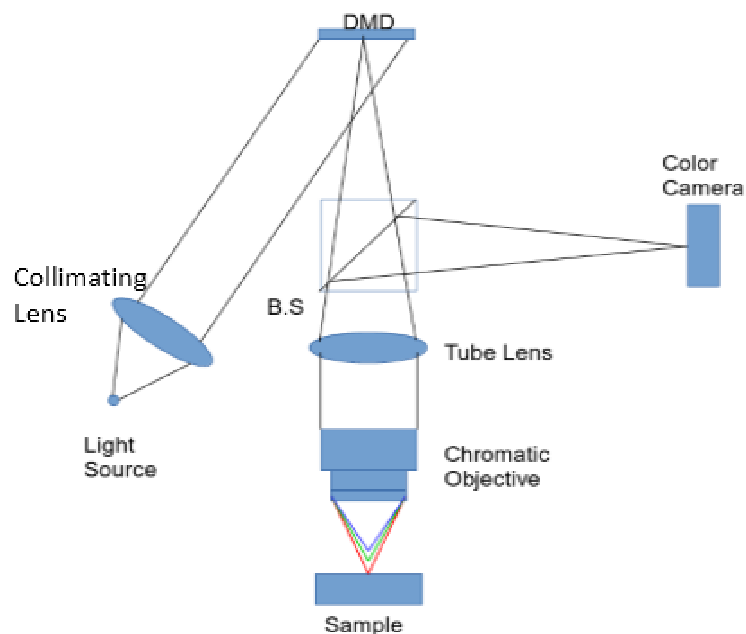

doi: 10.6342/NTU201601083

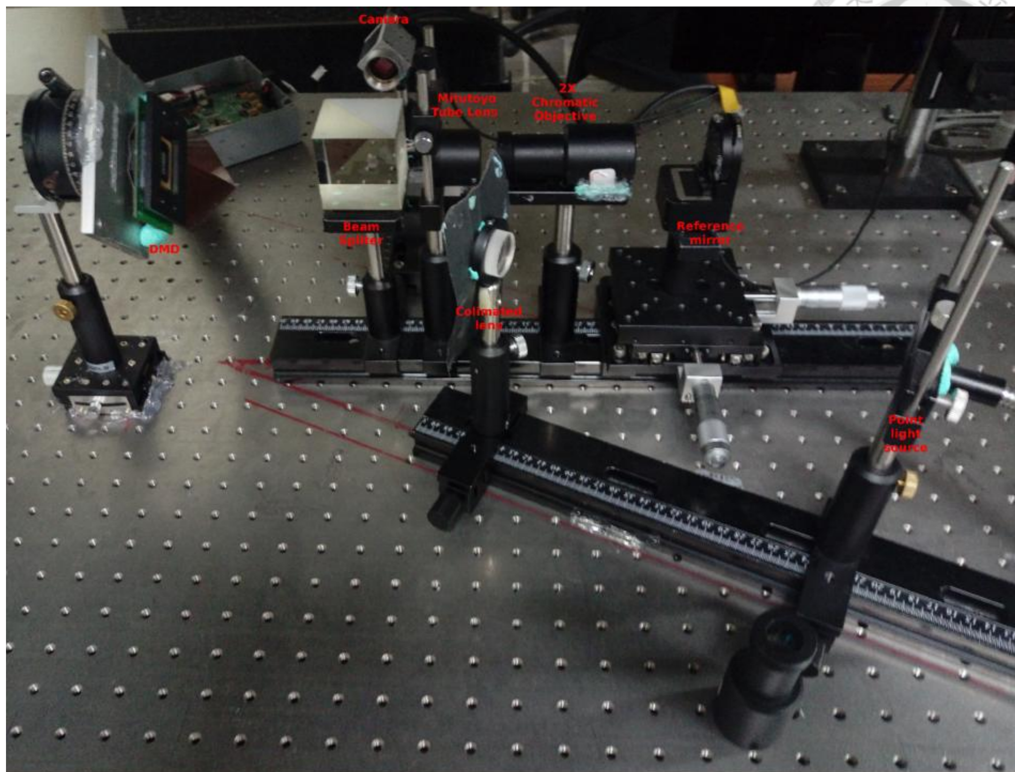

Figure 75 Optical system setup on anti-vibration table for digital diffractive-confocal imaging correlation microscope goes chromatic

5.2.2 Experiment result and analyses

Because of using a color camera and chromatic objective, digital diffractive-confocal imaging correlation microscope goes a chromatic system with two extra steps in working procedure. The flow chart of the developed system is described in Figure 76. The first extra step is to separate the color image into four different gray scale pictures corresponding to Bayer filter as described in Figure 39. Furthermore, in this system, no interpolation was applied to generate complete color for each pixel. For the reference database, color information just extracted from the raw color image format (Bayer RG 12bit). The second extra step was added after we performed normalized cross correlation calculation and detected peak valued in NCC response curve. Because of using color camera, we have four different diffraction pattern for depth mapping corresponding to three wavelengths, and then we need to decide which NCC–depth response curve is most reliable in the particular measurement range and use it as depth decoding reference. This extra step is to calculate the slope of each response curve. From peak point location, we chose two points having the same distance to peak point, and then calculate equation of

doi: 10.6342/NTU201601083

straight light going through each point and peak point. After calculating the slope for each NCC-depth response curve, we can choose the curve having the biggest slope as the depth decoding reference. As described in Figure 78, the NCC-depth response curve for green color having the biggest slope can be used as the depth decoding reference.

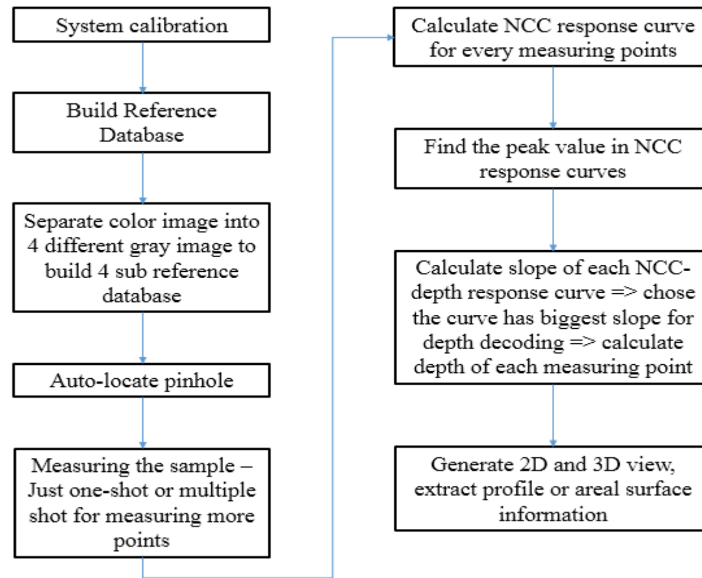

Figure 76 Flowchart of digital diffractive-confocal imaging correlation microscope

To check accuracy and precision of the developed system, we use the same designed DMD pinhole pattern as in the one in the digital diffractive-confocal imaging correlation microscope system. Because the sensor size of color camera is much smaller than the mono camera, the number of measuring points will be significantly reduced for almost 2000 points with quasi one-shot in FOV. However, using the color camera and specific designed chromatic objective, the measurement range can be increased up to 1100 μm for almost 2.5 times (using chromatic objective with the same magnification with a conventional objective 2x). Typical NCC-depth response curve for digital diffractive-confocal imaging correlation microscope goes chromatic at different depth positions are shown in Figure 78, 78 and 79 and.

doi: 10.6342/NTU201601083

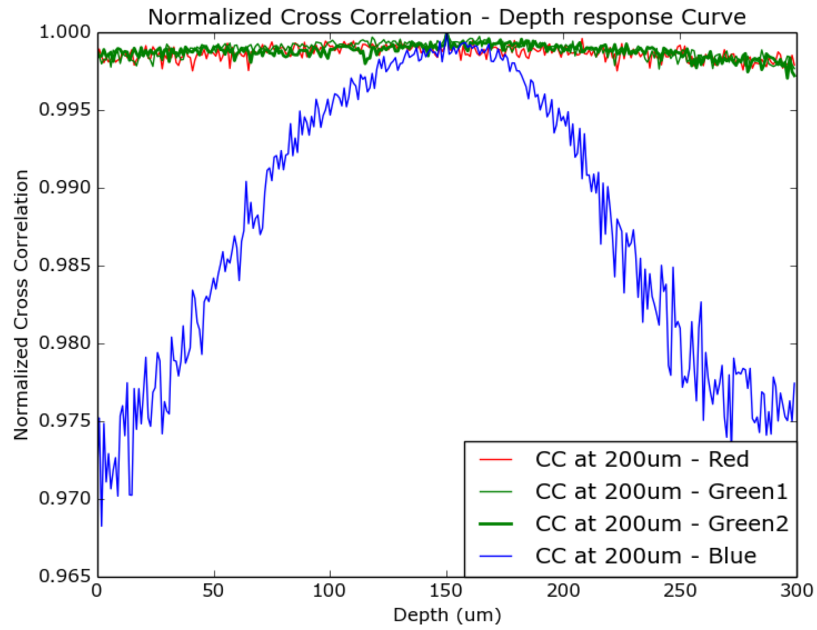

Figure 77 Typical NCC-depth response curve for digital diffractive-confocal imaging correlation microscope at position 1 – blue range

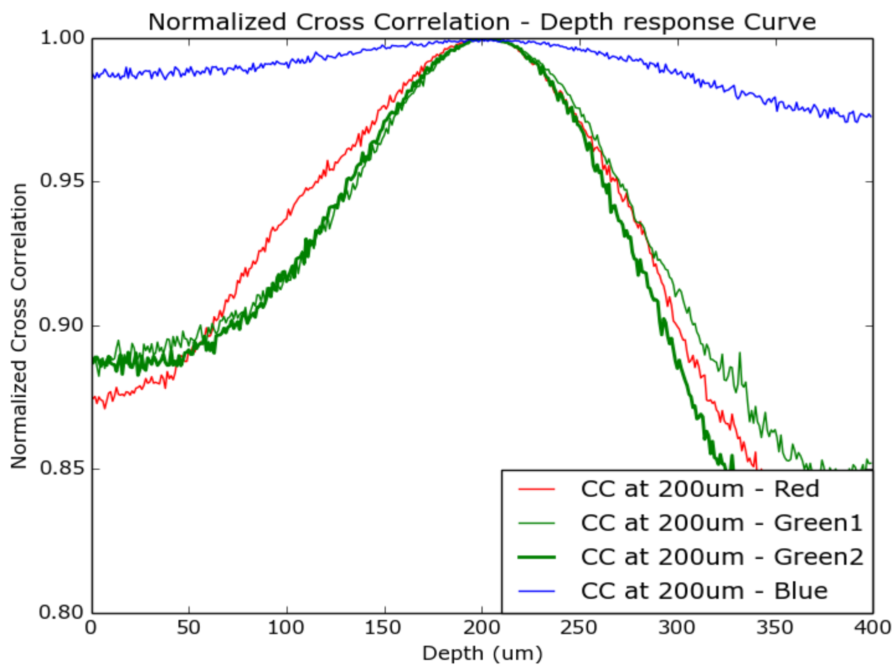

Figure 78 Typical NCC-depth response curve for digital diffractive-confocal imaging correlation at position 2 – green range

doi: 10.6342/NTU201601083

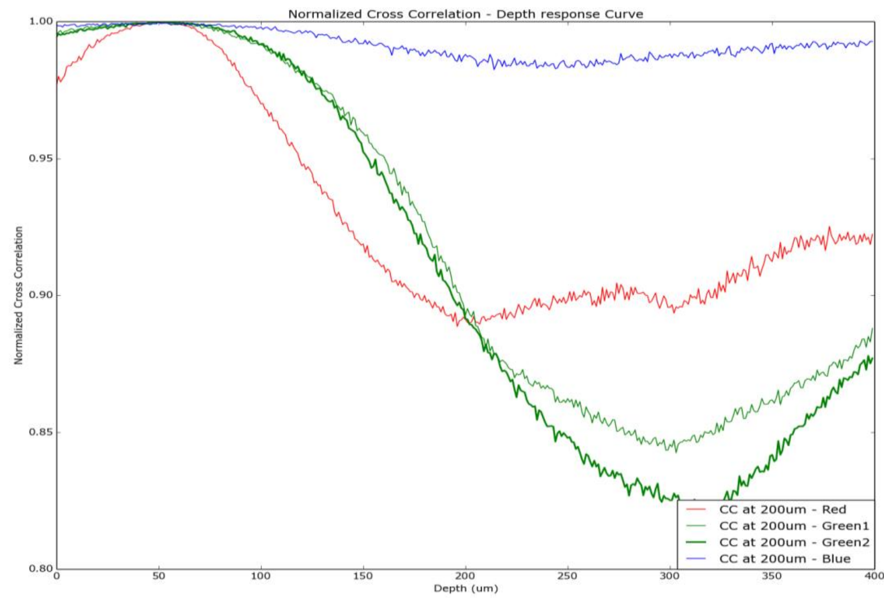

Figure 79 Typical NCC-depth response curve for digital diffractive-confocal imaging correlation microscope at position 3 – red range

To check the measurement accuracy of digital diffractive-confocal imaging correlation microscope, we took an experimental measurement on a calibrated step-height surface target with a step height of 150 μm. With the same setup with above experiment, the average height of target was 150.58 μm. 2-D and 3-D views of this measured step height were shown in Figure 80.

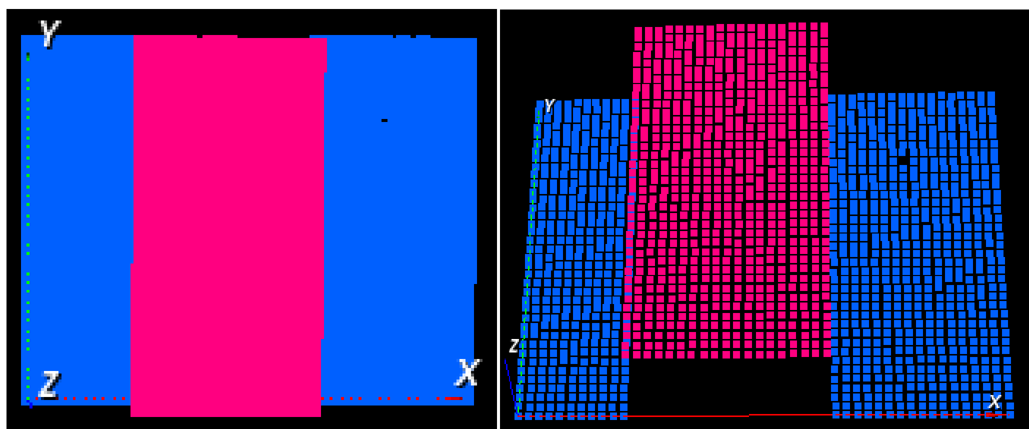

Figure 80 2-D and 3-D views of step-height sample

doi: 10.6342/NTU201601083

5.3 Chromatic confocal system included spectral area camera

5.3.1 General configuration

The system applied real-pinhole confocal setup to increase confocal effect. That means increasing sectioning capability (axial resolution) of our system. However, the setup is much more complicated and need many efforts for alignment. DMD was loaded with special designed pinhole arrangement to created pinhole array. A white-light light source beam is collimated by collimating a lens to illuminate the DMD. The reflected light from DMD is imaged on the focus plane of the chromatic objective. The mirror (or tested sample) is placed perpendicular to the optical axial of objective, so the reflected light from the mirror goes through the objective again. The reflected light after that will hit with DMD the second time and finally forms image on the spectral area-scan IMEC camera by the tube lens L2 and the beam splitter. The light goes through DMD twice, so the pinhole array created by DMD has effect on both detection and illumination sides. To build database of spectrum response patterns, the reference mirror is moved by a linear piezoelectric stage. The diagram of the optical system setup is described in Figure 81.

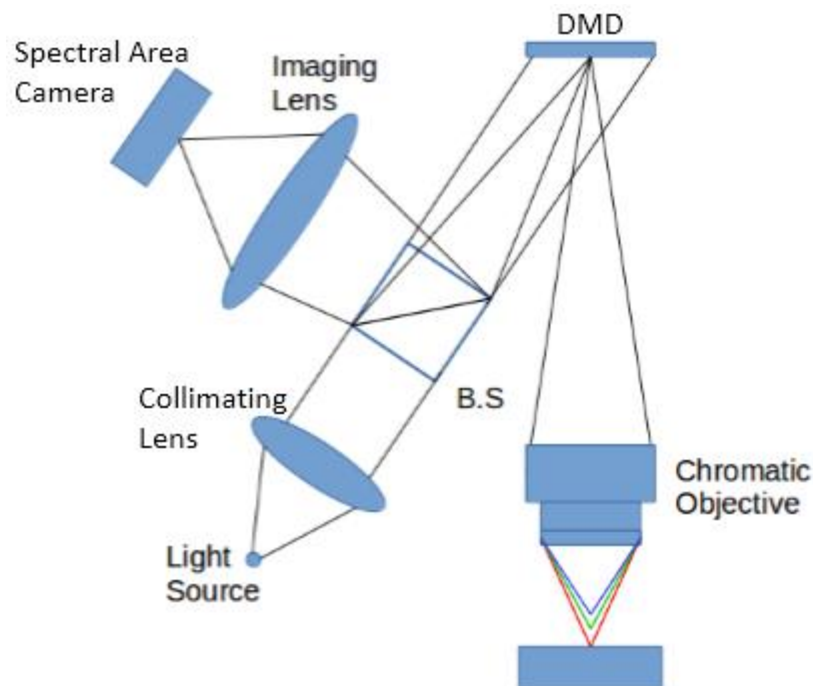

doi: 10.6342/NTU201601083

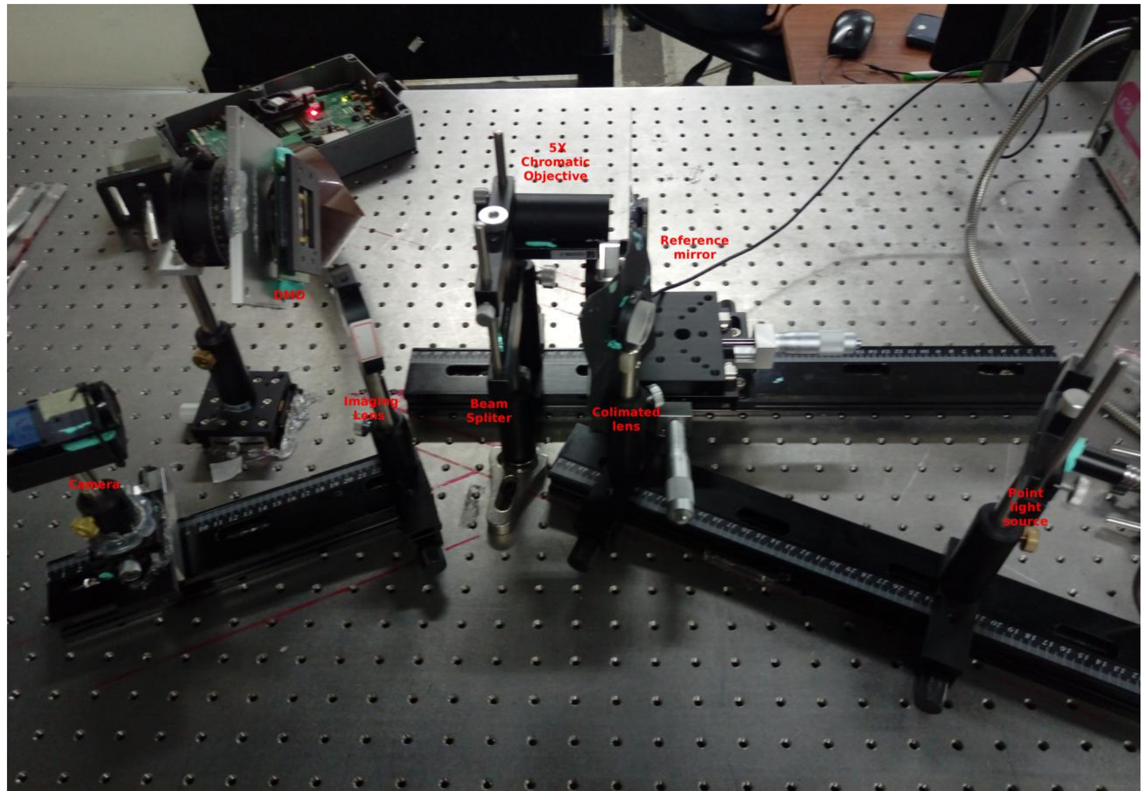

Figure 81 Optical system setup on anti-vibration table for chromatic confocal system using DMD and IMEC camera

5.3.2 IMEC camera calibration

IMEC camera need to be calibrated because of two main reasons: sensitiveness of IMEC filters with wavelengths outside of its active range and internal filter crosstalk.

In the first case, the incident light is conditioned using an appropriate band pass or rejection filter in front of the sensor. The primary goal of the rejection filter is to block all light with wavelengths outside of the active range. Therefore, the filters will remove spectral leaking and unwanted second order responses outside of the sensor's active range. Our IMEC filter working range is from 470 to 620 nm, so the rejection filter 450-640 nm was chosen.

Unlike the wavelengths outside of the active range, some unwanted responses cannot be removed using rejection filters. These unwanted responses typically are second order responses with a response to wavelengths leaking into the filters and response to filter crosstalk. These wavelengths contribute to the filter's total response and will be presented in the captured data. Their contribution to the signal can be suppressed by applying the spectral correction algorithm post-acquisition.

doi: 10.6342/NTU201601083

Our CMV2K SSM4x4 VIS sensor is a CMOSIS CMV2000 sensor with 16 filters active in the visual spectrum in a snapshot mosaic filter layout organized in patterns of four rows and four columns illustrated in Figure 82.

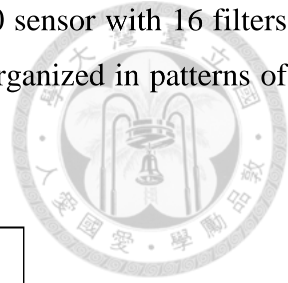

0 490	1 500	2 477	3 478
4 577	5 591	6 563	7 553
8 618	9 616 478	10 613	11 600
12 538	13 549	14 523	15 511

Figure 82 IMEC 16 bands snapshot mosaic filter layout

The post-acquisition of the spectral correction algorithm consists of multiplying the raw signal with a correction matrix. The resulting signal behaves as if it were captured by a sensor with ideal filters that have a single peak with a fixed FWHM (Figure 84). Correction matrix was 2-D matrix with 16 rows (16 bands) and 601 columns (in wavelengths range from 400 to 1000nm). Filter responses in active range of our VIS hyper spectral sensor are illustrated in Figure 83.

doi: 10.6342/NTU201601083

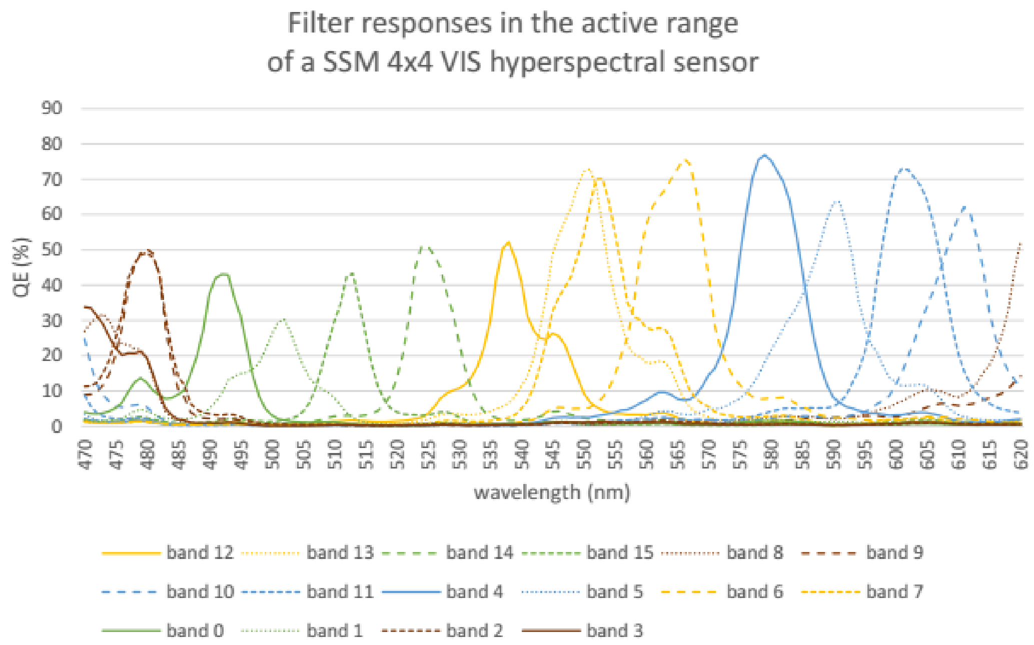

Figure 83 Filter responses in the active range of a SSM 4x4 VIS hyper spectral sensor

doi: 10.6342/NTU201601083

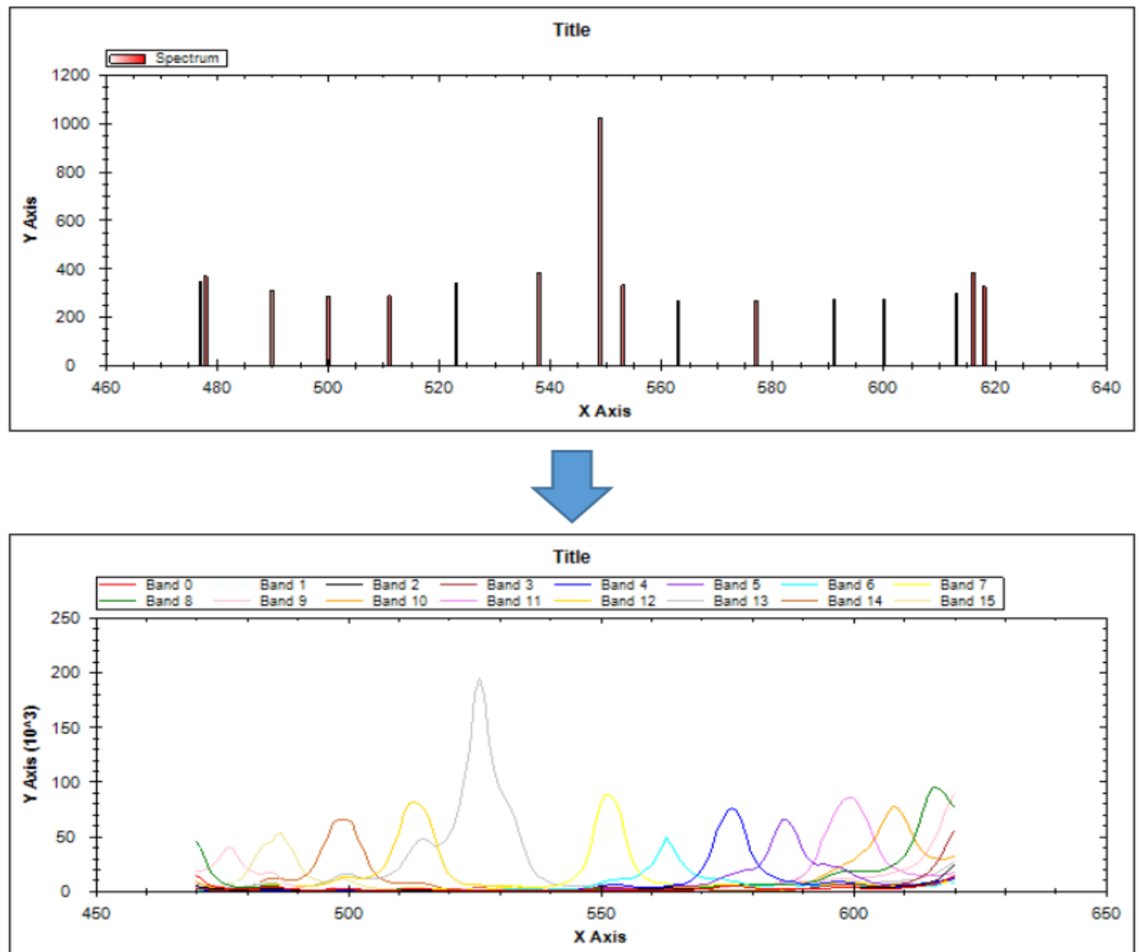

Figure 84 Spectrum response after calibration

5.3.3 Experiment results and analyses

In this setup, the lights go through DMD twice, so the pinholes created by DMD have double narrowing effect on both detection and illumination sides. The configuration will increase confocal effect that means increasing sectioning capability (axial resolution) of our system.

A white-light source beam is collimated by collimated lens, and then goes through a beam splitter to illuminate the DMD. Because of the DMD characteristic, the reflected light from DMD will be dispersed. The light goes directly to an infinite chromatic objective and focuses on the mirror (or test sample) surface which is placed perpendicular to the optical axial of the objective. The light will be reflected again, then go through DMD and beam splitter for the second time, then finally forms an image on a 12-bit color CCD camera by an imaging lens.

doi: 10.6342/NTU201601083

Typical response of the system was showed in Figure 85 and Figure 86. As described in those pictures, the system suffers from the vignetting problem of chromatic objective (which was specially designed for point-scan and line-scan chromatic confocal system – not for area-scan system). Therefore, number of measurement points limited to 90 points in the center of DMD. This limit can be further resolved by re-designing the chromatic objective.

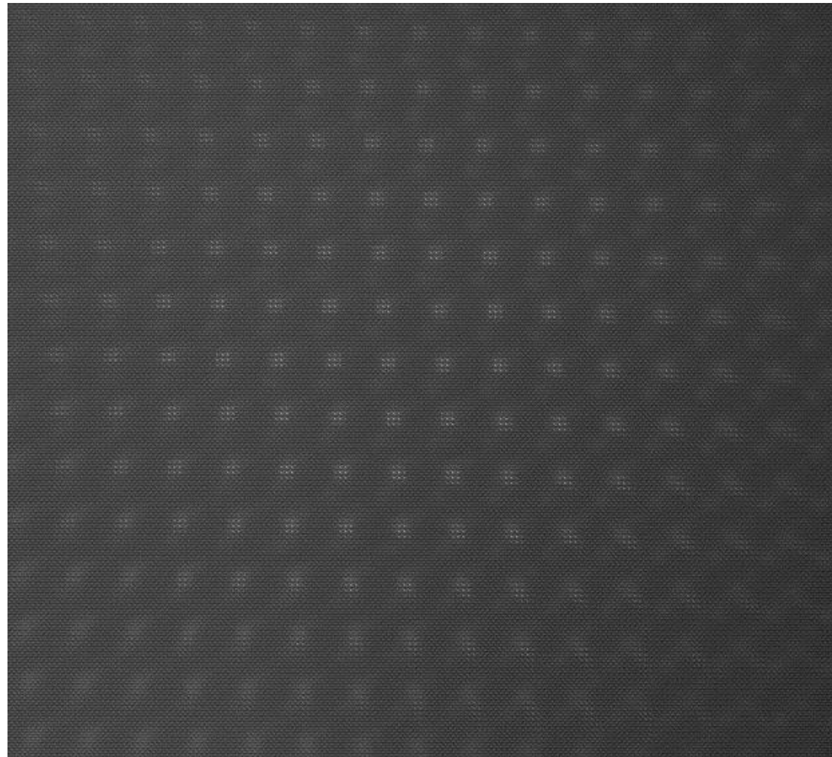

Figure 85 Typical response of IMEC camera (16 bands)

Figure 86 Typical response of IMEC camera (single bands)

doi: 10.6342/NTU201601083

The flow chart of the developed system is described in Figure 87. First, a system calibration procedure needs to be performed in order to optimize light intensity and find measurement range (IMEC camera works only on narrow range 465-630nm). The reference database was built by vertical scanning procedure being performed using a reference mirror and a linear PZT. After that, the software will process pinhole auto-locate algorithm. This algorithm needs extra steps compared to the one using in digital diffractive-confocal imaging correlation microscope system. First, the image taken by IMEC camera will be separated into 16 sub-images corresponding to 16 bands. The sub-image with the highest contrast will be used as input for auto-locate pinholes algorithm. When measuring the sample, the position of object, light source intensity and camera exposure time also need to be calibrated to achieve best image contrast and put the sample in the measurement range. To match the spectrum response curve of measuring point to database, 1-D NCC was employed.

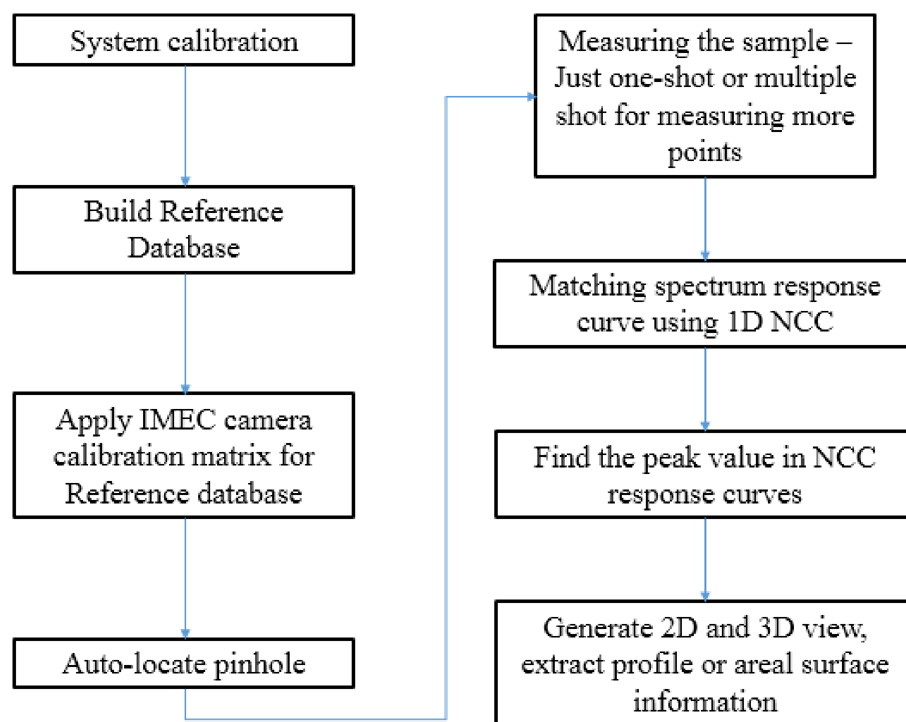

Figure 87 Flowchart of chromatic confocal system using DMD and IMEC camera

doi: 10.6342/NTU201601083

Figure 88 Auto-locate pinholes algorithm output

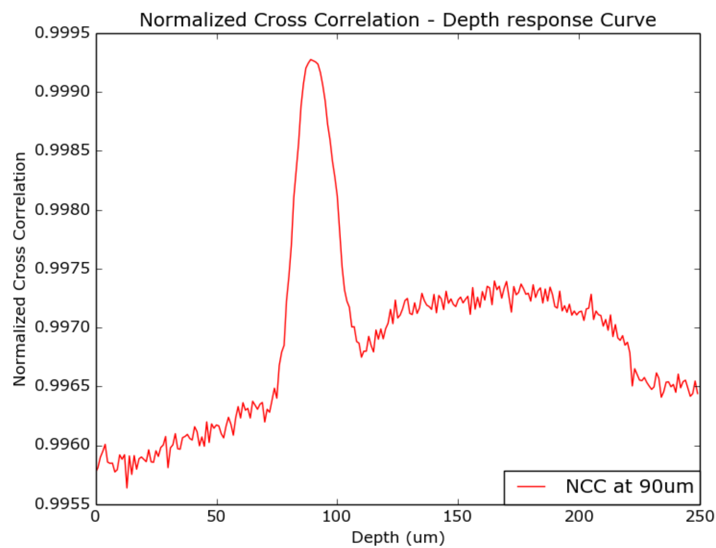

Figure 89 Typical NCC response

Because of IMEC filters characteristics, light intensity was reduced significantly compared to a normal mono CCD, to increase light sensitivity a DMD pinhole pattern with pinhole size 4x4 pixels and the pitch between two pinholes as 10 pixels was developed. However, because of chromatic objective's vignetting error, with the configuration we just can measure 90 points with quasi one-shot in center of DMD (for 27 times chromatic objective). Using this pinhole pattern and a standard flat mirror, we build reference database consists of 250 images for 250 steps; the distance between each step is one μm. After this, we change the mirror to an empty wafer and using PZT to move the wafer into measurement range. First, we took one shot, move the wafer to new location 50 μm apart from its previous location, and took another shot. From two

doi: 10.6342/NTU201601083

consecutive measured images, we can calculate the position of every measuring points and the distance of this measuring point between two measured times. We repeat this testing procedure for 30 times and then we performed statistical analysis to find out the sample measured mean value and random standard deviation. For different measure times, the sample mean values were varying in range from 51.25 to 51.29 μm and the random standard deviations was 0.12 μm calculated on 90 measure points. The graph below illustrated the measuring accuracy and precision in the tested result.

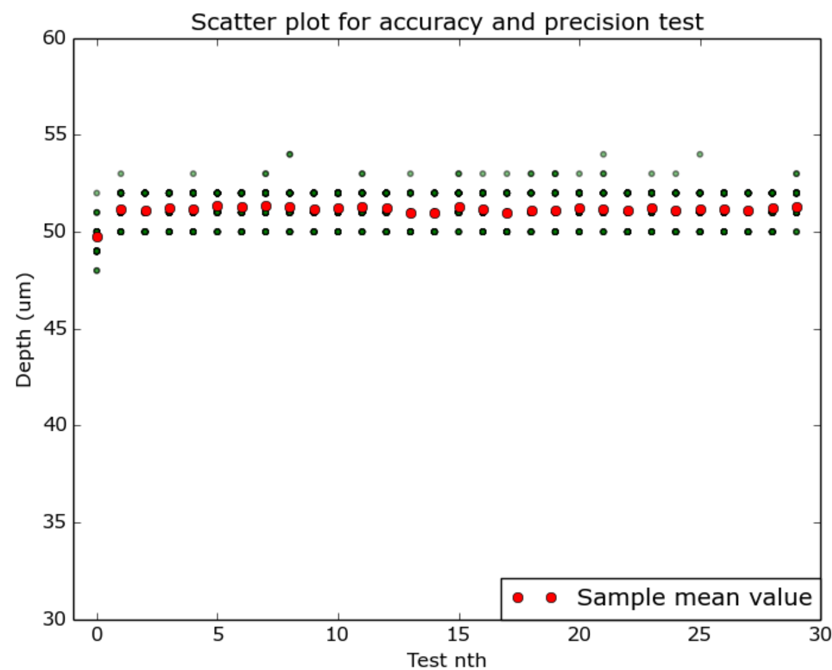

Figure 90 Scatter plot for accuracy and precision test

Furthermore, the accuracy and precision tests also performed on diffuse surface sample as described in Figure 91. The system was tested in diffuse surface in grinding and horizontal milling surface corresponding to Ra 0.4 and 1.6, respectively.

doi: 10.6342/NTU201601083

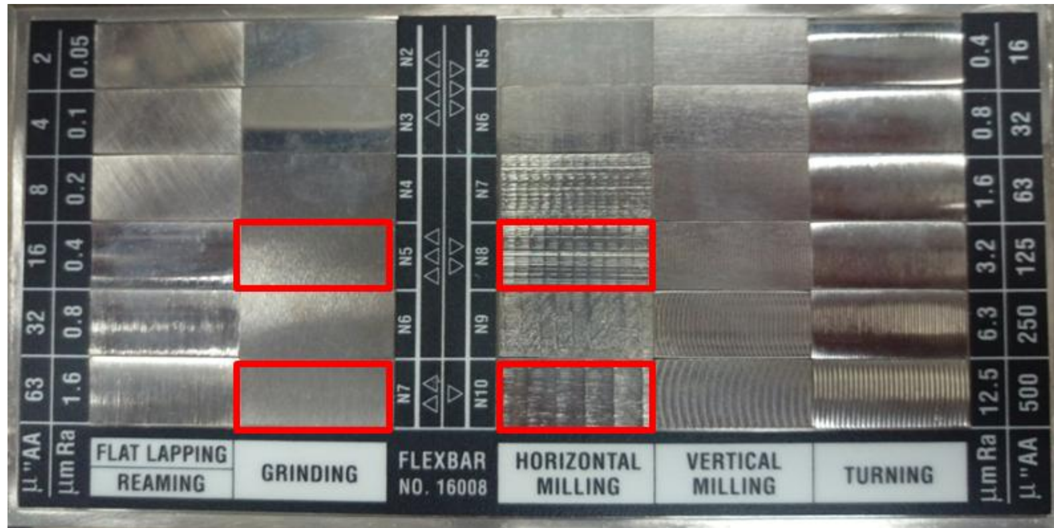

Figure 91 Diffuse surface sample

Using the same pinhole windows (in the center with 90 measuring point), we move the sample to the measuring range and took one shot then move the wafer to new location 30 µm apart from the previous location and took the other shot. From two consecutive measured images, we can calculate the position of every measuring points and the distance of this measuring point between two measured times. We repeated this testing procedure for 30 times and then performed statistical analysis to determine the sample mean value and the random standard deviation.

When measuring diffuse surface sample, there are two different type of NCC response curve being received. The first one will provide valuable information for depth measurement as in Figure 92. The other cannot find any correlation with reference database pattern because of light intensity is too weak at this measuring point as all the light have been scatter away. It may be also caused by the depth change frequency in this measured spot was two heights, so the pattern was alter significantly as described in Figure 93. By defining an evaluation threshold, the noise response can be removed.

doi: 10.6342/NTU201601083

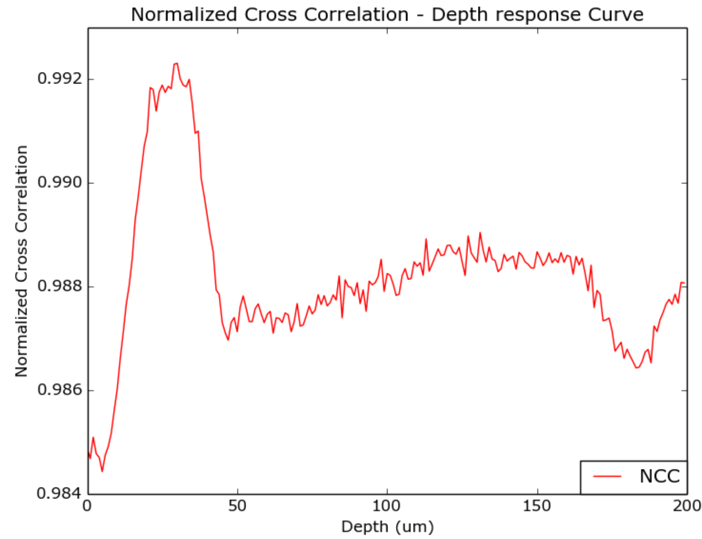

Figure 92 Typical NCC response

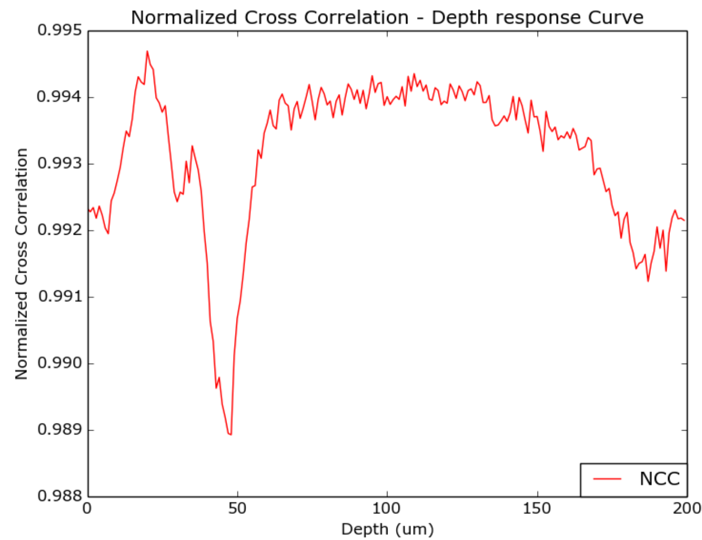

Figure 93 NCC response with noise

In order to remove noise and keep only useful data information, the definition of standard deviation, which is used widely in statistics, was employed as a threshold for evaluating the depth response curve. The standard deviation is formulated as:

$$\sigma = \sqrt{\frac{\sum_{i=1}^{n}(x_i - \bar{x})^2}{n-1}} \tag{28}$$

doi: 10.6342/NTU201601083

where σ is the standard deviation, n is the total number of data, x_i is the i-th sample data, and $\bar{x}$ is the average sample data.

For different measure times, sample mean values are in range from 28.44 to 28.75 μm and the random standard deviation was kept within 0.67 μm under 90 measured results. Figure 94 illustrates the measurement accuracy and precision in the tested result. Transparent green dots are shown as bad measured points with noise (which can be detected by using standard deviation threshold). Solid green points indicate good measured points.

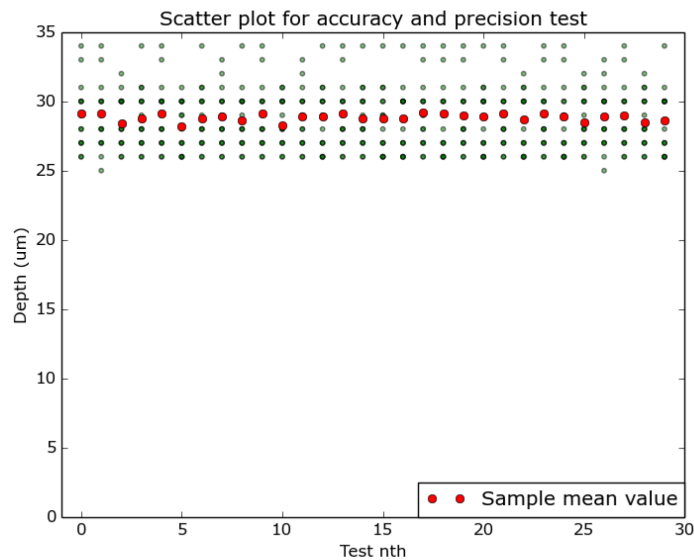

Figure 94 Scatter plot for accuracy and precision test of diffuse surface sample

Surface characteristics have important impacts in our measurement results. There are two factors has major role in our method efficiencies: Surface reflectance and roughness. Employing normalized cross correlation for diffractive pattern matching and spectrum response matching, our system was proved immune to light variation and surface reflectance disturbance. However, the formula just can work in case in spot size area when surface reflectance is uniform. On the other hand, surface roughness will affect our measure results when in spot size area, the depth change with high frequency. In this case, diffractive pattern or spectrum response will be mixed up with diffractive pattern or spectrum response of different height. Therefore, sometime we cannot find any correlation between the measured response and reference database.

doi: 10.6342/NTU201601083

doi: 10.6342/NTU201601083

6 Conclusions and future work

6.1 Conclusions

By using innovative devices such as DMD and IMEC camera and new developed measurement methods, this study has been initially completed an quasi one-shot full-field confocal microscope, which can further integrated in present product line. By using DMD, lateral scanning will be reduced and mechanical movement in the developed system can be minimized, so the measurement errors also are significantly reduced. Furthermore, with specific designed pinholes array arrangement created by DMD, cross-talk effect between adjacent measuring points can be significantly reduced, so lateral resolution could be improved. The vertical scanning process will be eliminated by using two different approaches: innovative digital diffractive-confocal imaging correlation microscope method and chromatic confocal system including spectral area camera. After eliminating all scanning process, those systems can achieve high-speed, high-resolution for volumetric measurement.

This research also focused on NCC algorithms using for digital diffractive-confocal imaging correlation microscope, and spectrum response curve reconstruction technique for chromatic confocal microscope using DMD and IMEC spectral camera system. On the other hand, the diffraction pattern of virtual pinhole being created by specific arrangement of micro mirrors on DMD was comprehensively investigated. Specific scientific and technological findings of this study are summarized as follows:

1. Summarizing and concluding the current developments and trends for a variety of domestic and international confocal microscopy techniques related to surface profilometry: This thesis provided in-depth discussion, comparison and analysis of different confocal microscope systems.

2. Using Fraunhofer diffraction model to explicate diffraction pattern of diffraction pattern of virtual pinhole which created by specific arrangement of micro mirrors on DMD: This diffraction pattern was simulated by Matlab software and then confirmed by practical experiment.

3. By applying 2-D normalized cross correlation to build normalized cross correlation–depth response curve in DDCIC microscope based on DMD and 1-D normalized cross correlation for spectrum response matching procedure in chromatic

doi: 10.6342/NTU201601083

confocal system including spectral area camera, the developed systems are immune to light intensity variation caused by light source's power fluctuating and reflectivity variation of sample's surface.

4. Quasi one-shot full-field surface profilometry using the digital diffractive-confocal imaging correlation microscope with DMD is developed for quasi one-shot microscopic 3-D surface measurement. Optical configuration was built with DMD to generate specific pinhole array arrangement for minimizing cross talk effect. From the preliminary experimental results with specular surface samples, it was verified that for digital diffractive-confocal imaging correlation microscope based on DMD, the repeatability with one-standard deviation on height measurement is 0.03 μm in a measuring depth rage of 400 μm while the maximum measured error is within 0.1 % of the measurable depth range.

5. In order to enhance performance of the developed NCC confocal microscope, the digital diffractive-confocal imaging correlation microscope using chromatic objective with a color CCD was proposed. Measurement range, light efficiency and curvature measuring capability of this system can be significantly improved.

6. Chromatic confocal microscope using DMD and IMEC area spectral camera was developed. 2-D signal matching algorithm was used to rebuild spectrum response curve from finite wavelength bands of IMEC camera and build the calibration curve based on the relationship between vertical distance and spectral intensity. For chromatic confocal system including spectral area camera, random standard deviations is lower than 0.12 μm for specular type samples. Applying the system in the case of diffuse surface samples with roughness Ra = 1.6, one-standard deviation on height measurement still can be kept within 0.67 μm.

6.2 Future work

All proposed systems in this thesis were developed in order accuracy, precision and other important characteristics. However, in order to make those systems become commercial product, which can be flexibly used in available product chain, the systems need to be improved by following the directions described below:

1. All systems were setup on anti-vibration optical table, so compact and rigid mechanic structure need to be designed and produced.

doi: 10.6342/NTU201601083

2. The system is currently using a piezoelectric displacement of the platform to scan basis, but take the stage area is too small, and can load only 1 kg. The future can be replaced by more appropriate displacement of nano-scale platform to carry out the measurement reference database.

3. The current systems uses camera with 10 and 12 bit resolution, without cooling system, they suffer from dark current phenomenon in camera's sensor and signal to noise ratio will be reduced. Using a 16-bit resolution cooled camera can partially address this problem.

4. Currently, the main flow controller of all system is PC software; this will somehow limit speed of the system. In future, the main flow control of all system needs to be a microcontroller and FPGA board which can control the boat camera (using external trigger mode) and DMD at the same time and storage data in its own ram. PC just act as processing unit and visualization device.

5. Chromatic confocal system using IMEC camera and DMD are suffering from vignetting phenomenon of specific chromatic objective designs (which mainly used in point-scan and line-scan chromatic confocal system). Therefore, it is necessary to design new chromatic objective for area-scan chromatic confocal system.

6. Simulation models using to illustrate diffraction pattern and in and out focus effect of confocal system were mainly depend on single wavelength. The models using multiple wavelength light source (broadband light source) need to be developed in order to illustrate those phenomena.

doi: 10.6342/NTU201601083

References

1. T. R. Corle and G. S. Kino, "CHAPTER 1 - Introduction," in Confocal Scanning Optical Microscopy and Related Imaging Systems (Academic Press, Burlington, 1996), pp. 1-66.
2. "Bibliography on confocal microscopy and its applications," Scanning 16, 33-56 (1994).
3. T. Wilson and B. R. Masters, "Confocal microscopy," Applied Optics 33, 565-566 (1994).
4. C. J. R. Sheppard and X. Q. Mao, "Confocal Microscopes with Slit Apertures," Journal of Modern Optics 35, 1169-1185 (1988).
5. T. Tanaami, S. Otsuki, N. Tomosada, Y. Kosugi, M. Shimizu, and H. Ishida, "High-speed 1-frame/ms scanning confocal microscope with a microlens and Nipkow disks," Applied Optics 41, 4704-4708 (2002).
6. C.-H. Lee and J. Wang, "Noninterferometric differential confocal microscopy with 2-nm depth resolution," Optics Communications 135, 233-237 (1997).
7. T. Jiubin, L. Jian, and W. Yuhang, "Differential confocal microscopy with a wide measuring range based on polychromatic illumination," Measurement Science and Technology 21, 054013 (2010).
8. S. Kimura and T. Wilson, "Effect of axial pinhole displacement in confocal microscopes," Applied Optics 32, 2257-2261 (1993).
9. A. K. Ruprecht, K. Korner, T. F. Wiesendanger, H. J. Tiziani and W. Osten, "Chromatic confocal detection for high speed micro topography measurements," Proceedings of SPIE 5302, 53-60 (2004).
10. C. S. Joseph, G. G. Jérôme and C. J. Pierre, "Quasi Confocal Extended Field Surface Sensing," Proceedings of SPIE 4449, 178-183 (2001).
11. K. Shi, P. Li, S. Yin, and Z. Liu, "Chromatic confocal microscopy using supercontinuum light," Optics Express 12, 2096-2101 (2004).
12. F. Bitte, G. Dussler, and T. Pfeifer, "3-D micro-inspection goes DMD," Optics and Lasers in Engineering 36, 155-167 (2001).
13. F. Bitte, G. Dussler, T. Pfeifer, G Frankowski “MicroScan: a DMD based optical surface profiler,” Proceedings. of SPIE 4093, 309–318 (2000).
14. W. Neu, M. Schellenberg, E. Peev “Time-resolved confocal microscopy using a digital micro-mirror device,” Proceedings of SPIE 7596, 75960F-1 (2010) .
15. Q. Li, X. He, Y. Wang, H. Liu, D. Xu, and F. Guo, "Review of spectral imaging technology in biomedical engineering: achievements and challenges," BIOMEDO **18**, 100901-100901 (2013).
16. L.-C. Chen, Y.-W. Chang, and H.-W. Li, "Full-field chromatic confocal surface profilometry employing digital micromirror device correspondence for minimizing lateral cross talks," OPTICE **51**, 081507-081501-081507-081510 (2012).

doi: 10.6342/NTU201601083